Fall 12-2021

Estimating the Risk of Future Plastic Marine Debris Resulting from the Urban Coastal Built Environment

Kelly C. Jones
Old Dominion University, kellyc.jones23@gmail.com

ESTIMATING THE RISK OF FUTURE PLASTIC MARINE DEBRIS RESULTING FROM THE URBAN COASTAL BUILT ENVIRONMENT

by

Kelly C. Jones
B.A. December 2018, Hartwick College

A Thesis Submitted to the Faculty of
Old Dominion University in Partial Fulfillment of the
Requirements for the Degree of

MASTER OF SCIENCE

OCEAN AND EARTH SCIENCE

OLD DOMINION UNIVERSITY
December 2021

Approved By:

Hans-Peter Plag (Director)

C. Ariel Pinto (Member)

Hannah Torres (Member)

John Klinck (Member)

ABSTRACT

ESTIMATING THE RISK OF FUTURE PLASTIC MARINE DEBRIS RESULTING FROM THE URBAN COASTAL BUILT ENVIRONMENT

Kelly C. Jones
Old Dominion University, 2021
Director: Dr. Hans-Peter Plag

The growing urban built environment in the coastal zone poses an unknown risk to the marine biosphere as a source of marine debris. Plastic, since its introduction in the mid- 1900s, is now used in nearly all aspects of human life. Growth in human population and urbanization in coastal zones has resulted in the accumulation of large stocks of plastic in the coastal built environment, and these stocks are still growing exponentially. The coastal zone is exposed to a number of hazards including storms, tsunamis, and sea level rise, and most of these hazards are expected to change in the future due to climate change. The accumulation of plastic and other potential marine debris in the coastal zone creates a growing risk of plastic marine debris originating from the coastal zone, which will impact future generations for a long time. Risk is the possibility of consequences where the outcome is uncertain, and here the consequence is additional plastic marine debris entering the ocean. To quantify this risk, the product of hazard probability, fragility of the urban coast, and the exposed assets, measured in the amount of plastic, is used. The hazard probability is determined by the changing hazard spectrum as a result of climate change. The fragility of the urban coast is identified for three case studies through analysis of the damage caused in these locations by specific hazardous events. Unfortunately, the production and use of plastic in society is not well documented and the available data cannot be used to calibrate and validate a comprehensive stock and flow model for plastic in the urban coast. Therefore, the amount of plastic exposed in the case study locations and globally is estimated by population and amount of plastic per person. Using the estimated hazard probabilities, the fragilities, and the exposed amounts, the quantification of risk resulted in understanding that, for example, by 2050, one or more tsunamis with a wave height less than 2 meters in Japan could result in, on average, 74,000 tons of plastic marine

debris. One or more cyclones making landfall in the Bahamas could result in, on average, 9,796 tons of plastic marine debris. For Jakarta, the city is likely to be abandoned and a scenario where leaving 20% of the plastic in urban built environment behind could result in 272,800 tons of plastic marine debris. These examples, along with other compiled in the study, indicate the scale of the risk for future generations.

Dedicated to Nain.
I know you would be proud.

ACKNOWLEDGMENTS

This research was supported by the Graduate Summer Award Program 2021 from the Graduate School and Office of Research at Old Dominion University, Norfolk, Virginia, USA. This research was supported by the Department of Ocean and Earth Science and the Graduate School at Old Dominion University, Norfolk, Virginia, USA through a Graduate Teaching Assistantship. I want to thank my adviser, Dr. Hans-Peter Plag, for sharing his knowledge and teaching me to think nontraditionally and to ask the hard questions. I also want to thank my committee, Dr. John Klinck, Dr. Hanna Torres, and Dr. Cesar A. Pinto for sharing their unique perspectives and for helping me finish. A large thank you to my mom and dad. I love you and thank you for being my biggest supporters. Finally, thank you to Matthew, Ruthie, and my close family and friends who believe in me and the work that I do.

ABBREVIATIONS

ACCI	Anthropogenic Climate Change Index
CRED	Centre for Research on the Epidemiology of Disasters
DHHS	Department of Health and Human Services
ENSO	El Niño Southern Oscillation
ECLAC	Economic Commission for Latin America and the Caribbean
GAAPP	Global Average Annual Plastic per Person
GCR	Global Catastrophic Risk
GMSL	Global Mean Sea Level
HC1	Hurricane Category 1
HC2	Hurricane Category 2
HC3	Hurricane Category 3
HC4	Hurricane Category 4
HC5	Hurricane Category 5
IDB	Inter-American Development Bank
IPCC	International Panel on Climate Change
LCZ	Low Climate Zones
MD	Marine Debris
MHHW	Mean Highest High Water
MIAC	Ministry of Internal Affairs and Communications
NCEI	National Centers for Environmental Information
NHC	National Hurricane Center
NOAA	National Oceanic Atmospheric Administration

NWS	National Weather Service
PDF	Probability Density Function
PMD	Plastic Marine Debris
PVC	Polyvinyl chloride
SLR	Sea Level Rise
SST	Sea Surface Temperature
SFM	Stock and Flow Model
TS	Tropical Storm
UBE	Urban Built Environment
UMD	Urban Marine Debris
UNEP	United Nations Environmental Program
UNPD	United Nations Population Division
UTC	Coordinated Universal Time
WH	Wave Height

TABLE OF CONTENTS

Page

LIST OF TABLES……………………………………………………………………………...x

LIST OF FIGURES……………………………………………………………………… xi

Chapter

1. INTRODUCTION 14
   1.1 REDUCING THE RISK OF FUTURE MARINE DEBRIS WHILE UTILIZING THE URBAN COASTAL ZONE.. 15
   1.2 THE URBAN COASTAL SYSTEM.. 17
   1.3 HAZARDS TO THE URBAN COAST 19
   1.4 FRAGILITIES OF THE URBAN COAST 20
   1.5 THE GROWING VALUE OF THE EXPOSED ASSETS IN A GROWING URBAN COAST 22
   1.6 DOCUMENT STRUCTURE.. 27

2. KNOWLEDGE ASSESSMENT 29
   2.1 RISK OF URBAN MARINE DEBRIS 29
   2.2 HAZARDS TO THE URBAN COAST 30
   2.3 FRAGILITIES 36
   2.4 VALUE OF THE EXPOSED ASSETS IN THE URBAN COAST.. 40
   2.5 RESEARCH QUESTIONS 44

3. METHODOLOGY 46
   3.1 HAZARD PROBABILITY DENSITY FUNCTION 47
   3.2 FRAGILITIES OF THE URBAN COAST 48
   3.3 AMOUNT OF THE EXPOSED ASSETS.. 49
   3.4 RISK ASSESSMENT.. 52

4. RESULTS 53
   4.1 STOCK AND FLOW MODEL CALIBRATION 53
   4.2 CASE STUDY: JAPAN 59
   4.3 CASE STUDY: THE COMMONWEALTH OF THE BAHAMAS 67
   4.4 CASE STUDY: JAKARTA, INDONESIA.. 77

5. DISCUSSION.. 86

REFERENCES 88

VITA.. 97

LIST OF TABLES

Table Page

1. City Structure Types “Local Climate Zones commonly names ‘’LCZ XX” (XX from 1-Compact High-rise to G-Water). LCZs from 1-9 correspond to urban climate zones defined by Oke (2004).” (Taubenböck *et al.* 2020). 42

2. Table of plastic sources. Title, date, author of the paper and then name of the plastic data sourced used in that paper. 56

3. Poisson Probability of no events, 1 event, and 1 or more tsunami events occurring in 30, 80, and 200 years by water inundation height. The recurrence time is based on past tsunami events (NCEI 2021). 61

4. Fragility Scenarios created to understand the relationship between WH and damage. As the relationship is not clearly defined, the scenarios cover the spectrum of possibilities. 63

5. Poisson Probability of no events, 1 event, and 1 or more cyclone events occurring in 30, 80, and 200 years by cyclone storm strength base on past cyclone data. 69

6. Poisson Probability of no events, 1 event, and 1 or more cyclone events occurring in 30, 80, and 200 years by cyclone storm strength with recurrence times of the future. 70

7. This table shows the casualties and damage from Hurricane Dorian in the Bahama Islands. [1] is from the Health Minister in the Bahamas, [2] is from the Bahamas Weather Service. Information from table source: Avila *et al.* (2020). 72

8. Portion of the Bahamas Islands impacted by Hurricane Dorian (IDB 2019). 73

9. The fragility scenarios for the Bahamas Islands. 74

10. Poisson Probability of no events, 1 event, and 1 or more events occurring in 10, 30, 80, and 200 years. 78

11. The fragility scenarios of the UBE of Jakarta where different portions of material are left behind. 81

LIST OF FIGURES

Figure Page

1. High-level conceptual model of the ocean-terrestrial environment, encompassing the UBE. The flows from the Terrestrial Area (green) and the Ocean Area (blue) represents the potential flow of PMD. 17

2. This is a low-level conceptual model of the ocean-terrestrial environment, encompassing the UBE. The terrestrial land is represented in green; the estuary, bay, and fluvial environments represented in teal; and the ocean in blue. The black arrows show the flow of plastic. 18

3. Conceptual model showing the exogenic hazards between the urban system, terrestrial system, and marine system as well as the endogenic hazards within them. The arrows show the hazard leaving one system becoming exogenic for the other. 20

4. Coastal zone and coastal population changes. Major coastal cities, the average population per country, and the amount of alteration found along the shorelines in the coastal zone. Republished by Rekacewicz 2002. 22

5. Coastal zone and coastal population changes. Population per 30” cell inland versus along the coast (Sale *et al.* 2014). Reprinted from (Sale *et al.* 2014) with permission from Elsevier. 23

6. World Population from 1900 to 2020, projected to 2100. Reprinted from Roser *et al.* 2013. 24

7. A. Graph of average annual number of births globally. Reprinted from UN 2019a. B. Graph of average annual number of deaths globally. Reprinted from UN 2019a. 25

8. Change of population from urban to rural areas. Reprinted from Ritchie & Roser 2018. 26

9. Average global population from 1700 - 2020 (blue dots). Represents the average coastal population with a standard deviation of 10% to show potential fluxes in the 40% number (red). Data used from the HYDE Database for years 1700 - 1940 (Goldewijk et al. 2017) and from UNPD for years 1950 to 2020 (UNPD 2019). 27

10. A conceptual model of the urban coastal built environment system, the inherent fragilities, and the relevant hazards that can exploit them. 37

11. Global primary plastics production according to industrial use sector from 1950 to 2015. Republished from Geyer *et al.* 2017b. 44

Figure Page

12. The methodology to assess the risk of PMD originating in the UBE. 46

13. SFM of the flow of plastic in the UBE including the different stocks (boxes) And the flow of plastic (arrows).There is also a loss factor for each flow, not portrayed in the visual model. 50

14. The risk equation as an outline form the Results Chapter. Each section is separated by case study to identify the variables of the Risk Eq. (1), resulting in the risk assessment. 53

15. World Population 1950-2019. Low, medium, high, and no change variant projection from 2020 to 2100. Data source: (UNPD 2019). 57

16. Global Population in the coastal zone (40%; Sterzel *et al.* 2020) multiplied by the estimated amount of plastic in the UBE from 1950-2015. Global projected population variants (UNPD 2019) from 2016 to 2100 multiplied by 40% to identify coastal projections at the proportion, then used with the plastic in the UBE to determine potential future projections of annual plastic in the coastal UBE, globally. 59

17. Population of Japan with UNPD population projection variants (UNPD 2019). 64

18. The annual amount of plastic in Japan's national UBE compared to in Japan's coastal UBE. 65

19. Risk Scenario. Risk of 1 or more tsunami events, specified by wave height, in Japan in 30, 80 or 200 years where $WH_{(A)}$ creates 40%, 60% and 80% of the damages as $WH_{(B)}$. 67

20. Population of the Commonwealth of the Bahamas (UNPD 2019). 75

21. The current amount of exposure in the Bahamas Islands in terms of PMD. The total plastic and UBE plastic in the Bahamas are the same because the islands are relatively flat and therefore all plastic could be open for transport, rather than that just in the UBE as construction and consumer uses. 76

22. Risk Scenarios. Risk of 1 or more cyclone events making landfall in the Bahamas Islands in 30, 80, and 100 years where HCa creates A (40%), B(60%), or C(80%) of the damages as $HC_{(a+1)}$ and the fragilities are 10%, 20%, and 40% of the damaged material enters the ocean. 77

23. Land subsidence data for 2.5cm/yr (Budiyono *et al.* 2016), 3 cm/yr, 5 cm/yr, 7 cm/yr, 10 cm/yr (Abidin *et al.* 2015). 79

Figure Page

24. Population of Indonesia (UNPD 2019). 82

25. Population of Jakarta, Indonesia (WPR 2021). 83

26. The amount of exposed assets annually in the Jakarta, Indonesia (the UBE) in terms of tons of plastic. 84

27. Risk graph showing scenarios of fragilities. The fragilities are based on how much material is left behind during retreatment (20% to 90%). 85

CHAPTER 1

INTRODUCTION

Marine Debris (MD), also known as ocean litter, is a global pollution problem impacting a multitude of systems in the ocean environment. MD is defined by United Nations Environmental Program (UNEP) as "any persistent, manufactured or processed solid material discarded, disposed of or abandoned in the marine and coastal environment" (UNEP 2009). While ocean dumping has occurred for many centuries, the introduction of plastic and other non-biodegradable material has greatly changed the impact of dumping on the ocean systems (Sheavly & Register 2007). The rapid expansion of the Urban Built Environment (UBE) in the coastal zone has resulted in far more materials moving into the coastal zone and this has increased the MD that could potentially enter the ocean from the coastal UBE. The US Department of Health and Human Services (DHHS) defines the UBE as all structures, areas, and products created by people, including buildings, recreation zones, transportation systems, overhead lines, and underground waste disposals (DHHS 2004). The UBE in flood zones is a potential source of MD that could enter the ocean, and thus, is a potential hazard to the ocean system. The MD distributed in the ocean occur in both organic and inorganic forms. Although much of it is plastic, MD can also be classified as other organics that include woods and natural fibers, or inorganics including metal, glass, and concrete (Engler 2012). Plastic Marine Debris (PMD) is a threat to the ecosystems. This extreme hazard, caused by humanity's disregard for the planet and future generations, exploits many of the fragilities in Earth's systems.

The problem of plastic is directly linked to human needs and consumption. The increasing population and the increasing demand of materials, in turn, increases the amount of plastic in the coastal zone. The stocks of plastic in flood zones, specifically in coastal areas, can eventually turn into PMD. The threat posed by the urban coast as a potential source of MD to current and future generations depends on the extent and design of the urban coast, the hazards the urban coast is exposed to, and the fragilities of the urban coast with respect to these hazards. Section 1.1 introduces the complex societal planning problem, known as a wicked problem, of reducing the risk of future MD originating in the urban coast while continuing to utilize the coastal zone for a growing UBE. The urban coastal system is outlined in Section 1.2. In Section 1.3, the hazards to the UBE are introduced, and in Section 1.4 the fragilities of the UBE with respect to these hazards are considered. Finally, Section 1.5 discusses the extent of the exposed assets using population, and Section 1.6 gives an overview of the document structure.

1.1 REDUCING THE RISK OF FUTURE MARINE DEBRIS WHILE UTILIZING THE URBAN COASTAL ZONE

Risk is the possibility of consequences where the outcome is uncertain (Pinto & Garvey 2012), and here the consequence is additional PMD entering the ocean. Risk is typically discussed in terms of economic loss whereas the risk here refers to amount of PMD entering the ocean and not the impact of the MD on the ocean. A quantitative measure for risk can be defined as the product of hazard probability multiplied by the fragility of the exposed assets to the hazards multiplied by the value of the exposed assets (Plag & Jules-Plag 2013). In many cases, vulnerability is used in this measure, instead of fragility (e.g., Plag & Jules-Plag 2013). However, fragility is more closely related to the constitution of an exposed asset, and therefore it is used here.

Coastal zones are areas of transition between the marine and terrestrial environments. They are the most productive and valuable ecosystems on Earth (Baztan *et al.* 2015). The coastal zones are important areas of productivity and are buffers between the terrestrial environments and the marine environments. Changing this delicate buffer zone could result in major catastrophic events. Global Catastrophic Risk (GCR) is referred to as "a risk that might have the potential to inflict serious damage to human well-being on a global scale" (Bostrom & Cirkovic 2008). While humanity is exposed to a growing number of GCRs (Avin *et al.* 2018), future MD originating in the coastal UBE has the potential to increase the Anthropocene risk to the ocean. This is not only due to the growth of the built environment, but also because of the type of material now moving into these systems. The plastics, heavy metals, and electronics being added to these fragile zones compared to stone and wood of the past creates the GCR to the ocean due to the potential impacts of the PMD that can result from the urban coast. The risk associated with current building materials in the urban coast under climate change and a changing hazard spectrum is valuable scientific knowledge for tackling the wicked problem of reducing the risk associated with PMD while continuing to develop the urban coast.

Wicked problems are complex societal planning problems rooted in the environment and are, to a large extent, defined by the desired future (Rittel & Webber 1972). They are characterized by incomplete and often contradictory knowledge, a large number of stakeholders involved with conflicting opinions and interests, and high economic burdens. Tackling wicked problems requires transformative knowledge (Brown *et al.* 2010). Wicked problems were first defined by Rittel & Webber (1972) as problems that fit ten specified criteria:

1. Wicked problems have no definitive formulation.
2. Solutions are better or worse, not right or wrong.
3. Each employed solution to a wicked problem is a one-shot opportunity.
4. Every problem is a symptom of another problem.
5. The explanation of the problem determines the solutions.
6. The solver has no right to be wrong.
7. There is no defined set of options and solutions.
8. There is no immediate test for solutions.
9. There is no stopping rule. A wicked problem can never truly be ‘solved’.
10. Every problem is essentially unique. (Rittel & Webber 1972)

Tackling wicked problems requires a transdisciplinary approach, which includes unique, scientific, and transformative knowledge. This approach includes assessing the system and determining the stakeholders. Ideally, a stakeholder meeting takes place where the relevant stakeholders communicate their perspectives, and the group creates a shared goal statement. The system identification is finalized which allows for the fragilities of the system to be clarified. At the same time, the hazards that exploit these fragilities can also be determined. The transdisciplinary approach uses this information to create a full spectrum of possible futures and the risk associated with them. Interventions that would lead to the desired future are explored and assessed. Recommendations come from these interventions and the goal statement created by the stakeholders. The changing development of the urban coast impacts the risk of PMD, resulting in the question of how the development of the urban coast has changed in the past, as well as how it is projected to change in the future, in terms of land area and of the material used. The risk assessment will create the scientific knowledge valuable for those tackling the wicked problem of minimizing the PMD that could originate in the urban coastal zone. Specifically, the study will assess the risk associated with the current and projected futures of building materials in the urban coast under climate change and a changing hazard spectrum. In the next section, the system will be determined, identifying the fragilities and hazards.

1.2 THE URBAN COASTAL SYSTEM

There are more people moving into the coastal zones, resulting in urban sprawl and larger UBEs. The growing coastal urban settlement also causes more human-made consumer goods to move into these fragile transition zones. The mass movement of these environmentally hazardous goods to coastal zones creates the potential for a GCR to terrestrial and marine systems and, through feedback loops, to humanity. The expanding coastal population and the growing UBE are exposed to a changing spectrum of hazards that can exploit the inherent fragilities of these systems. The coastal built environment is systematically fragile with respect to the hazards.

The system representing the challenge of PMD resulting from the urban coast separates into the terrestrial system containing the urban coast and the ocean potentially receiving PMD originating from the urban coast (Fig. 1). The terrestrial environment stock contains the UBE, rural environment, and fluvial and floodplains; while the ocean environment shows the marine biosphere, physio-sphere, and geo-chemisphere. The ocean-atmosphere interaction is the source for many of the hazards the urban coast is exposed to. In order to identify the flows, conceptual models were created starting with the high-level model in Fig. 1.

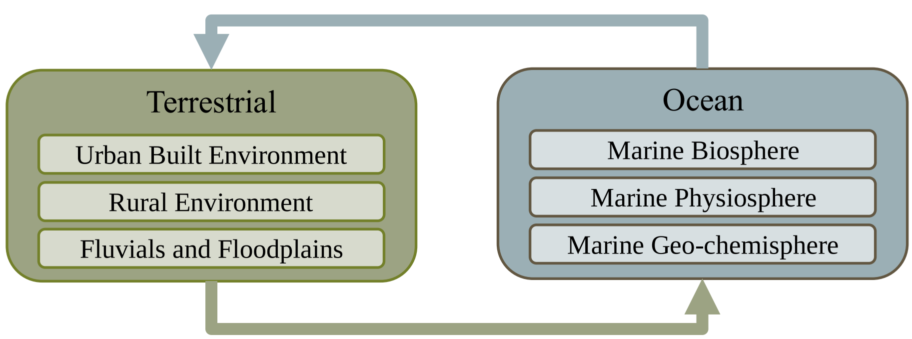

Figure 1. High-level conceptual model of the ocean-terrestrial environment, encompassing the UBE. The flows from the Terrestrial Area (green) and the Ocean Area (blue) represents the potential flow of PMD.

The high-level conceptual model (Fig. 1) was then further assessed to have more detail in a low-level conceptual model (Fig. 2). This low-level model shows the flows of plastic from the terrestrial system to the ocean system, starting at the UBE, which notes the inclusion of where plastic could originate from. Plastic can flow from UBE to the terrestrial non-built and rural built environments as well as the rivers, estuary systems and the ocean directly. The low-level conceptual model prepares for a Stock and Flow Model (SFM), discussed in Section 3.3 that more specifically shows how the plastic travels through the system.

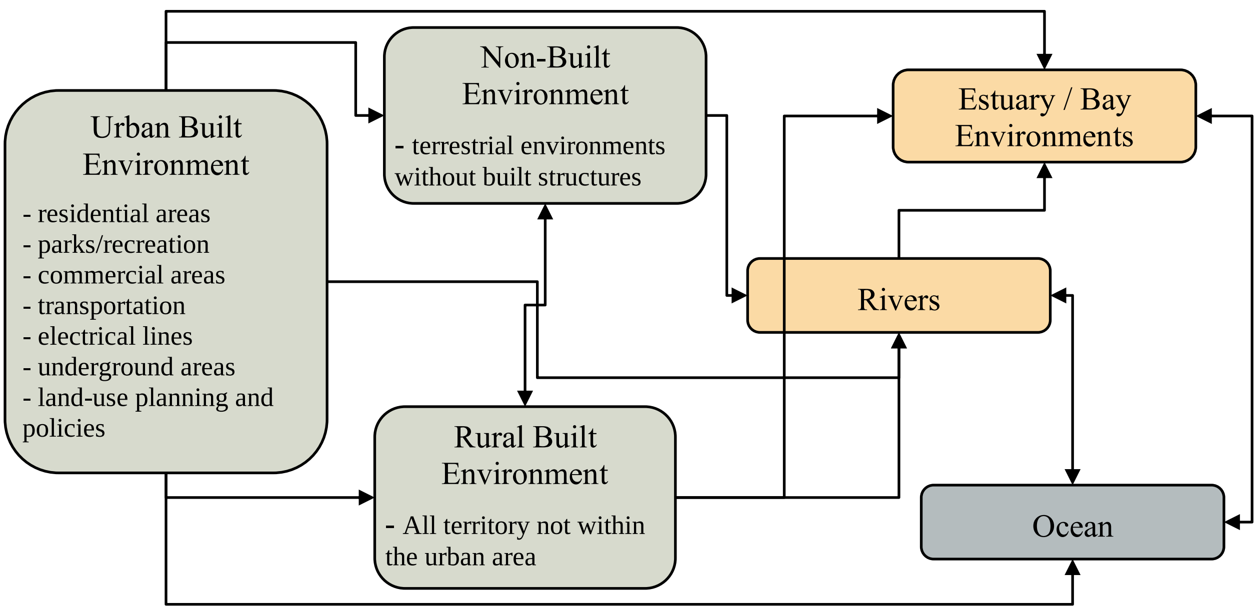

Figure 2. This is a low-level conceptual model of the ocean-terrestrial environment, encompassing the UBE. The terrestrial land is represented in green; the estuary, bay, and fluvial environments represented in yellow; and the ocean in blue. The black arrows show the potential flow of plastic.

The urban coasts are exposed to the impacts of climate change and Sea Level Rise (SLR), including the increasing exposure to hazards such as inundation and storms. The coastal UBE is expected not only to continue to grow but to grow faster than the total urban environment, worsening the GCR associated with PMD. A large fraction of the coastal zone has changed greatly, and will likely continue to change, due to both the increased human civilization and the increased threat of climate change.

1.3 HAZARDS TO THE URBAN COAST

Hazards can be identified as exogenic to a system or endogenic. Here, exogenic hazards are those that originate in the environment surrounding the system, while endogenic hazards originate within the system itself. The initial hazards tend to be exogenic, and often cannot be prevented or mitigated. Endogenic hazards are the hazards that often can be addressed because they originate within the system. For the urban coast, exogenic hazards originating in the terrestrial environment would include river floods, landslides, tornadoes, and earthquakes causing harm to the system within that environment (Fig. 3). Exogenic hazards originating in the adjacent marine environment include storm surges, cyclones, tsunamis, and SLR. Endogenic hazards in the UBE include cascading hazards that can increase the destruction such as fires and explosions as well as litter, sewage, air, and water pollution that can impact human lives. While these are endogenic to the UBE, they are potentially exogenic hazards to the marine systems as shown in Fig. 3. The litter available for creation from hazardous events impacting the urban system poses a severe exogenic hazard to the marine system.

Both the terrestrial UBE and ocean systems are exposed to hazards that are endogenic or exogenic and, due to the nature of the systems, these hazards overlap (Fig. 3). For example, an exogenic hazard to the urban coast is a hurricane which causes stress on the coastal built environment from wind, rain, and storm surges, exploiting the fragility of poorly constructed structures and sewer systems. The endogenic hazard for the built environment would be falling debris or the sewage leakage that causes human harm. The same hazard of the sewer leakage is an exogenic hazard to the ocean systems through fragilities in the marine ecosystems. Similarly, ocean litter is an exogenic hazard to the ocean system from the UBE and exploits the ocean system's fragilities by introducing plastics, rubbers, oils, and other harmful litter into the ocean.

Exogenic hazards to the urban coast can cause a string of endogenic hazards due to improper preparedness to decrease the inherent fragilities. The amount of debris resulting from hazardous events can differ greatly depending on preparedness of the system, the system fragilities, and the materials used to construct the urban coast. These can all be changed to decreases the risk of harmful debris entering the marine system. In order to decrease the risk of coastal built environments on the marine environment, the UBEs can become more prepared, decrease the fragilities, and use less harmful materials. Even if exogenic hazards from the natural environment to the UBE were to increase and/or become more dangerous, the endogenic hazards would be limited and therefore less endogenic hazards could impact the marine system.

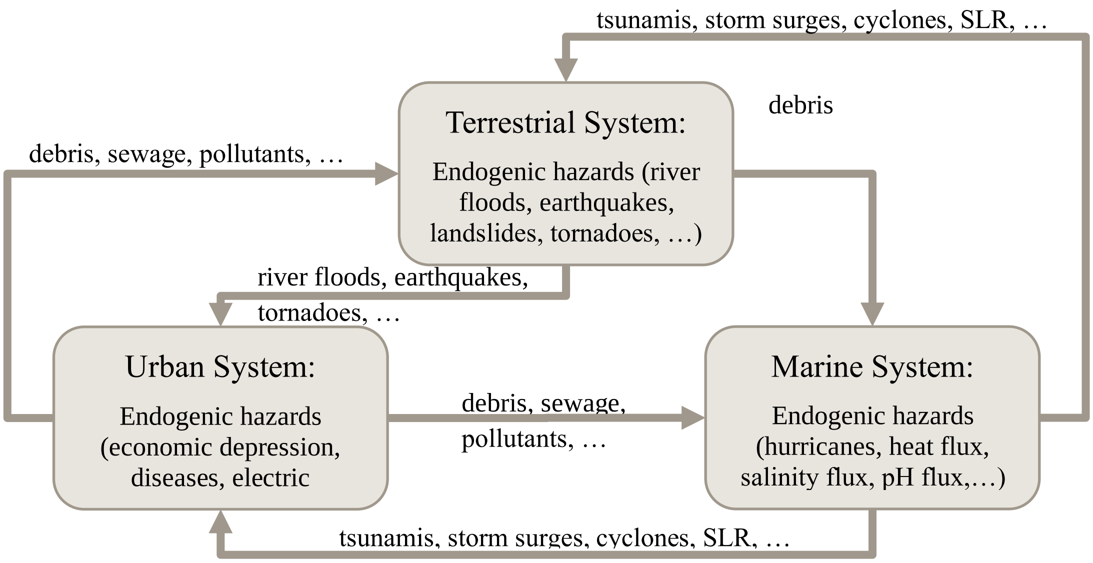

Figure 3. Conceptual model showing the exogenic hazards between the urban system, terrestrial system, and marine system as well as the endogenic hazards within them. The arrows show the hazard leaving one system becoming exogenic for the other.

1.4 FRAGILITIES OF THE URBAN COAST

The high-level conceptual model (Fig. 1) displaying the system and the potential hazards (Fig. 3) leads to further analysis of the system fragilities. First, however, the term must be defined. According to Merriam-Webster (2020a), the definition of fragile is to be easily broken or destroyed. A fragility is an inherent property of a system (Nilsson & Grelsson 1995) that can result in a degradation of the system when acted upon by a hazard. Therefore, the main fragilities are constitutional, but there are fragilities in processes of the system (e.g., in the disruption of supply chain) as well. In many studies (e.g., McGranahan *et al.* 2007) the word used to denote this meaning is vulnerability. However, the definition of vulnerability to some extent implies the presence of a threat and is not clearly restricted to constitutional properties of a system. Therefore, the word fragility will be used throughout this thesis.

Inherent fragilities remain if the system is frozen in time, while process fragilities and hazards are event-based and would disappear from a system in stasis. Fragilities are associated with the changes in the flows in the system. An initial list of fragilities will be determined based on the system defined in Section 1.2. The ocean and terrestrial systems are interconnected but have separate fragilities. Case studies are used to develop estimates of the fragility of the urban coast relevant to the hazards. The fragility is how much PMD could be created. Three different cases are being studied reflecting varying probabilities of hazards, fragilities, and exposure. This will allow for the collection of the scientific knowledge required for the risk assessment in these three cases. The three case studies chosen to identify fragilities include the 2019 Hurricane Dorian; the 2011 Japan Tohoku tsunami; and the present land subsidence in the city of Jakarta, Indonesia. These cases show a varying level of natural hazards on the coastal city and also a varying level of urban expansion.

- The 2019 cyclone, Hurricane Dorian impact on the Bahamian Islands is a case where the probability of the hazard as well as the level of exposure was increasing. This resulted in a catastrophe to the human and nonhuman systems.
- The case of the 2011 tsunami in Japan has a changing exposure, but not a changing probability of the hazard. The population is increasing and so is the UBE, changing the risk through increased exposure to the exogenic hazard.
- The city of Jakarta is an example of high-probability hazards (SLR due to land subsidence and river floods) presently occurring resulting in a retreat out of the city.

The case studies are important to informing the answer to the question: Can we ignore the low-probability, high impact tail of the Urban Marine Debris (UMD)-Probability Density Function (PDF)? It is important to recognize that there are other case studies that would assist in answering this question, but the focus is on events in urban coastal areas that are caused by high-probability hazards compared to urban coastal areas that have low- probability hazards.

1.5 THE GROWING VALUE OF THE EXPOSED ASSETS IN A GROWING URBAN COAST

The change in population towards living in the coastal zones has an impact on the shorelines (Fig. 4; Rekacewicz 2002). The number of urban areas located in flood zones is growing, particularly in coastal flood zones (Fig. 5; Sale *et al.* 2014). In 2020, 40% of the world population inhabited the coastal zone (Sterzel *et al.* 2020). The coastal zones are fragile areas and the human migration into these areas greatly alters the environment.

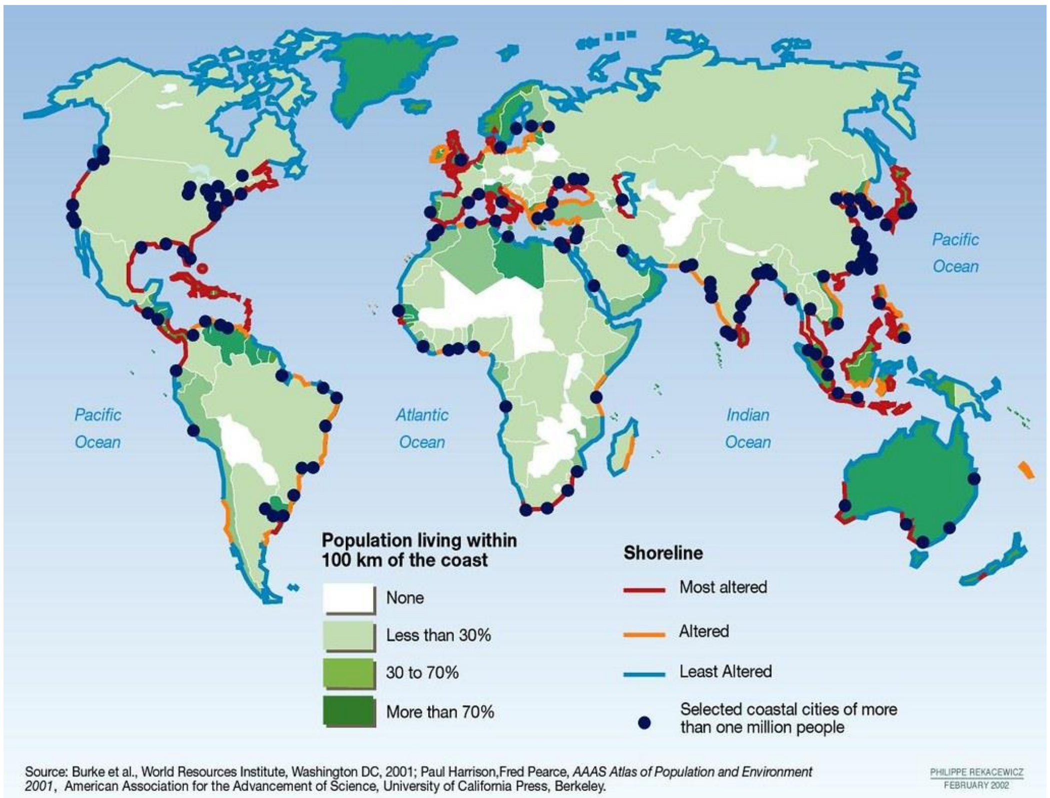

Figure 4. Coastal zone and coastal population changes. Major coastal cities, the average population per country living in the coastal zone, and the amount of alteration found along the shorelines. Reproduced from Rekacewicz 2002.

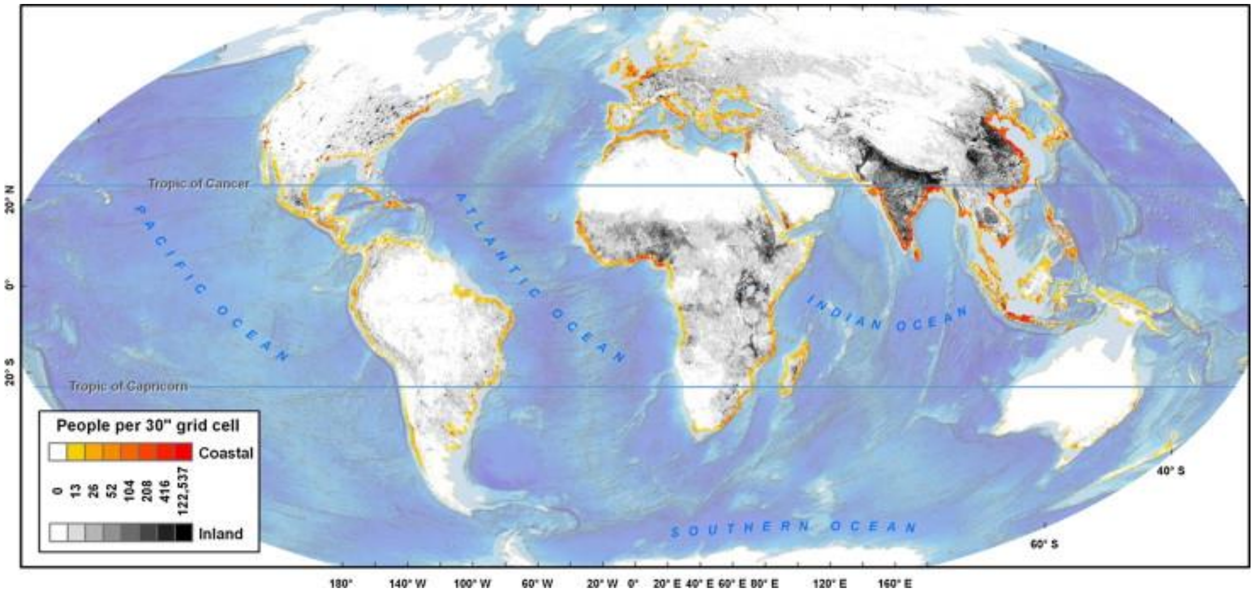

Figure 5. Coastal zone and coastal population changes. Population per 30" cell inland versus along the coast (Sale *et al.* 2014). Reprinted from Sale *et al.* 2014 with permission from Elsevier.

The global population has been increasing rapidly in the last 100 years (Fig. 6). In 1919, the global population was 1.85 billion people but a hundred years later, the population reached 7.71 billion people and is continuing to grow (UN, 2019a). The United Nations (UN) determined that the growth rate of the world's population is no longer increasing, and that this rate had peaked between 1965 and 1970. Compared to a population growth rate of 2.1% from 1965 to 1970, the rate has decreased below 1.1% between 2015 and 2020 and is expected to continue to slow through the 21st century (UN, 2019a).

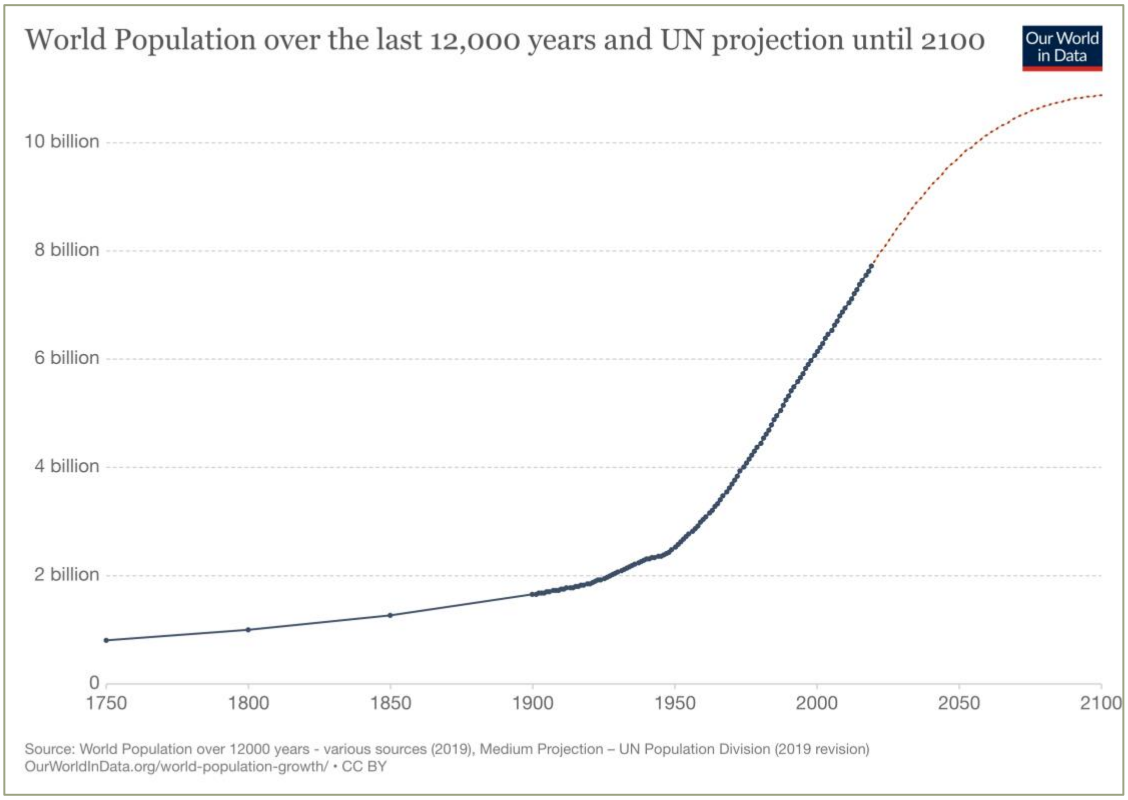

Figure 6. World Population from 1900 to 2020, projected to 2100. Reprinted from Roser *et al.* 2013.

While the growth rate is expected to continue declining, it is still expected to stay above 0. Birth rates are not the only factor that determine population growth, death rates must also be included. In the year of 1950, 97.40 million people were born, and, on average, births increased to the most recent number in 2015 of 140.87 million births (Fig. 7a). However, the number of deaths did not increase at the same rate as births. In 1950 there were 51.27 million number of births is expected to flatten through the 21st century, while the deaths and in 2015 there were 57.22 million (UN 2019a) (Fig. 7b). The number of deaths is expected to increase due to current generations dying of old age (UN 2019a). The projections for births and deaths are outlined in Fig. 7. Not only has population increased, the share of the population that lives in the urban environment compared to the rural environment has increased (Fig. 8; Richie & Roser 2018). In 1950, 70% of the world's population lived in rural areas. In 2020, it was closer to 40% and is continuing to decline.

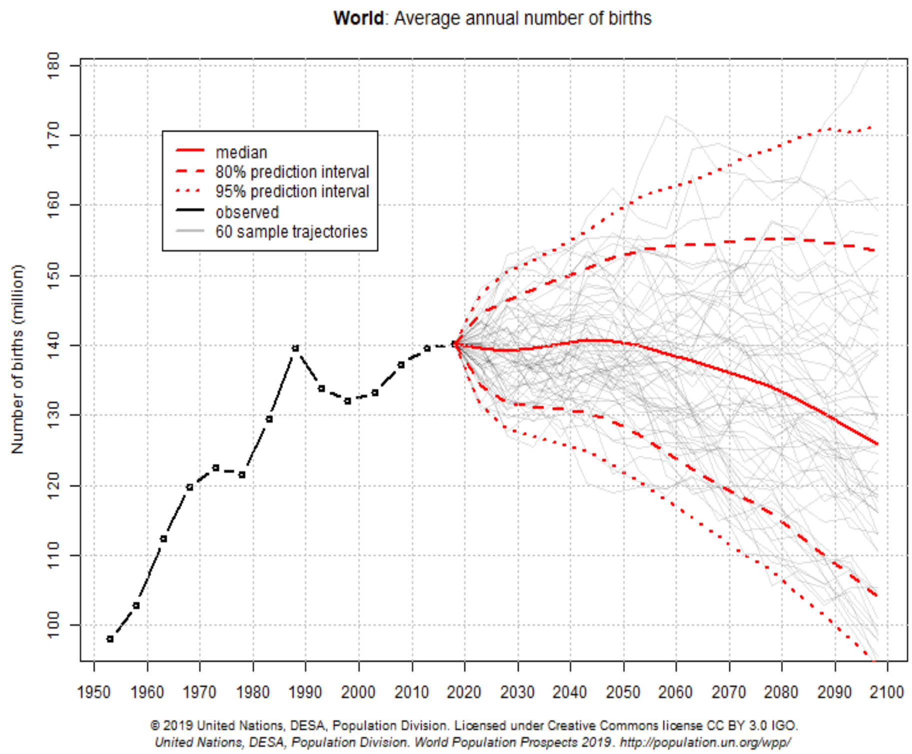

A.

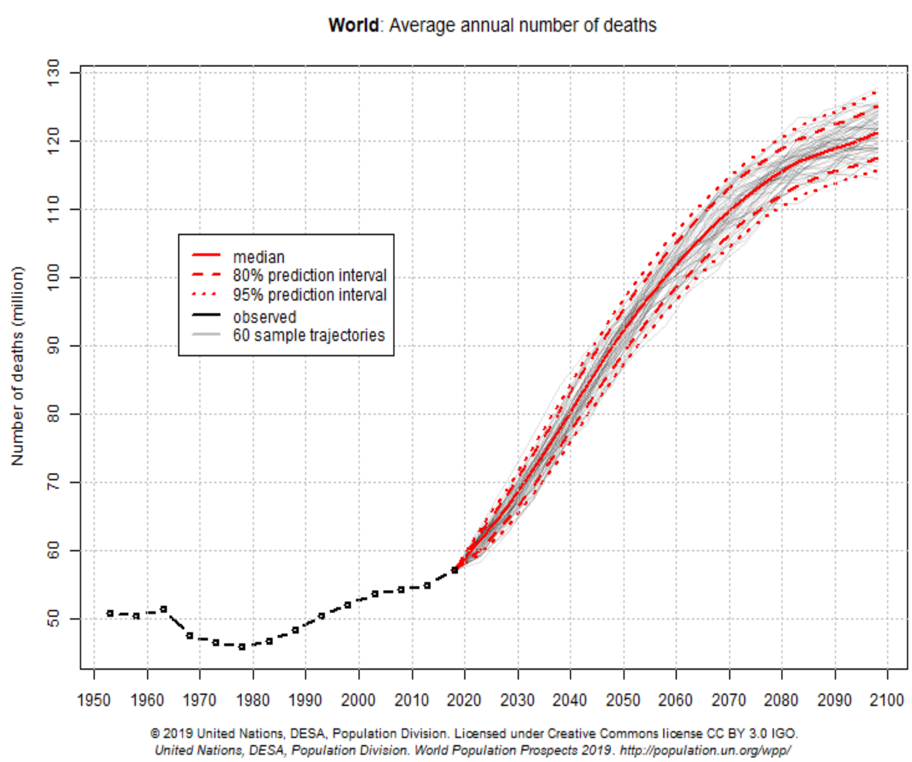

B.

Figure 7. A. Graph of average annual number of births globally. Reprinted from UN 2019a. B. Graph of average annual number of deaths globally. Reprinted from UN 2019a.

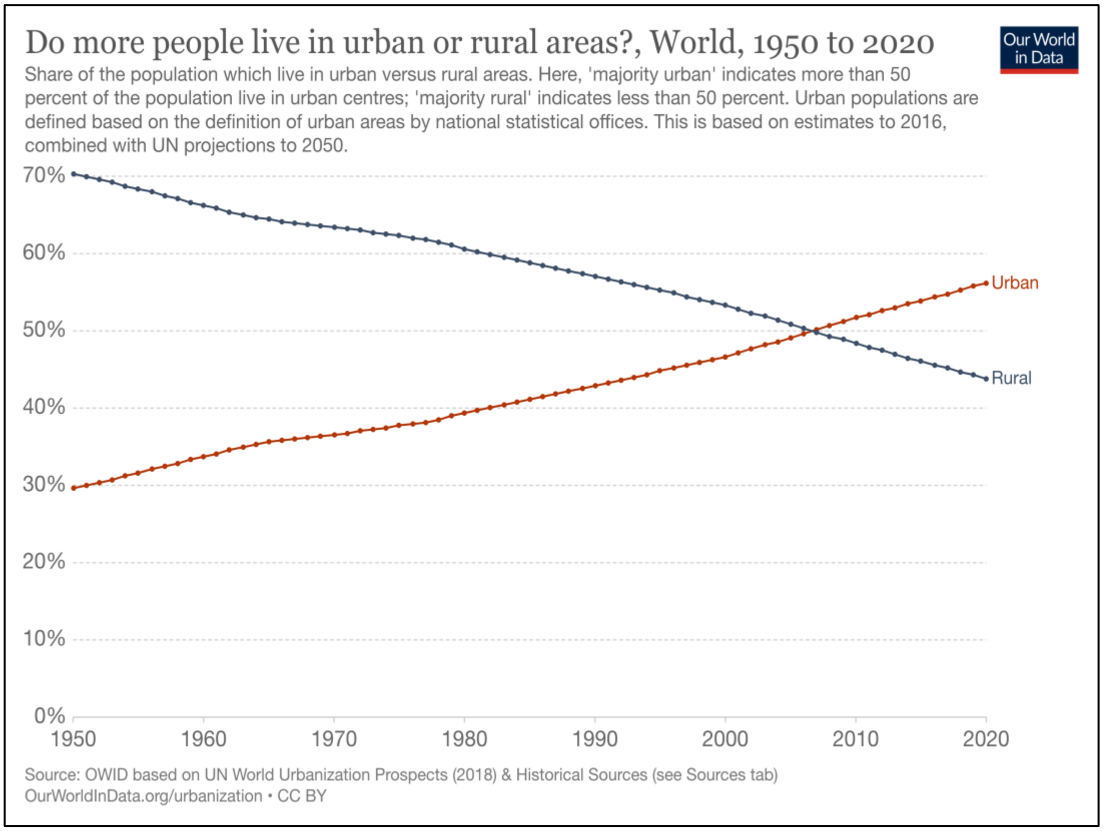

Figure 8. Change of population from urban to rural areas. Reprinted from Ritchie & Roser 2018.

By 2030, the world's population is expected to reach 8.5 billion, 9.7 billion by 2050, and 10.9 billion by 2100 (UN 2019a). A spectrum of projections was created based on 95% population prediction intervals as well (UN 2019a). As stated earlier, approximately 40% of the world population inhabits the coastal zone (Sterzel *et al.* 2020). Using the numbers listed above and the assumption that 40% of the population lives in coastal zones, a preliminary estimate shows a coastal population of 3.4 billion by 2030, 3.88 billion by 2050, and 4.36 billion by 2100 (Fig. 9). These numbers, along with Fig. 9, show a general idea of what the population would be in the coastal zone at the 40% proportion. This extreme and rapid growth in population, despite the declining rate, also has led to rapid growth in construction, built materials, and consumer goods in fragile coastal zones. The problem of meeting the increasing demands of the urban coastal population while reducing the amount of litter entering the ocean poses a wicked problem to society. Tackling this problem requires a fundamental rethinking of the design of the urban coast.

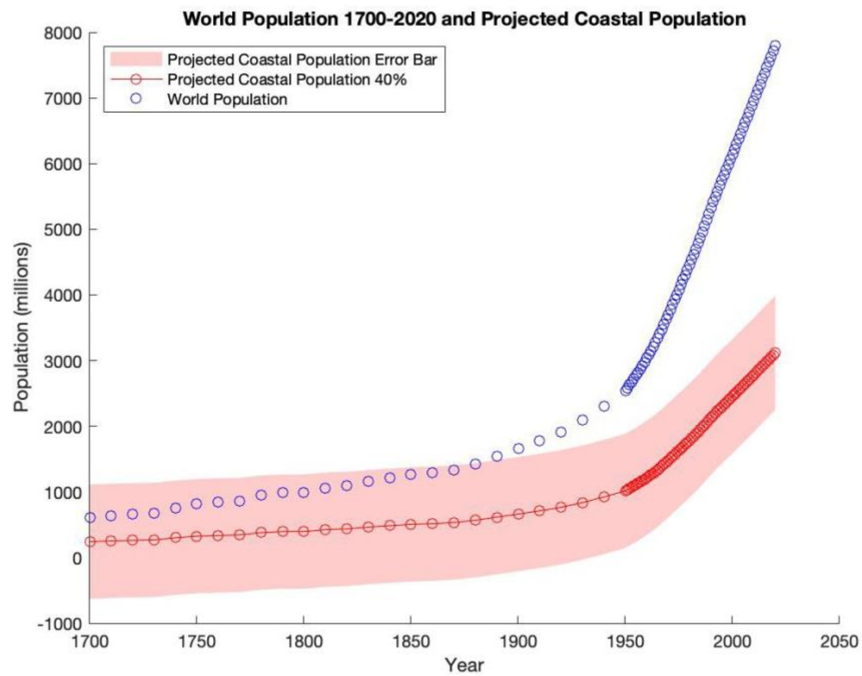

Figure 9. Average global population from 1700 - 2020 (blue dots). Represents the average coastal population with a standard deviation of 10% to show potential fluxes in the 40% number (red). Data used from the HYDE Database for years 1700 - 1940 (Goldewijk *et al.* 2017) and from UNPD for years 1950 to 2020 (UNPD 2019).

1.6 DOCUMENT STRUCTURE

Chapter 1 introduced the thesis. First, identifying the link between population and plastic production in order to define the system's approach to the urban coast. From here, the chapter identified the fragilities and hazards the coast is exposed to and introduced the concept of risk for the urban coast. Finally, Chapter 1 introduced the case studies that will be used to complete the thesis: Hurricane Dorian impacting the Bahama Islands in 2019; the tsunami impacting Japan in 2011; and SLR in Jakarta, Indonesia in present day.

Chapter 2 assesses the current knowledge available to address these questions. In order to completely evaluate the future of the urban coast, the history must be established. From here the potential futures can be researched. Chapter 2 will look at the current knowledge of the fragilities of the system, including fragilities of the urban coast and the marine system. The hazards impacting the urban coast are extensive and requires an expansive analysis of research to establish baseline information and find potential trends. The current knowledge along this topic must be fully assessed to determine the probability and the risk of hazards. Finally, Chapter 2 will analyze the current knowledge around the risk associated with PMD. The main knowledge gaps were identified, and research questions were formulated.

Chapter 3 establishes the goals of the thesis and the methodology used to complete the project. The research questions are outlined to determine what the project intends to address. The methodology explains the process of data collection, modeling, and necessary assumptions to answer the research questions.

Chapter 4 outlines the PDFs, the fragilities, and the exposed assets of the UBE for the four case study locations. The current and future PDFs are determined for relevant hazards for the case studies are established. The fragilities are determined through case study events and different scenarios. The exposed assets of plastic are estimated through coastal population estimates and plastic usage estimates. The combination of these variables allows for risk to be determined.

Chapter 5 discusses the results that were found, the issues with the methodology, and establishes a space for future work. The study is then concluded to address future research questions.

CHAPTER 2

KNOWLEDGE ASSESSMENT

The ability to assess the risk of Plastic Marine Debris (PMD) is dependent on the current knowledge. The current knowledge includes how the coastal Urban Built Environment (UBE) is evolving; what hazards the UBE is exposed to; what of those hazards could lead to Plastic Marine Debris (PMD) leaking from the UBE into the environment and the ocean. This chapter discusses the history and potential futures of the urban coast and the knowledge concerning fragilities is evaluated with the goal to identify relevant knowledge gaps. The risk equation discussed in the next section establishes the structure of the chapter. First the knowledge of the risk of Urban Marine Debris (UMD) is analyzed. From here, knowledge about the exposure of the UBE to hazards, historically and in the potential futures, must be assessed. The fragilities of the UBE establishes the weaknesses in the UBE that can be exploited by hazards. Finally, an assessment on the historic, current, and potential futures of the exposed assets of the UBE to those hazards is completed.

2.1 RISK OF URBAN MARINE DEBRIS

PMD is a hazard to the ocean that exploits the fragilities of the marine system. The risk of PMD entering the ocean system is growing with increased population and increased UBE in coastal zones. Risk is the possibility of consequences where the outcome is uncertain (Pinto & Garvey 2012). A quantitative measure to determine the risk of plastic entering the ocean from the urban coast is the product of PDF of the hazards to the UBE multiplied by the fragility of the exposed assets multiplied by the value of the exposed assets in terms of the amount of plastic in the UBE (Plag & Jules-Plag 2013). One equation used to quantitatively estimate risk related to a hazard is the Risk Eq. (1), where R is the risk relative to a hazard, P is the probability of that specific hazard to occur, F_A is the fragility of the exposed assets to that specific hazard and V_A is the value of those assets.

$$R(H) = P(H) \times F_A(H) \times V_A\,, \tag{1}$$

Some risk assessments have been conducted for the urban coast, but they are focused on specific hazards and/or specific cities (e.g., Copenhagen (Hallegatte *et al.* 2011), Shanghai City

(Sun *et al.* 2021)). Other risk assessments are from specific coasts (e.g., Mediterranean coast of Egypt (Frihy & El-Sayed 2013), Taiwan (Hsu *et al.* 2017)). A literature review conducted by Hunt & Watkiss (2011) discusses the impacts of climate change and the adaptations in cities to them. The determination of this study suggests that research is in its infancy and more research is needed to include physical and financial flows as well as a full evaluation of climate hazards. In order to assess the risk of PMD associated with the UBE, the terms of the Risk Eq. (1) have to be explored. The relevant 'natural' hazards must be identified and understood. The fragilities of the urban coast to these hazards will be assessed by case study analysis (Section 2.3). The value of the exposed assets will be estimated in terms of amount of plastic rather than in economic value (Section 2.4).

2.2 HAZARDS TO THE URBAN COAST

Hazards are events that exploit the inherent fragilities of a system to cause damage, also defined as "a source of danger" (Merriam-Webster 2020b). As discussed in Section 1.3, hazards can be identified as exogenic or endogenic to a system. The fragilities of the terrestrial system and those of the ocean system show the weaknesses that hazards can exploit and, therefore, can cause other hazards to occur. PMD originating in the urban coast poses an exogenic hazard to the marine system, and in order to better understand the risk associated with this hazard, PDFs for the hazards to the urban coast need to be developed. The knowledge available on the hazards exogenous to the urban coast is extensive. The main hazards exogenic to the urban coast include hydrometeorological and geologic hazards. These hazards include climate change and SLR as well as the impact they have on precipitation, cyclones, storm surges, tsunamis, and earthquake shaking. The resulting endogenic hazards within the urban coast include fire, explosions, sewage, air and water pollution, and PMD. Exogenic hazards to the ocean that originate in the urban coast include oil, rubber, sewage, PMD and other marine debris and are relatively new compared to the hydrogeological and geohazards, resulting in relatively limited knowledge. The previous studies about the PDF of UMD are assessed in this chapter with the goal to identify the knowledge gaps and to establish the research questions.

2.2.1 CLIMATE CHANGE AND SEA LEVEL RISE

While there are many hazards that impact the coast, the change in the risk is a result of the changing hazard spectrum due to the impacts of climate change. The International Panel on

Climate Change (IPCC) states in the 4th Assessment Report on Climate Change that the \warming of the climate is unequivocal" (IPCC, 2007). Global average annual air temperature has increased (IPCC, 2007), as of 2017, by about 1°C since 1901 (Wuebbles *et al.* 2017). Global Mean Sea Level (GMSL) has risen 17.78 cm - 20.32 cm since the beginning of the 20^{th} century, but more than half of this change has occurred in the past 25 years (Wuebbles *et al.* 2017). GMSL is important for understanding the global hazard probabilities, but when addressing local sea levels, isostatic rebound and land subsidence must be considered. Isostatic rebound is "the rise of land masses that were depressed by the huge weight of ice sheets during the last ice age" (NSIDC 2021). Land subsidence influences local sea level to varying degrees based on geologic locations. The case study locations reflect this variety.

The changing climate results in a warming climate; increasing atmospheric water vapor; SLR; heat flux in surface, atmosphere and in the ocean; ocean acidification; and shrinking sea ice and snow cover (Wuebbles *et al.* 2017; IPCC 2007). These aspects of global climate change are leading to changing hazards spectrums, and therefore, changing risk. GMSL is predicted to continue to rise; atmospheric and marine heatwaves are likely to become greater and more frequent; decreasing snowpack leading to decreasing amount ofmelt are expected to continue (Wuebbles *et al.* 2017; IPCC 2007). The magnitude of these trends resulting from global climate warming is dependent on global atmospheric greenhouse gas emissions, such as CO^2 (IPCC 2007; Wuebbles *et al.* 2017). When looking specifically at risk due to coastal cities, the hazards associated with climate change reflect those relevant to the coast. Climate change results in exogenic hazards to the UBE, particularly in low-lying coastal areas (McGranahan *et al.* 2007). Historically, civilizations have been drawn to coastal zones and floodplains, but the changing sea level changes the risk associated with these areas (McGranahan *et al.* 2007). It is important to recognize that anthropogenic climate change has resulted in exogenic hazards that can destroy the coasts. With population increasing and a growing coastal UBE, the risk of climate change is also great for the marine environment.

An important acknowledgment for the future study is that moving people out of the coastal zones is considered costly. Some studies have been conducted in order to determine the cost of climate change based on hazardous events and the ensuing damages (e.g., Frame *et al.* 2020). In New Zealand, two droughts were assessed to find that of the NZ$4.8 bn damage, NZ$800 mil of that is associated with climate change (Frame *et al.* 2020). The damages of Hurricane Harvey to find that US$67 bn of the US$90 bn costs of the damages can be associated with climate change (Frame *et al.* 2020). This is a large portion of the total costs and makes it hard to argue that it is more expensive to move out of the coastal zone, than to withstand these climate change costs. The cost of climate change is yet to be fully understood.

2.2.2 FLOODING

Flooding is a hazard exogenic to the urban coast that can be caused by precipitation, storm surges, and tsunamis. River flooding occurs when the outflow of the river is less than the inflow (Leopold 1994) and can be caused by increased precipitation in the upstream watershed, as well as increased inflow from tributaries such as from melt water or anthropogenic infrastructure damage. Precipitation is expected to increase in frequency (Tabari 2020). Water availability, atmospheric circulation (Tabari 2020), and thermodynamics (Pfahl *et al.* 2017) are critical variables in the concentration of atmospheric water vapor. Temperature increase is thought to increase atmospheric water vapor by approximately 7% per °C temperature rise (Skliris *et al.* 2016), resulting in extreme precipitation events. This does not mean that more rain will occur globally, but depending on the region, extreme precipitation events are more likely to occur (Tabari 2020). Increases in extreme precipitation can be associated with increasing flood events. When addressing coastal zones, flooding from rain events is coupled with flooding from the ocean, called compound flooding (Bevacqua *et al.* 2019). Compound flooding is particularly dangerous to the coast zones and has been for tens of thousands of years. With extreme precipitation events increasing and GMSL rising (IPCC 2007), compound flooding poses a greater risk. This, with the increasing UBE in coastal areas (Neumann *et al.* 2015), creates a potentially extreme risk for both the coastal zone and the marine environment. The probability of compound flooding along European coasts based on meteorological drivers of flooding is predicted to increase along some coasts and not along others (Bevacqua *et al.* 2019).

2.2.3 CYCLONE BEHAVIOR

Cyclones and non-tropical storms are prominent threats to coastal zones between 5°N to 50°N and 5°S to 50°S (Emanuel 2003). Cyclones cause hazards of wind stress, increased precipitation, and storm surge when interacting with the coastal zone. Cyclones can be potentially damaging to the UBE. The potential changes in frequency and/or intensity of a cyclone and the potential change in the storm surge itself is critical. The possible futures of hurricanes have been studied extensively and is still partially debated (e.g., Webster *et al.* 2005; Kishtawal *et al.* 2012; Marsooli *et al.* 2019). In 2005, no trend was found to be associated with sea surface temperature (SST) and the number of cyclones, however, when assessing cyclone intensity there was an increasing trend in the North Atlantic (Webster *et al.* 2005). The intensity of tropical cyclones is increasing with climate changes (e.g., Holland & Bruyère 2014; Kishtawal *et al.* 2012; Marsooli *et al.* 2019) while the frequency change is still debated (Holland & Bruyère 2014; Marsooli *et al.* 2019). The changes in the proportion of intense hurricanes relative to the total number of hurricanes through the Anthropogenic Climate Change Index (ACCI) between 1975 and 2010 resulted in no global trend as a whole with increasing ACCI but noted an upward trend in intense hurricanes (Holland & Bruyère 2014). The ACCI is the difference between climate models with and without anthropogenic forcings (Holland & Bruyère 2014). Holland & Bruyère (2014) used, on all variance, a 5-year smoothed annual time series to remove the El Niño Southern Oscillation (ENSO) variability. The proportion of intense cyclones have been increasing compared to the total number of cyclones and will continue to increase with warming ocean waters (Holland & Bruyère 2014). The results also show that the number of hurricanes is increasing in the Atlantic Ocean and maintain an upward trend in the Hurricane Category 4 (HC4) and Hurricane Category 5 (HC5) proportions (Holland & Bruyère 2014; Kishtawal *et al.* 2012). Changes in tropical cyclone intensification for major ocean basins using satellite data observations from 1986-2010 resulted in statistically significant evidence of changing intensification of tropical cyclones rather than a changing amount of tropical cyclone occurrence (Kishtawal *et al.* 2012). The global average amount of time for a tropical cyclone to mature was reduced by about 9 hours (Kishtawal *et al.* 2012).

In the Atlantic Ocean, specifically along the US eastern coast, increasing flood levels induced by tropical cyclones suggest that frequencies, intensities, and sizes of the storms could increase by 2100 (Marsooli *et al.* 2019). Simulated models show tropical cyclone frequency and intensity is larger in South-Eastern US and in the Gulf of Mexico than in the Mid-Atlantic and North-Eastern regions (Marsooli *et al.* 2019). There is also an increase in the number of slow-moving tropical cyclones which leads to increased wind and, therefore, increased size and length of coastal flooding. It has been established that the intensities of the cyclones are increasing with climate change (e.g., Marsooli *et al.* 2019), the change in number of cyclones is still being determined. Another important factor to coastal zones and the UBE in terms of cyclones is the resulting storm surge and precipitation events.

2.2.4 STORM SURGE

A storm surge is defined by the National Oceanic Atmospheric Administration (NOAA) National Hurricane Center (NHC) as “an abnormal rise of water generated by a storm, over and above the predicted astronomical tide” (NHC 2021a). When assessing the risk of storm surge flooding, the impact of climate change on the hazards that influence storm surges is critical. Typically, these surges are caused by cyclones and non-tropical storms, while some surges can result from other weather front types resulting in low pressure zones (NHC 2021a). While the potential change in cyclone behavior is one component in the risk of storm surge floods, another is the potential change in storm surges resulting from the cyclone. Storm surges are a major threat to coastal UBEs. The rapid inundation not only destroys parts of the UBE, if not all of it, but also creates a rapidly accessible flow for debris to go into the ocean systems. Storm surges arise from the atmospheric forcings on the body of water, which then generates oscillating waves with varying periods (WMO 2011). The PDF of storm surges with a rising ocean temperature is vital to studying the impact of natural hazards on coastal zones. Storm surges, or meteorological tides, are major components of extreme water levels in coastal areas (Vousdoukas *et al.* 2016). During a time of global warming, conditions that are important for cyclone generation include SST and vertical wind shear (Grinsted *et al.* 2013). Increased temperature is favorable for cyclone behavior, while increased vertical wind shear is not favorable (Grinsted *et al.* 2013).

2.2.5 TSUNAMI WAVES

Tsunami waves are formed by a sudden displacement in the water column (NOAA 2021a). Tsunamis have been defined as affected by refraction and diffraction, gravity waves due to the manner in which tsunami waves are formed; long wave phenomena with wavelength ranging from 100 – 150 km; and shallow water waves due to the wavelength far exceeding the water column depth (Röbke &Vött 2017). These sudden events are caused by a number of geologic processes including earthquakes, volcanic eruptions, submarine landslides, subaerial landslides, and rockfalls. Seismic activity, such as earthquakes, cause approximately 82% the majority of tsunamis (Röbke &Vött 2017). Gravitational Mass Wastings account for about 9%, volcanism accounts for nearly 5%, and the rest are a result of atmospheric disturbances, meteorite impacts, and other causes (Röbke &Vött 2017). Tsunamis are, mainly, due to geologic occurrences not influenced by atmospheric changes, such as climate change. Therefore, climate change has a minor impact on the occurrence of tsunamis. Climate change will exacerbate tsunami impacts due to SLR. As these events occur rapidly, preparedness efforts are crucial to human safety and to ocean safety.

2.2.6 EARTHQUAKE SHAKING

Earthquakes are a result of Earth's crust suddenly releasing stored energy to create seismic waves (British Geological Survey 2021). Natural processes that cause earthquakes include tectonic stress changes, crustal fluid dynamics, tides, surface ice and snow loading, heavy precipitation, atmospheric pressure changes, and sediment unloading (Kundu *et al.* 2015). All of these causes explain how changes in rock stress occurs and ultimately result in rock failure, allowing for the energy release. Human-induced earthquakes has become a point of major research recently. Total industrial project induced seismically are severely under-reported, however, pore pressure in fault zones greatly influences seismicity, concluding that groundwater extraction influences earthquakes (Foulger *et al.* 2018). While earthquakes are, mostly, caused by tectonic changes, there are other influences that causes changes in stress enough for seismic activity. A number of studies suggest that earthquakes were induced by changes in weather, such as heavy rainfall and pressure changes from typhoons. Some earthquakes in Taiwan have been known to be triggered by typhoons and the extent of atmospheric pressure-based earthquakes in one of the most active plate boundaries is under determination (Liu *et al.* 2009). The study identifies strain data with a negative strain that occur during a typhoon and no strain events in the typhoon-free months, the first four months of the year. In order for triggering to be consistent with only some typhoons and earthquakes to also occur without a typhoon, the fault in question must be critically close to failure (Liu *et al.* 2009).

While cyclones impact on slip faults is still not made clear, mass fluctuations on Earth's surface are linked to seismic activity. Post-glacial seismicity increase can be explained by changes in volume of ice or lakes (Hampel *et al.* 2010). Two- and three-dimensional numeric models of the crust were created with faults embedded and then simulated pressure representing ice or water volume, resulting in fault slips that accelerated during unloading and rebound compared to the low-level of seismicity when the load is present (Hampel *et al.* 2010). While earthquakes are a geologic phenomenon caused by changes in rock stress, variability in pressures above the crust play a key role in these stressors. Climate change has no bearing on the geology or tectonic activity of the Earth, but the retreatment of ice and rebound do impact the seismicity. This increases the potential of the exogenic hazard of earthquake shaking and potential for tsunamis, resulting in an increased potential of litter and pollution to become MD.

Earthquakes and volcanic eruptions are geologic hazards not impacted by atmospheric changes directly. The indirect effect of melting icesheets has the potential to change pressure conditions within the earth's magmatic system resulting in potential change in volcanic activity (Sigmundsson *et al.* 2010). A loss of 1 m of ice, with an average density correlates with a 9 kpa normal stress change on the surface of the earth (Sigmundsson *et al.* 2010). This is one order of magnitude smaller than the stress variation of 1 bar (100 Pa) often referred to in earthquake triggering studies. Changes in the stress leads to changes in the earthquakes (Sigmundsson *et al.* 2010).

2.3 FRAGILITIES

Fragilities are inherent properties of a system that can be exploited by the hazards described in Section 2.2. The high-level conceptual model, the fragilities of the system, and the relevant hazards that exploit the fragilities are identified in Fig. 10. The important fragility in this system to estimate the risk associated with PMD from the UBE is the destruction of the UBE. Exploitation of this fragility allows for the plastic in the urban coast to flow into the marine environment. Inundation is another fragility that must be explored to estimate the risk. An inundated urban area creates a new flow path for the destroyed UBE to move from the UBE to the ocean.

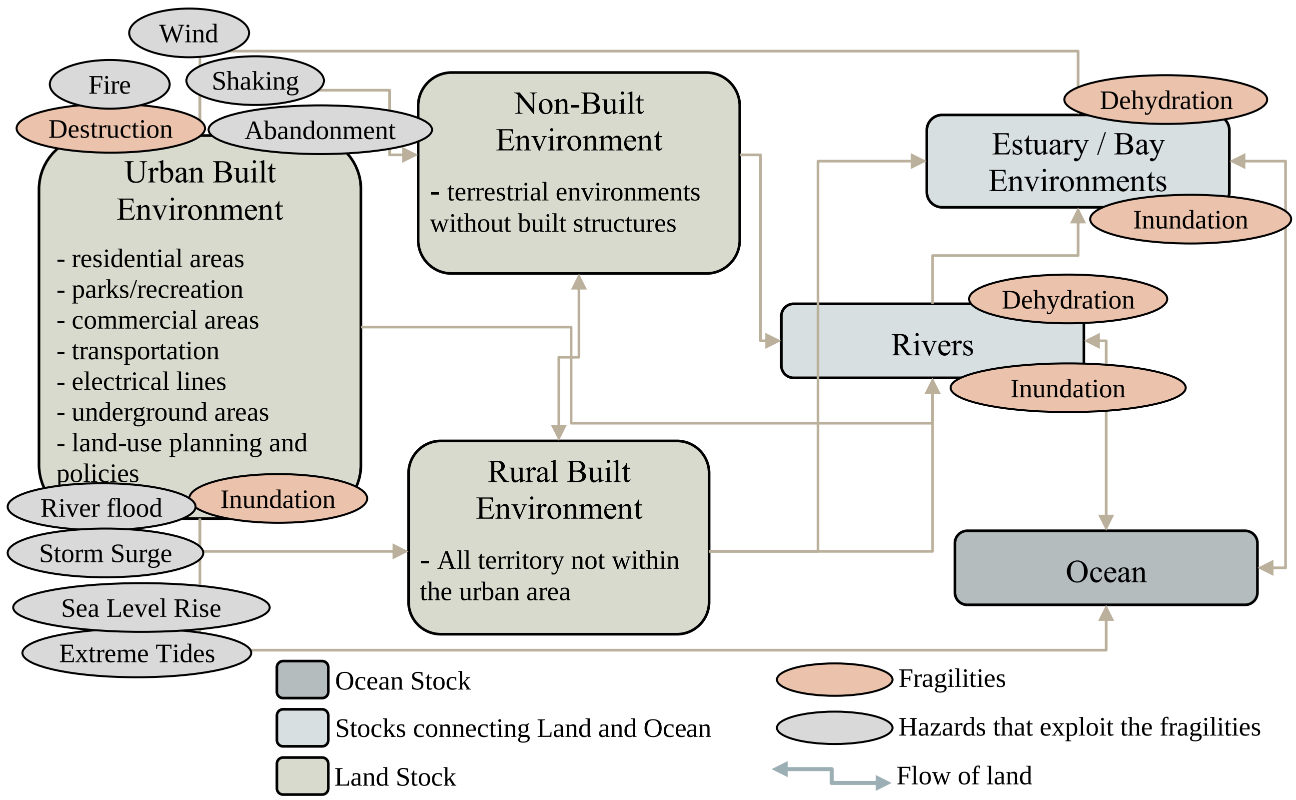

Figure 10. A conceptual model of the urban coastal built environment system, the inherent fragilities, and the relevant hazards that can exploit them.

2.3.1 FRAGILITIES OF THE TERRESTRIAL URBAN COAST

The terrestrial UBE contains many sources of plastic. This includes homes and residential buildings; schools, hospitals, and workplaces; parks, recreational areas, and greenways; business areas and transportation systems; electric transmission line; underground infrastructure such as waste disposal sites and subway systems. Plastic is also in the materials and items that are within these areas, such as toys and home goods, office materials, and other materials. The UBE is fragile to building and infrastructure destruction, deterioration from erosion and economic loss preventing upkeep, changes in rules and regulations for businesses and health, changes in human population, among others. The focus of this project is on the UBE and human population that leads to increased exogenic hazards to the ocean systems. The fragilities of the UBE lead to the risk of the exogenic hazards to the ocean.

TOHOKU EARTHQUAKE AND TSUNAMI IN JAPAN, 2011

Japan is an island nation located off the eastern coast of the Eurasian continent between approximately 20°N and 45°N and 123°E to 154°E (USGS 2021). The Japanese Island Arcs are formed from the collision of the Pacific Plate which subducts under the North American Plate (USGS 2021). This collision results in large amounts of stress along the fault line. When the stress is released, the seismic energy is released and results in an earthquake (USGS 2021). Japan is an island archipelago that resides above this subduction zone and therefore, is frequently prone to earthquakes (MIAC 2020) on land and originating in the ocean. Earthquakes that occur beneath the ocean floor can result in tsunami waves from the displacement of water (NOAA 2021a). Historically, the earthquake hazard is not new to the people living there and neither is the threat of a tsunami. On March 11th, 2011, on earthquake occurred off the coast of Tohoku, Japan in the Pacific Ocean resulting in a massive tsunami to impact eastern Japan (Mimura *et al.* 2011). The magnitude 9.0 Great East Japan Earthquake occurred at 2:46PM JST had an epicenter at 38°N and 142.9°E with an estimated depth of 24 km (Mimura *et al.* 2011). Shortly after the earthquake, the first tsunami wave hit the east coast of Japan. The highest waves reached the coastline roughly 30 minutes later between 3:15PM and 3:20PM JST (Norio *et al.* 2011). Many tidal stations record high levels around 8 m before being destroyed, except for the Onagawa which recorded a wave height around 13 m above mean sea surface elevation at 3:30PM JST (Norio *et al.* 2011). Eyewitness accounts and damage to the UBE result in wave height estimates to be closer to 24 m – 36 m (Norio *et al.* 2011). Japan is located along a fault line that regularly produces earthquakes and tsunamis, but the coastal UBE and urban population in Japan has expanded exponentially. This results in a change in the future potential risk due to the changing exposure.

HURRICANE DORIAN LANDFALL IN THE BAHAMA ISLANDS, 2019

The Commonwealth of the Bahamas historically has been at risk of cyclone landfall (Neely & Read 2019). Hurricane Dorian was the strongest recorded hurricane to hit the Bahamas Islands in modern history (Avila *et al.* 2020). Dorian was marked as a Tropical Storm (TS) on August 24th, 2019 and reached the windward islands on August 27th as a compact cyclone, building to a 65 kt hurricane when moving over St. Croix in the US Virgin Islands (Avila *et al.* 2020). Rapidly intensifying to a HC5 on the Saffr-Simpson Hurricane Wind Scale, Dorian made land on Great Abaco Island in the Bahamas on September 1st with estimated winds of 160 kt and minimum central pressure of 910 mb (Avila *et al.* 2020). Landfall caused the storm to slow allowing for the storm to remain over Great Abaco Island with at least tropical-storm-force wind for many hours, causing immense destruction. Slowly moving toward Grand Bahama Island, the eye made landfall on September 2nd and moved off the island 6 hours later towards the east coast of the US (Avila *et al.* 2020).The storm moved north- northwest until finally dissipating September 9th off the coast of Nova Scotia, Canada. The storm surge prediction given on August 30th noted that the surge could be up to 3 m – 4.5 m above normal tide levels (Avila *et al.* 2020). A tide gauge on the western top of Grand Bahama Island measures a water level of 1.9 m about Mean Highest High Water (MHHW) suggesting that the surge levels were 1.8 m – 2.1 m above ground level on the island (Avila *et al.* 2020). Eyewitness accounts state that inundation was closer to 6.1 m (Avila *et al.* 2020). The slow but intense movement of the storm over the Bahamas coupled with a massive storm surge resulted in catastrophic damages to the UBE. The intense winds and the huge storm surges resulted in more than 75% of the homes and buildings on Great Abaco and Grand Bahamas Island to be damaged (Avila *et al.* 2020). The future potential risk of PMD is expected to change with changing hazard PDF and changing exposure.

FLOODING IN JAKARTA, INDONESIA PRESENT DAY

The Republic of Indonesia is an island nation located in Southeast Asia and Oceania between the Pacific and Indian Oceans. Indonesia contains approximately 17,500 islands, 7,000 of which are uninhabited (Britannica 2021). The island archipelago is created from the complex tectonic zone which has resulted in seismicity, volcanic activity, collision, and uplift (Hall 2014). Jakarta is the largest city and the capital of Indonesia and is located on the northwest coast of Java Island (Hall 2014). To the south of the Jakarta province there are mountains that have rivers flowing north to a delta, which has been developed to become the city of Jakarta, containing 13 rivers (Yamazaki *et al.* 2021).

Jakarta has a population of 10.2 million people, as of 2013, within about 660 km^2. There are 13 rivers flowing through the city, forming the main drainage system, and also causing many riverine and coastal flooding events, historically (Abidin *et al.* 2015). Another major physical driver causing the flooding events is land subsidence. Land subsidence is ranging from a rate of 1 cm - 15 cm per year in different locations of the city (Budiyono *et al.* 2016) due to excessive groundwater extraction, natural soil consolidation, infrastructure loads, and tectonic activities

(Abidin *et al.* 2015). Jakarta is an actively hazardous location due to the historical river flooding coupled with land subsidence. This is an extremely important case to follow because of the retreat plans of the city. The risk of PMD entering the ocean from the UBE is dependent on these retreat plans.

2.3.2 FRAGILITIES OF THE MARINE SYSTEM

The fragilities of the marine system are described to understand the potential impact of the plastic in the marine biosphere. However, the impact is not addressed in this thesis and therefore, the fragilities of the marine system are not quantified. The ocean system includes subsystems of chemical, biological, geological, and physical systems. These are all systems of their own but are also interconnected and cannot be separated from one another. Each ocean system contains different stocks and flows, and therefore, has its own inherent fragilities. A key component of this project is to analyze the flow of PMD from the coast into the ocean during a time of SLR and climate change. The most prevalent fragilities of the marine biosphere, or biological ocean subsystem include temperature changes, pressure changes, salinity changes, changes in the food source, and changes in marine habitats. The physical ocean system is fragile to temperature changes and salinity changes. The chemical ocean subsystem is fragile to changes in chemical flows, changes in biological and physical mixing, changes in available elements. Finally, the geological ocean subsystem does not contain any fragilities relevant to PMD or climate change but is an important sink of the high-level system. Conceptually understanding the marine system fragilities helps in understanding the need for the risk of PMD entering the ocean from the coastal UBE.

2.4 VALUE OF THE EXPOSED ASSETS IN THE URBAN COAST

The final variable in the Risk Eq. (1) is the amount of the exposed assets to hazards. The exposed assets here refer to the amount of plastic material in the UBE. The urban coast is expanding. More people are moving into coastal zones causing varying degrees of urban sprawl and for the built environment to increase. Historically, population was fewer; a lower percentage of people lived in the coastal zone; and the exposed assets in the UBE in the coast was less dense. The lack of technology and materials to move massive amounts of sediments and create barriers did not allow for a highly populated urban coast. However, coastal living is not a new phenomenon.

During the Holocene, sea levels steadied, and the period became known as a safe-operating space for humanity (Rockstrom *et al.* 2009). People began to settle due to the steadied sea level, either living inland for farming and agriculture or living in the coastal zones for transportation and seafood sources. However, the amount of people was fewer (Roser *et al.* 2013) and the materials used were natural (i.e., wood, stone). Population has increased greatly, causing the boundaries identified by Rockstrom *et al.* (2009) for the safe-operating space for humanity to be potentially surpassed. Along with the population increase, more people have moved to coastal zones and are using building materials potentially harmful to marine systems. Sea levels were still relatively stable, so the risk of these harmful materials entering the environment was less. People who live in coastal zones are equipped for the historically stable tidal ranges and sea level changes that have shown for many generations. However, what they are not equipped for is the change in these rates or exposures, such as those caused by climate change creating a new risk to societies.

2.4.1 THE URBAN MARINE DEBRIS – PROBABILITY DENSITY FUNCTION

The UMD – PDF is the scientific knowledge needed to address the wicked problem of a growing UBE and growing risk of PMD. The knowledge available regarding this function includes information about city archetypes, spatial configurations, and the changing risk perception that assist in defining the UBE and resulting potential for PMD. Six archetypes of low-lying urban and rural coastal areas include open and urbanized coasts with beach and/or sand dunes; open rural coasts; urban deltas; rural deltas; urban estuaries; rural estuaries (Haasnoot *et al.* 2019). Open areas refer to a coast with sediment but without river mouths, delta areas refer to a deltaic coast with wetlands, and an estuary refers to an estuarine coast with wetlands. An urban area was defined as densely populated and containing costly building stock and/or tourist attractions, while rural was defined as predominantly agricultural and containing few dwellings and low populations, noting that purely natural coastlines were not considered (Haasnoot *et al.* 2019). It is also important to include not only low-lying areas, but also elevated areas and acknowledge the structural differences between cities.

Another way to group cities is those that consist of similar spatial configurations. Cities with cumulative populations proportional to the city populations on a continental level for land-use and land-cover descriptions allowed for 17 Low Climate Zones (LCZ) to avoid cultural bias (Table 1; Taubenböck *et al.* 2020). 7 Clusters of cities correlating the LCZ with geographical cultural spaces resulted from the initial 17 LCZ (Taubenböck *et al.* 2020). Coupling these clusters with the 3 archetypes determined by Haasnoot *et al.* (2019) will give this project the archetypes for urban coastal systems. These then will be used to analyze and develop the UMD – PDF. Coastal urban areas are not uniform globally. The topography, building structure, economic activities, and infrastructure change the fragilities of the system and must be evaluated as a part of this thesis. However, another important factor in the hazard of climate change, apart from physical hazards, is the risk perception associated with it.

Table 1. City Structure Types "Local Climate Zones commonly names "LCZ XX" (XX from 1-Compact High-rise to G-Water). LCZs from 1-9 correspond to urban climate zones defined by Oke (2004)." (Taubenböck *et al.* 2020).

Built Types	Non-Built Types
LCZ – 1 Compact high-rise	LCZ – A Dense trees
LCZ – 2 Compact midrise	LCZ – B Scattered trees
LCZ – 3 Compact low-rise	LCZ – C Bush, scrubs
LCZ – 4 Open high-rise	LCZ – D Low plants
LCZ – 5 Open midrise	LCZ – E Bare rock or paved
LCZ – 6 Open low-rise	LCZ – F Bare soil or sand
LCZ – 7 Lightweight low-rise	LCZ – G Water
LCZ – 8 Large low-rise	
LCZ – 9 Sparsely built	
LCZ – 10 Heavy industry	

2.4.2 HISTORICAL EXPOSURE OF THE URBAN COAST

This is not the first time humans have faced environmental risks from the coast. Major flooding and storms are noted globally throughout history, such as on the Dutch Coast and the German Coast (Wikipedia 2020a). During the 18th century, there have been several historic floods along the coast of the Netherlands (Wikipedia 2020b). Two of the largest storm surge flood events during this time occurred in 1717 and 1775 (Baart *et al.* 2011). In 1717, a "Christmas flood" took place due to a cyclone that lasted from December 24th to December 27th, bringing severe rain and hail, as well as major flooding in the northern part of the Netherlands, Germany, and Denmark where 10,000 victims were reported (Baart *et al.* 2011). In November of 1775, the largest storm surge of the 18th century took place. Noting by a description in Baart *et al.* (2011), the surge was higher than every flood before it. The description also noted that the coast after the event consisted of many shipwrecks and bodies. The Dutch population in the 18th century grew from around 1.905 million to 2.08 million (Paping 2014). In 2020, this population is 17.16 million (UN 2019c) with a much greater UBE along the coast. Surges the magnitude describe from 1717 and 1775 would cause more damage and disaster than they did then, which was noted to be extreme.

Along the German coast, many notable storm surge floods have been acknowledged in both the North Sea and the Baltic Sea for over a thousand years (Wikipedia 2020c). In 340 B.C., a storm surge along the North Sea coastline caused the settlers to move out of the area (Jensen & Muller-Navarra 2008). It is not said in this article how many deaths, but the population in 340 B.C. was a small fraction of what it is today. Extreme surges from the North Sea took place from this point until today, noting how much of the coast became flooded, but not the height of this until the 1900s. In 1953, 1962, and 1976, extreme surges were believed to be a result of wind surges due to North - Northwest gale-force winds (Jensen & Muller-Navarra 2008). In the Baltic Sea, these winds are in the East - Northeast direction and are referred to as Seiches which have accounted for many surge floods that reached between 2 m and 3 m in height (Jensen & Muller-Navarra 2008). Looking back to the population in 1950 in Germany, which was around 70 million people poses less risk than in 2019, which was 84 million (UN 2019b). A 3 m surge today has larger consequences than even 70 years ago. The purpose of revisiting past coastal flooding events is to note that coast flooding is not a new hazard. The risk has been changing due to increased population, increased coastal migration, and increased toxic materials in the coastal zone, coupled with a changing climate. The increased population increases human risk to exogenic hazards, but also increases the risk of marine debris entering the ocean system.

2.4.3 POTENTIAL FUTURES OF THE URBAN COAST

The future predictions show population growths to slow (Fig. 6; Roser *et al.* 2013) but the increasing coastal migration to continue to rise (Neumann *et al.* 2015; Crossett *et al.* 2020). Plastic production has been increasing exponentially since 1950 and is expected to continue as well (Fig. 11; Geyer *et al.* 2017a). With population globally increasing, population in coastal zone increase, and a probable future of increased plastic production, the UBE is expected to become a stronger risk to marine debris. SLR and climate change pose an increasing threat to the coastal zones, including the UBE. The hazards lead to a flow of plastic and other materials from the UBE, which is growing, into the natural terrestrial environment to river systems and estuary systems to terminate in the ocean.

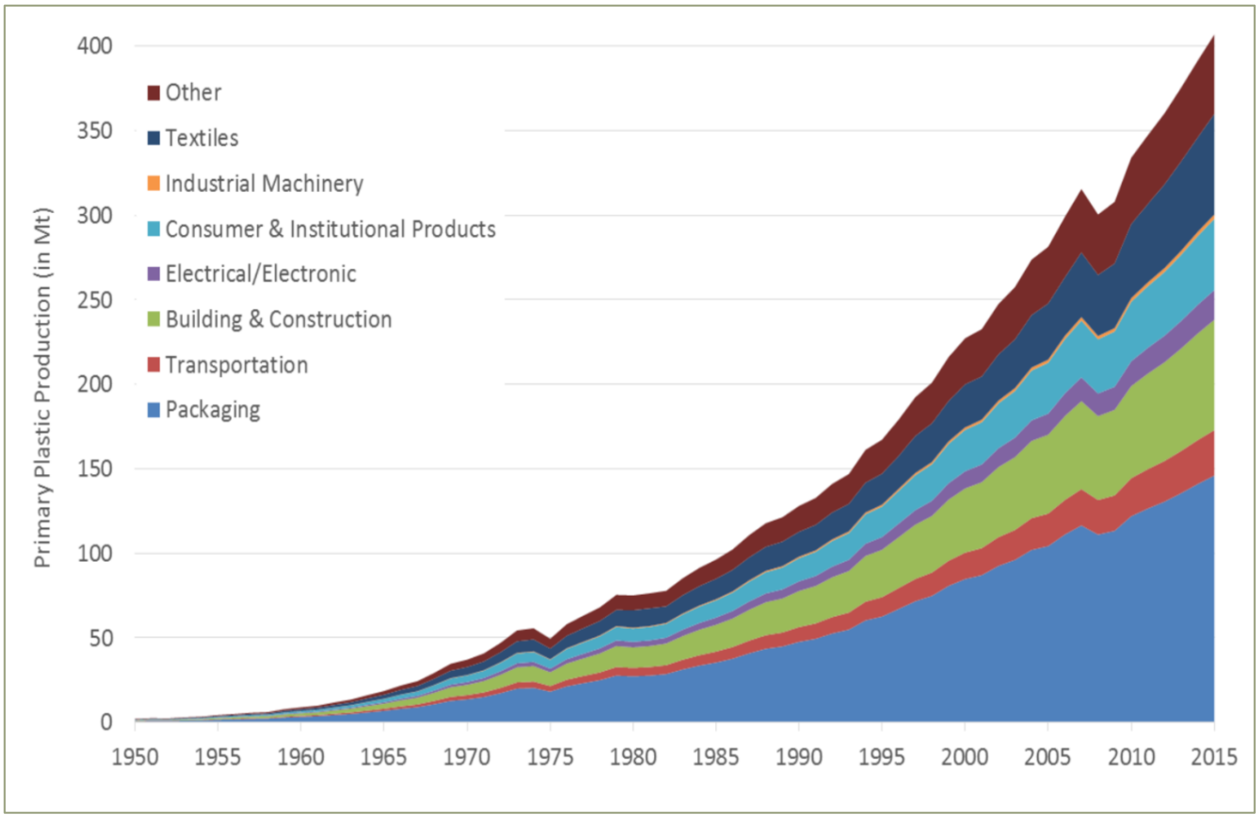

Figure 11. Global primary plastics production (in million metric tons) according to industrial use sector from 1950 to 2015. Reprinted from Geyer *et al.* 2017b.

2.5 RESEARCH QUESTIONS

The assessment of the existing knowledge shows that coastal zone is historically impacted by hazards such as tsunamis, cyclones, and storm surges. Climate change and SLR are changing the spectrum of hazards, increasing the intensity of cyclones, and increasing the extreme precipitation events. However, the specific changes are location specific in severity. The knowledge assessment has resulted in the clear understanding that: Increasing population and increasing coastal migration has expanded the coastal urban built environments; Plastic is an important and widely used material in the UBE; and climate change is a present and future major threat to coastal areas.

While the hazards to the urban coasts including climate change and SLR are widely studied, research pertaining to the plastic available to become marine debris is lacking. Assessing the risk of MD leaking out of the urban coast into the ocean provides valuable knowledge to guide the future development of the urban coast. As pointed out in Section 1.1, this risk depends on the past and future development of the urban coast (exposure), the design of the urban coast (fragilities), and the development of the hazards the urban coast is exposed to. In order to assess the risk, the following research questions will be addressed:

1. How is the UBE expected to evolve in the 21st century in terms of size and materials used?

   The urban coast is expanding due to population growth and the desire to live near the coastal zone. The materials used to manage the urban growth are harmful to the ocean and marine systems. This changing material and population expansion changes the risk of MD.

2. What are the fragilities of the urban coast that could lead to marine debris?

   The urban coast is made up of a variety of materials that have inherent fragilities. The exploitation of these fragilities leads to hazards that can cause a lot of damage to the ocean system, particularly the marine bio-chemosphere. Establishing the fragilities of the UBE allows for an accurate depiction of risk of exogenic hazards exploiting these fragilities.

3. What are the PDFs of the hazards the urban coast is exposed and how will these PDF change during the 21st century?

   After identifying the fragilities of the UBE, the hazards that exploit these fragilities can be determined. Assessing the hazard spectrum and determining the potential change in the hazards associated with exploiting the fragilities of the urban coast. How the hazards change the UBE can lead to the hazard of marine debris entering the ocean systems.

Answering these questions will then allow for a quantitative assessment of the risk of MD originating in the urban coast.

CHAPTER 3

METHODOLOGY

The methodology for this thesis was determined by the variables described by the Risk Eq. (1). Fig. 12 shows the structure of the methodology used to complete this assessment. Currently, the risk associated with growing coastal urban areas and the flow of Plastic Marine Debris (PMD) to the ocean is unknown. The goal of this thesis is to provide a conservative estimate of the risk. The risk assessment and the modeling provide the detailed data necessary to fulfill the equation. The Risk Eq. (1) requires an assessment of the hazards to the Urban Built Environment (UBE), the fragilities of the UBE to those hazards, and the amount of the exposed assets.

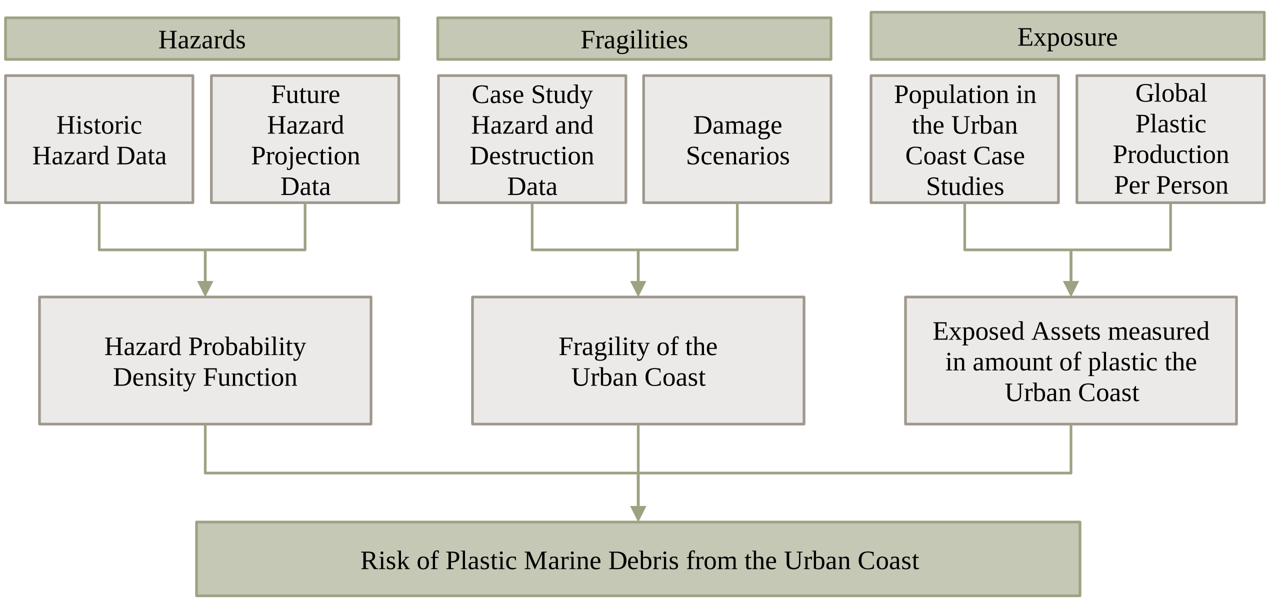

Figure 12. The methodology to assess the risk of PMD originating in the UBE.

This required data is outlined in Fig. 12. The hazard data required for the model is freely available for collection based on previous studies that have hazard change projections and probabilities. The data is used alongside a model to find an estimation of the amount of plastic in the coastal zones. The methodology for collecting the hazard probability is discussed in Section 3.1.

The fragilities of the UBE must also be established. This data is collected through analysis of the three case studies, through event analysis. Each case study is a specific location with a specific disaster resulting from a specific hazardous event. The fragilities, while inherent to the UBE system, are quantified because they were exploited during the specific hazardous event. The methodology to identify each case study's fragilities is discussed further in Section 3.2.

To determine the value of the exposed assets, the initial methodology includes a detailed model describing the amount of plastic in the UBE. The model was intended to be detailed, establishing the plastic stocks in the UBE such as: buildings, consumer goods, and the plastic used for the processes of construction and demolition. The result of tedious research did not allow for this detailed of a model as described in Section 3.3. Therefore, a generalized estimation was created using plastic production and population, detailed in Section 3.3 and the results established in Chapter 4. Finally, risk of Urban Marine Debris (UMD) is quantified by utilizing the Risk Eq. (1), discussed in Section 3.4.

3.1 HAZARD PROBABILITY DENSITY FUNCTION

The hazard PDFs associated with the case studies are critical to understand the potential risk of PMD created from the coastal UBE. The hazardous events associated with the case studies must be assessed in order to understand the PDFs. Historical data is collected and assessed for size, impact, and for future projected changes to the hazard spectrum. The PDF must be created based on type of hazard, discrete or continuous. The discrete events include event-based hazards such as cyclones, tsunamis, and flooding. The PDFs for these hazards are determined using the Poisson Probability Distribution Eq. (2), where P is the probability of $x = k$ event to happen in a given time interval (e.g., 100 years), and μ is the average number of events to happen in such a time interval.

$$P(x = k, \mu) = \frac{\mu^k}{e^{\mu} \times k!} \quad , \tag{2}$$

To determine μ for each hazard, the recurrence time first needed to be determined, Eq. (3). The recurrence time is equal to the number of events N divided by the number of years n over which the events took place.

$$R = \frac{N}{n} \quad , \tag{3}$$

The data collection was conducted to establish the recurrence times of these events, sorted by size, for each hazard. To calculate μ, Eq. (4) was used, where R is multiplied by desired time span (t). Each case study uses μ found from Eq. 3.3 in the Poisson Eq. to determine the PDF for 2050, 2100, and 2220.

$$P(x = k, \mu) = R \times t \quad , \tag{4}$$

The PDFs based on past data are necessary to understand the current risk. Further data collection was completed to find probable future changes in the hazard spectrum. These changes are then applied to the current PDF of SLR in the 21st century was based on published estimates. While the to understand the future PDF and, therefore, future risk of PMD. The PDF of land subsidence is not used because the subsidence is ongoing, so the probability of occurrence is 1.

3.2 FRAGILITIES OF THE URBAN COAST

To identify the fragilities of the urban coast, three case studies are carried out. A conceptual model (Fig. 2) was created to show the urban coast and the fragilities for each coast to relevant hazards, discussed in Section 2.1. In each case study, the UBE is fragile to being destroyed but the degree of destruction varies by the hazard that exploited it. The fragilities for 2 of the case studies are determined analysis of destruction created by a specific hazardous event. There is minimal data regarding the amount of material that entered the ocean, but the data regarding the destruction can be used in scenarios to understand the potential PMD.

3.2.1 TOHOKU EARTHQUAKE AND TSUNAMI IN JAPAN, 2011

To understand the fragilities in Japan, the 2011 Great Eastern Tsunami, also known as the Tohoku tsunami, is analyzed for damages. Approximately 5 million tons of debris created from Tohoku tsunami, March 2011 and 70% of that sank nearshore, while 30% was high wind items such as foam and plastics (NOAA 2014). The assumption was made that 30% of the debris created by the tsunami was PMD. Establishing the portion of the total coastal UBE that was turned to PMD allows for a scenario-based approach to be used to estimate damage from other size tsunamis. The results are described in Section 4.2.2.

3.2.2 HURRICANE DORIAN LANDFALL THE BAHAMA ISLANDS, 2019

Hurricane Category 5 (HC5) Dorian greatly impacted the Bahamian islands and is known for major destruction on Great Abaco and Grand Bahama Islands. The destruction data used to estimate the fragilities of this area is taken from a NOAA report (Avila *et al.* 2020). Understanding the amount of the UBE destroyed in a HC5, such as Hurricane Dorian, can be used in scenarios to understand the potential damage for a Hurricane Category 4 (HC4), Hurricane Category 3 (HC3), Hurricane Category 2 (HC2), Hurricane Category 1 (HC1), and a Tropical Storm (TS). This relationship between storm category and damage is poorly understood. While there it is clear that as storm category increases, amount of damage increases (NHC 2021b), the specific proportion of damage compared to another category is not clear. This is dependent on the preparedness of the landfall area. The Bahamas is prepared for small storms but is clearly not prepared for the larger ones. The fragilities create scenarios for the amount of damage created from storms based on the amount created during Hurricane Dorian. Then scenarios are created to determine how much of the destroyed material enters the ocean.

3.2.3 FLOODING IN JAKARTA, INDONESIA PRESENT DAY

Jakarta, Indonesia is the first city to decide to retreat due to the major compound flooding that is increasing as a hazard, mainly from land subsidence (Abidin *et al.* 2001). The city contains numerous rivers that run through it and have been known to flood in the past (Wijayanti *et al.* 2017). The rapidly increasing sea level due to constant land subsidence and the rivers at maximum carrying capacity has caused major flooding to occur muchmore frequently (Budiyono *et al.* 2016) throughout the city rather than just along the coastline. The specific event for this assessment is the ongoing challenge of land subsidence. The scenarios of fragilities are determined by the different retreat scenarios that ask the question: How much material is left behind during the retreat?

3.3 AMOUNT OF THE EXPOSED ASSETS

The methodology used to determine the amount of the exposed assets measured in PMD that could originate in the UBE utilizes a model approach. A detailed Stock-and-Flow Model (SFM) for the urban coast in each of the three case studies was to be created. This detailed model is described in Section 3.3.1. However, the lack of sufficient data on the production and use of plastic did not allow for calibration. An alternative modeling approach is therefore used to determine the estimated value of the exposed assets through global plastic production and population in the coastal zone, described in Section 3.3.2.

3.3.1 A DETAILED STOCK-AND-FLOW MODEL

A detailed SFM was created based on the conceptual model (Fig. 2) to identify the specific stocks of plastic in an UBE to show the accumulation of plastic. Fig. 13 shows, visually, the stocks and flows of plastic in the UBE. The detailed SFM is ideal for understanding how much material accumulated in the UBE. The stocks had been identified and the flows have been estimated, but without the data necessary to fill the equations, the model could not be calibrated. To understand the results of this research, see Section 4.1.

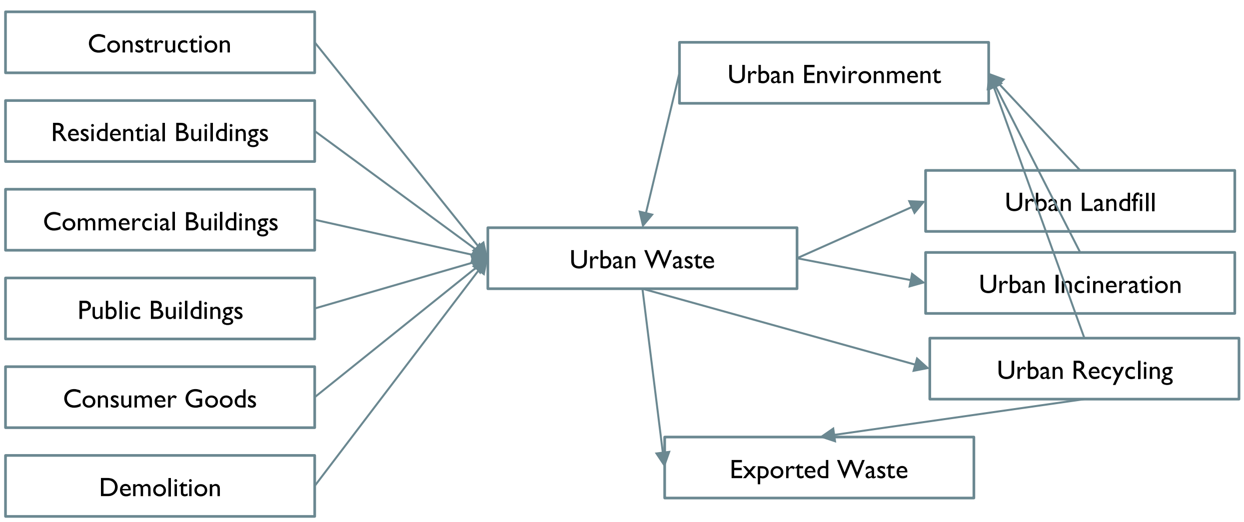

Figure 13. SFM of the flow of plastic in the UBE including the different stocks (boxes) and the flow of plastic (arrows).There is also a loss factor for each flow, not portrayed in the visual model.

3.3.2 A PROXY DATA APPROACH

Acknowledging the challenges with the first attempt to model the UBE, this second attempt has resulted in a higher-level, more generalized, and conservative estimate of the amount of plastic in the coastal zones. In order to quantify the value of the exposed assets, population data and plastic pro duction data are used. First, it is important to understand the population and urbanization is different for each case study. From the attempt to model specific stocks in the UBE of the three case studies, a new simplified model was created using the Model Eq. (5), where $V_A(t)$ is the value of the exposed UBE expressed as the amount of plastic in a specific coast at a specific time interval; N (t) is the number of people living in the coastal zone at that interval; and $A_N(t)$ is the accumulation of plastic in the UBE. $A_N(t)$ is estimated through the summation of Global Average Annual Plastic per Person (GAAPP) between 1985 to 2015 in the given UBE.

$$V_A = N(t) \times A_N(t) \quad , \tag{5}$$

Population data was collected from the UNPD (2019) which contained population change from 1950 to 2019 globally and by country. Global plastic production and sector uses data was collected from (Geyer *et al.* 2017a). The industrial use sectors are identified in Geyer *et al.* (2017a). The model defines the UBE as specific industrial use sector stocks: "Building & Construction" and "Consumer & Institutional Products". The sector stock of "Building & Construction" is referred to as Construction for this study and the "Consumer & Institutional Products" is referred to as Consumer Goods. Data was also collected to establish how many people are in each coastal zone.

After the data had been collected and made into a usable format, a proxy data model was created to determine over time how much plastic is in the coastal zone globally and in the three case studies. The simplified equation is used to determine a rough estimate of the amount of plastic in the coastal zone at a given time. This will be done for the three case study locations identified in Section 3.2 from 1950 to 2019 and projected to 2100: Japan; The Commonwealth of the Bahamas; Jakarta, Indonesia.

To generalize the amount of plastic in the three case studies, the global cumulative plastic production data from 1950 to 2015 by use sector is used from Geyer *et al.* (2017b). The cumulative plastic production by use sector was assessed to determine the annual average use sector plastic production. The annual production was then divided by the global population for the same years (UN 2019a). This created the GAAPP. To determine the amount of plastic in the UBE, the use sectors of "Building and Construction" and "Consumer & Institutional Products" are used. These use sectors are multiplied by the coastal population and summed to determine the amount of annual plastic production in a specific coastal UBE. This method is not highly detailed and therefore, not highly accurate, but provides the general amount needed to understand the potential risk associated with the urban coast in terms of PMD.

For all of the case studies, population is gathered from UNPD's global population data sheet that spans from 1950 to 2019. This dataset provides global, per region, and per country populations. For the risk assessment, the data used will be the annual total population for each case study. In the case of Jakarta, Indonesia, further specification is needed to look at the specific city. Each case study population is compared with populations recorded by each country themselves. By using population per year, plastic per person per country can be used to establish plastic in the country.

The assessment of plastic includes understanding the global plastic production recorded by as many sources as possible. The method for collecting plastic data will be a literary review regarding the production and use of plastics. Plastic waste, which appears to be a much wider discussion of plastic, is not considered as a part of this thesis. The waste cycle is important to understanding how much plastic stays in the coastal urban areas. However, understanding how much plastic is being produced and how much plastic is moving into the coastal zone provides for more information regarding the amount of plastic potentially available as marine debris. While the percentage of plastic material used to construct the UBE varies by country or even city, this is not included in the new estimation for the exposed assets as there is not enough detail in the data.

3.4 RISK ASSESSMENT

The Risk Eq. (1) is critical for determining the risk associated with increasing urban areas and the flow of PMD. The previous subsections have outlined the structure for determining the three components of the Risk Eq. (1): the probability of the hazard, the fragility of the exposed asset relative to the hazard, and the value of the exposed asset as expressed in tons of plastic. The risk assessment will be completed when combining these components, mathematically. After understanding a spectrum of exposed assets, a spectrum of hazards, and the fragilities of the urban coast, the risk will be clear. From these three variables in the Risk Eq. (1), the risks of the urban coast on the potential flow of PMD can be determined.

CHAPTER 4

RESULTS

In reporting the outcomes of the research, the result section is structured according to the Risk Eq. (1) as seen in Fig. 14. The hazard Probability Density Function (PDF) discusses the PDF of various hazards relevant to case study locations. The fragilities are also determined by case study using a scenario-based approach. The value of exposed assets is outline for global analysis and by the Urban Built Environment (UBE) of each case study. Finally, the risk analysis is created by combining the three components of the Risk Eq. (1).

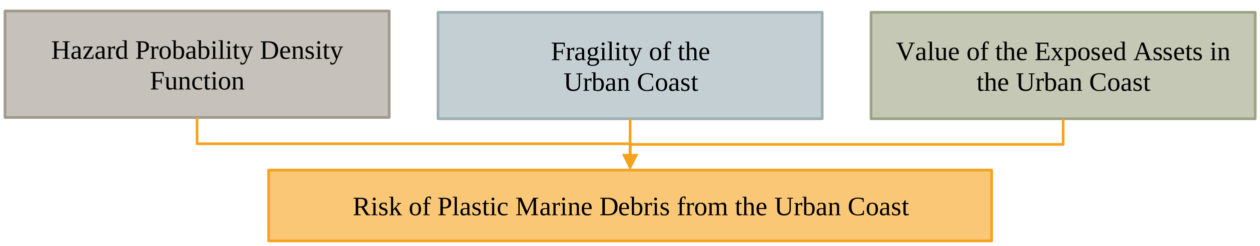

Figure 14. The risk equation as an outline forms the Results Chapter. Each section is separated by case study to identify the variables of the Risk Eq. (1), resulting in the risk assessment.

4.1 STOCK AND FLOW MODEL CALIBRATION

As previously discussed, there are three factors in the Risk Eq. (1) that need to be determined in order to understand the risk of the UBE in terms of PMD in coastal zones to the marine biosphere. The value of the exposed assets is measured in amount of plastic, rather than in cost. To estimate the amount of plastic, a detailed model of the urban coast was to be created to answer the question: How much plastic is available for transport to the marine systems?

4.1.1 MODELING THE EXPOSED ASSETS

In the urban environment, plastic is mainly located in buildings. It is a part of the building process through use of plastic film to protect pieces and equipment, to the plastic bottles used on site for construction workers, to the building structure as well. It is used in Polyvinyl chloride (PVC) piping, flooring, electrical wiring, and more. Plastic is also used in the consumer goods that fill the buildings, from desks and office equipment to technological equipment such as routers and computers, to lighting fixtures, to clothing and household goods. Plastic is well understood to be used in massive amounts for everyday life. It is likely that a lot more plastic will be used in the buildings in the future. The stocks of plastic were identified and the flow between them understood. The stock and flow variables were established, and the equations were being created when the challenge of available data became clear.

Initially, the stocks and flows of the model did not appear to include unreasonable information. As research continued, it became clear that this detailed model was not feasible due to a lack of data calibration and the inability to finalize equations. This is the first result of this thesis. The model (Fig. 13) shows the specific stocks and flows the UBE has in regard to plastic. This model is important for accurately depicting the amount of plastic in the urban coast. Without this detailed model, it is not possible to know the full extent of the amount of plastic in the UBE. Furthermore, it is not possible to know the full extent of the risk of plastic in the coastal UBE. The model does not require extraneous or challenging data in order to run, but requires information such as:

1. How much plastic is used in construction that does not end up in the building?
2. How much plastic, by weight, volume, or percentage is used in the building itself?
3. Does the amount of plastic in different types of buildings vary? How so?
4. How much plastic is used in the demolition process that did notoriginate in the building?
5. How much of these materials are reused or recycled into other buildings?

These questions were not able to be answered due to a lack of data and therefore, it cannot be determined how much plastic is in a specific building or in the UBE as a whole. The lack of data records is extremely important result of this thesis. The users of plastic, including construction companies, consumers, and sellers, are not recording how much plastic they are purchasing, using, or discarding during building projects, or in everyday life. The data is nearly nonexistent.

While there are many sources who study and discuss the production and use of plastics (i.e., Geyer *et al.* 2017a), the data which these papers refer to ultimately comes from one apparent source: PlasticsEurope. This is the second major result of this thesis. Table 2 is a diagram that shows different sources and the data used to conduct their studies. There are no studies that have collected or used plastic production data independent of PlasticsEurope, which is an organization of plastic producing companies.

PlasticsEurope is "a leading pan-European association and represents plastics manufacturers active in the European plastics industry" (PlasticsEurope 2021). The group networks with more than 100 companies who produce more than 90% of all polymers across the European Union (EU), Norway, Switzerland, Turkey and the United Kingdom (UK) (PlasticsEurope 2021). PlasticsEurope represents the plastic producers, so collecting data from an independent source is critical. Table 2 shows for a variety of papers that the original source of data is from PlasticsEurope publications regarding production and use of plastics. These "Plastics - the Facts" are produced annually. The publications do not indicate how the data is collected, if it is reproducible, or where the files can be accessed. When contacting the company regarding this problem, the organization was non-responsive (Martin 2021).

Due to these initial results and the understanding that modeling the UBE is not possible without more data, the methodology changed tounderstanding a general estimation of the value of the exposed assets of the UBEs of three case studies.

Table 2. Table of plastic sources. Title, date, author of the paper and then name of the plastic data sourced used in that paper.

Document Title	Year	Authors	Original Source
Global Plastic Production by Industry	2018	Jason Treat and Ryan T. Williams, National Geographic	Source: Roland Geyer, University of California, Santa Barbara
Production, use, and fate of all plastics ever made	2017	Roland Geyer, Jenna R. Jambeck, Kara Lavender Law	PlasticsEurope, 2006; PlasticsEurope, 2016
Marine Anthropogenic Litter	2015	Bergmann *et al.*	PlasticsEurope. 2013; PlasticsEurope 2014/ 2015
Plastics and microplastics in the oceans: From emerging pollutants to emerged threat	2014	IUCN: Florian Thevenon, Chris Carroll and Jo˜ao Sousa	PlasticsEurope, 2008; PlasticsEurope, 2009.; PlasticsEurope's Views on the Marine Litter Challenge, April 2010
River plastic emissions to the world's oceans	2017	Laurent C.M. Lebreton, Joost van der Zwet, Jan-Willem Damsteeg, Boyan Slat, Anthony Andrady and Julia Reisser	Plastics Europe. 2016
Toward the Integrated Marine Debris Observing System	2019	Maximenko *et al.*	Geyer, R., Jambeck, J. R., and Law, K. L. (2017). doi:10.1126/sciadv.1700782
Mare Plasticum - The Plastic Sea: Combatting Plastic Pollution Through Science and Art	2020	Streit-Bianchi *et al.*	Geyer R, Jambeck J, Lavender Law K (2015); PCI Wood Mackenzie (2017); PlasticsEurope (2018); PlasticsEurope (2019); European Bioplastics (2018)
The geological cycle of plastics and their use as a stratigraphic indicator of the Anthropocene	2016	Colin Waters, Anthony Barnosky, Patricia Corcoran, Alejandro Cearreta	PlasticsEurope (2013); PlasticsEurope (2015); Thompson, R.C., Moore, C., vom Saal, F.S., Swan, S.H., 2009
Sustainable Plastic Strategy	2020	Contributing partners: SusChem, Cefic , PlasticsEurope, EuPC, ECP4	(original)
PlasticsEurope	2016	PlasticsEurope	(original)
PlasticsEurope Operation Clean Sweep Report 2019	2019	PlasticsEurope	(original)

4.1.2 MODELING THE CASE STUDIES URBAN BUILT ENVIRONMENTS

Establishing the value of the exposed assets in terms of amount of plastic in each case study required a generalized Model Eq. (5). The variable in this equation requires data for population in the coastal zone and average amount of plastic per person produced annually. The first variable in this Eq. (5) is population. The UN Population Division (UNPD) provides a database with annual population globally (Fig. 15) and per country from 1950 to 2019 (UNPD 2019). Population data for the case study countries was extracted and analyzed. Using the medium variant projections for total population and population density. The second variable is the percent of the population of a specific country living in the coastal zone (*C*) in a given year. This data was identified for case study dependent on the topography and urban structure. Third, the global plastic production data from 1950 to 2015 was used from Geyer *et al.* (2017a). This paper cites the original source of their plastic data to be from PlasticsEurope, but the original data is not available.

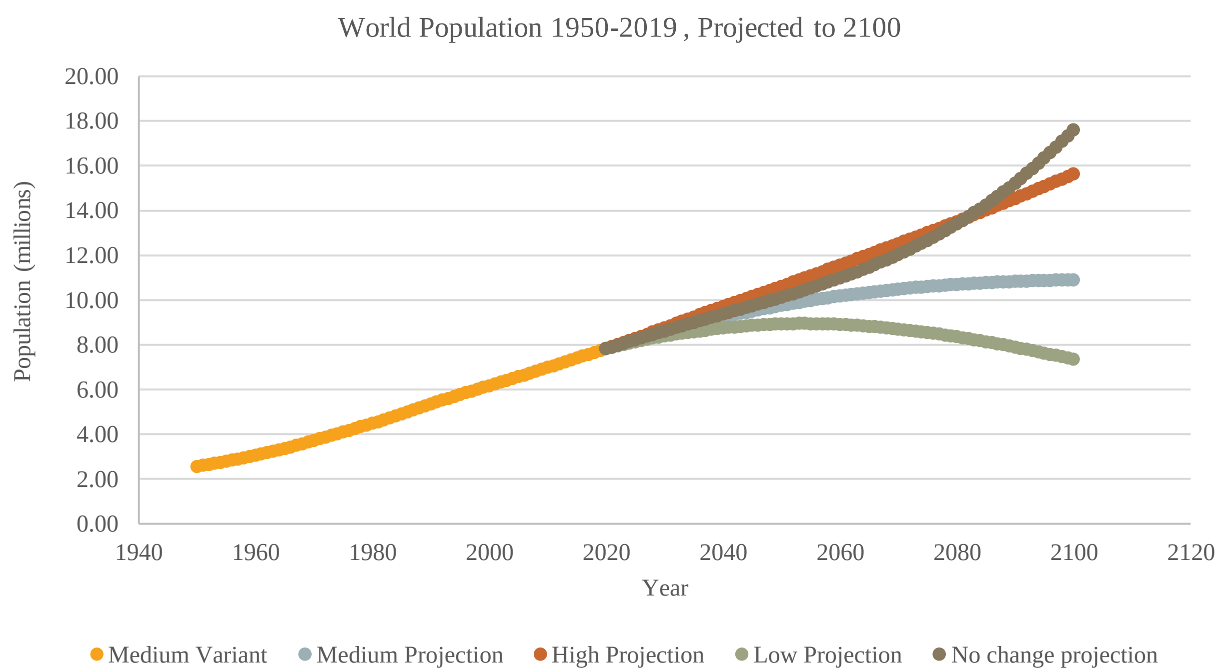

Figure 15. World Population 1950-2019. Low, medium, high, and no change variant projection from 2020 to 2100. Data source: (UNPD 2019).

The plastics data shows from 1950 to 2015 the cumulative plastic production in million tons. First, the annual plastic production is determined by subtracting the amount of plastic in the year before, starting with 1950 and 1951. For example, the annual plastic production in 1951 is equal to the cumulative plastic production in 1951 minus the cumulative plastic in 1950. This was determined for each year in the data set. From here, the global annual production is divided by the global population to identify the GAAPP. Geyer *et al.* (2017b) also provides information on the portion of plastics produced that were used specific use sectors. As mentioned in Section 3.3.2, to determine the UBE the use sections of “Building & Construction” and “Consumer & Institutional Products” are used. These sector proportions were applied to the GAAPP to determine the amount of plastic per person in the UBE. This amount is then multiplied by a specific coastal population to determine the amount of plastic in a specific coastal UBE annually. When determining the risk of the coastal UBE to creating PMD, an accumulation of plastic must be used.

Now that the amount of plastic per person in the UBE is identified, accumulation must be estimated. Building & Construction has an average use time of 35 years, while Consumer & Institutional Products have an average use time of 3 years (Geyer *et al.* 2017a). The estimated accumulation of plastics can be set equal to the sum of annual plastic production for the past 30 years. While the average use time of consumer goods is only 3 years, this material is the most likely to stay within the UBE after use, whether in a internal waste stream or within the environment. Building & construction has an average use time of 35 years but the standard deviation is approximately 7 years (Geyer *et al.* 2017a). Due to these factors the accumulation of plastics in a specific coastal UBE is equal to the sum of annual plastic production from 1985 to 2015 for the specific coastal population. The waste is considered by limiting the years used in the production accumulation.

Using this plastic production and use data annually as well as the national population annually, but the annual amount is a poor indicator for how much plastic a person represents since average use times in some sectors are up to 35 years in a specific country from 1950 to 2015 is estimated. To determine more specifically how much plastic a person consumes or uses in a specific coastal UBE Eq. (5) requires the amount of the population living in the coastal zone.

4.1.3 GLOBAL ESTIMATION OF PLASTIC IN COASTAL ZONES

The global estimation of plastics in the coastal zone is understood through global population (Fig. 15) multiplied by the global average coastal population of 40% (Sterzel *et al.* 2020). The amount of plastic per person in the UBE has been described in Section 4.1.2. This is then multiplied by the coastal population to determine an estimate of the amount of plastic in the coastal UBE globally (Fig. 16). The global estimation is important for understanding how much of this hazardous material is available for destruction and the potential risk of becoming PMD.

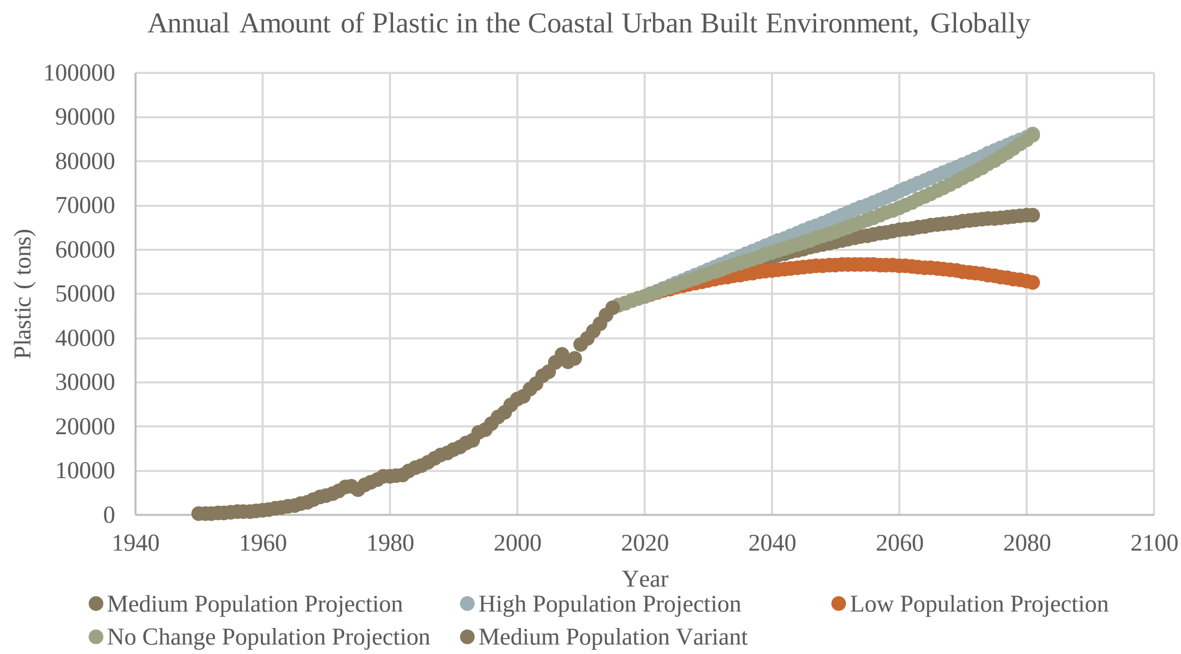

Figure 16. Global Population in the coastal zone (40%; Sterzel *et al.* 2020) multiplied by the estimated amount of plastic in the UBE from 1950-2015. Global projected population variants (UNPD 2019) from 2016 to 2100 multiplied by 40% to identify coastal projections at the proportion, then used with the plastic in the UBE to determine potential future projections of annual plastic in the coastal UBE, globally.

4.2 CASE STUDY: JAPAN

The case study of Japan is used because the risk assessment includes a stable hazard with changing exposure. Historically, there have been earthquake and tsunami hazards in Japan, and the frequency of these events is not likely to change with climate change. However, the exposure of the UBE is changing and understanding the fragilities provides for necessary information to inform the risk.

4.2.1 THE HAZARD PROBABILITY DENSITY FUNCTION

The hazard relevant to the current UBE of Japan is the tsunami waves that threaten it. The tsunami wave data was collected from the National Centers for Environmental Information (NCEI 2021) for tsunamis 1800-2020. This data was then sorted as explained in Section 3.1 to find the recurrence time (R) for tsunamis for different wave heights (Table 3). From here, the probability for each wave height was determined for 30 years (2050), 80 years (2100), and 200 years (2220), as seen in Table 3, to represent different generations.

Tsunamis are a geological hazard and are not expected to change with the changing climate (Röbke & Vött 2017). To understand the current PDF for tsunami waves in Japan, the Poisson Eq. (2) was used. Table 3 shows the variables in the equation, the water height, and the probability of no events, 1 event, and 1 or more events occurring. The current tsunami PDF can be applied for the future of tsunamis as well. The future PDF of tsunamis is not different than the current. This, in combination with the fragility and the value of the exposed assets, can be used to identify the current and future risk of PMD entering the ocean from the Japan coastal UBE.

4.2.2 JAPAN 2011, FRAGILITIES ASSESSMENT

TOHOKU EARTHQUAKE AND TSUNAMI, MARCH 2011

The event in this case study refers to the eastern Japan earthquake and tsunami that resulted in major damage to the coastal zone on Honshu Island. On March 11th, 2011 a 9.0 magnitude earthquake occurred at 14:46 Tokyo time (Norio *et al.* 2011). The epicenter was estimated at 38.322°N and 142.369°E, 77 km off the eastern coast of Honshu Island, Japan (Norio *et al.* 2011). The earthquake was the third highest ever recorded since recording started around 1960, globally (Norio *et al.* 2011).

Table 3. Poisson Probability of no events, 1 event, and 1 or more tsunami events occurring in 30, 80, and 200 years by water inundation height. The recurrence time is based on past tsunami events (NCEI 2021).

Poisson Probability for Tsunamis in Japan with Past Recurrence Times						
Water Height (m)	Year (t)	R	μ	No Tsunami Events in t Years	1 Tsunami Event in t Years	1 or More Tsunami Events in t Years
All	2050	4.30	6.98	9.33E-04	6.51E-03	9.99E-01
	2100		18.60	8.32E-09	1.55E-07	1.00E+00
	2220		46.51	6.31E-21	2.94E-19	1.00E+00
WH_A 1-1.9	2050	11.32	2.65	7.06E-02	1.87E-01	9.29E-01
	2100		7.07	8.50E-04	6.01E-03	9.99E-01
	2220		17.67	2.11E-08	3.73E-07	1.00E+00
WH_B 2-4.9	2050	15.36	1.95	1.42E-01	2.77E-01	8.58E-01
	2100		5.21	5.47E-03	2.85E-02	9.95E-01
	2220		13.02	2.21E-06	2.88E-05	1.00E+00
WH_C 5-9.9	2050	21.50	1.40	2.48E-01	3.46E-01	7.52E-01
	2100		3.72	2.42E-02	9.01E-02	9.76E-01
	2220		9.30	9.12E-05	8.48E-04	1.00E+00
WH_D 10.1-15	2050	53.75	1.95	1.42E-01	2.77E-01	8.58E-01
	2100		5.21	5.47E-03	2.85E-02	9.95E-01
	2220		13.02	2.21E-06	2.88E-05	1.00E+00
WH_E 15.1-30	2050	71.67	0.42	6.58E-01	2.75E-01	3.42E-01
	2100		1.12	3.27E-01	3.66E-01	6.73E-01
	2220		2.79	6.14E-02	1.71E-01	9.39E-01
WH_F 30.1+	2050	71.67	0.42	6.58E-01	2.75E-01	3.42E-01
	2100		1.12	3.27E-01	3.66E-01	6.73E-01
	2220		2.79	6.14E-02	1.71E-01	9.39E-01

While the earthquake was large, the major disaster to the coast was a result of the tsunami that was triggered by this earthquake. Within minutes of the Tohoku earthquake, the tsunami waves reached the eastern coast of Honshu Island, inundating a maximum distance of 10 km from the coastline and an estimated height of 24 m - 36 m (Norio *et al.* 2011). The total land area covered by the tsunami is 561 square km (Koshimura *et al.* 2014). The wave affected nearly the entire

Pacific coast, including 20 countries that issued tsunami warnings. This massive energy release resulted in a variety of geophysical impacts. The Island of Honshu, Japan was moved approximately 3.6 m to the east and the earth's axis shifted about 25 cm and increased the planet's rotation by about 1.8 microseconds (Norio *et al.* 2011).

THE RESULTING DISASTER

The Tohoku earthquake and tsunami resulted in major death and destruction of the UBE along the east coast of Japan. In total, 15,899 people were killed, 2,526 people were reported missing, and 6,167 people injured (NPA 2011). Most of the personnel damages took place in Miyagi, Iwate, and Fukushima Prefectures, respectively. While these are notable, the identification of fragilities is reliant on understanding the damages to the UBE. Property damages consisted of 122,000 buildings totally collapsed, 283,117 partially collapsed, 731,573 partially damaged, and 11,276 inundated (NPA 2011). Roads, bridges, dikes, and railways were also damaged during the tsunami (NPA 2011). Understanding the extent of damages clearly identifies the fragilities in the system for a storm of this size. Reports detail the buildings collapsed, damaged, inundated, and burned down as well as the lost material stock by type (NPA 2011). Plastic is not included in the list of materials.

FRAGILITIES OF THE URBAN COAST

To determine the fragilities, the damage is estimated in relation to wave height, as categorized in Section 4.2.1. The Tohoku tsunami of 2011 reached an inundation height of 24 m - 36 m, categorizing it in the $WH_{(F)}$ 30+ m wave height category, the maximum assessed in the PDF of tsunamis. Approximately 5 million tons of marine debris was created from the tsunami (NOAA 2014). Of all that material, an estimated 70% sank nearshore, while 30% was determined to be high-wind items such as foam and plastics (NOAA 2014). This creates the assumption that 30% of the MD created is PMD, resulting in approximately 1.5 million tons of PMD created from the Tohoku tsunami. Based on Value of Exposed Assets (discussed in Section 4.2.4), in 2011 28.6 million tons of plastic production was introduced to the coastal UBE. As a results, the tsunami created 5% of the UBE to become PMD. From here, scenarios were created to identify the fragilities of other wave height tsunamis.

Table 4 identifies the fragility scenarios which are assessed by Wave Height (WH): $WH_{(A)}$:

1-1.9 m, $WH_{(B)}$: 2-4.9 m, $WH_{(C)}$: 5- 9.9 m, $WH_{(D)}$: 10-14.9 m, $WH_{(E)}$: 15-29.9 m, and $WH_{(F)}$: 30+ m. The scenarios created for the fragility of UBE to destruction is defined by assuming the smaller wave height creates a specific percent of damage as the wave height group higher. For example, $WH_{(A)}$ creates 80% of the damage as $WH_{(B)}$ in relation to the damage created by the 2011 Tohoku Earthquake.

1. $WH_{(A)}$ creates 80% amount of the PMD as $WH_{(B)}$
2. $WH_{(A)}$ creates 60% amount of the PMD as $WH_{(B)}$
3. $WH_{(A)}$ creates 40% amount of the PMD as $WH_{(B)}$

The fragility scenarios reflect potential portion of the coastal UBE that is fragile to becoming PMD. The value of the exposed assets is critical for the risk assessment.

Table 4. Fragility Scenarios created to understand the relationship between WH and damage. As the relationship is not clearly defined, the scenarios cover the spectrum of possibilities.

Wave Height	Wave-Damage Scenarios	Percent of UBE becoming Plastic Marine Debris
WH_A 1-1.9	80%	1.72%
WH_B 2-4.9		2.15%
WH_C 5-9.9		2.69%
WH_D 10.1-15		3.36%
WH_E 15.1-30		4.20%
WH_F 30+ (2011)		5.24%
WH_A 1-1.9	60%	0.41%
WH_B 2-4.9		0.68%
WH_C 5-9.9		1.13%
WH_D 10.1-15		1.89%
WH_E 15.1-30		3.15%
WH_F 30+ (2011)		5.24%
WH_A 1-1.9	40%	0.05%
WH_B 2-4.9		0.13%
WH_C 5-9.9		0.34%
WH_D 10.1-15		0.84%
WH_E 15.1-30		2.10%
WH_F 30+ (2011)		5.24%

4.2.3 VALUE OF THE EXPOSED ASSETS

The UBE must be understood through analysis of the material in the coastal zone. First, to determine population from 1950 to 2019, data is collected from UNPD (2019) and Ministry of Internal Affairs and Communication (MIAC 2020). The population of Japan in 1950 was 82,802,084 and in 2010 was 128,542,349. Fig. 17 shows the population from 1950 to 2019 and UNPD projected population variants from 2020 to 2100 (UNPD 2019). Population has leveled off and started to decline from 2005-2019 and is projected to continue declining at varying projections based on birth and death rates (UNPD 2019). Japan is a coastal nation that has 50%, 53%, and 80% of the population living in the coastal zone in 1950 2970, and 1997, respectively (Hinrichsen 1999). The assumption that the portion of the population living in the coastal zone remains at 80% from 1997 to 2100 is created to understand the exposure. While it is unlikely that the coastal zone stopped growing, assuming the population remained at 80% allows the value of the exposure to remain conservative rather than overestimating.

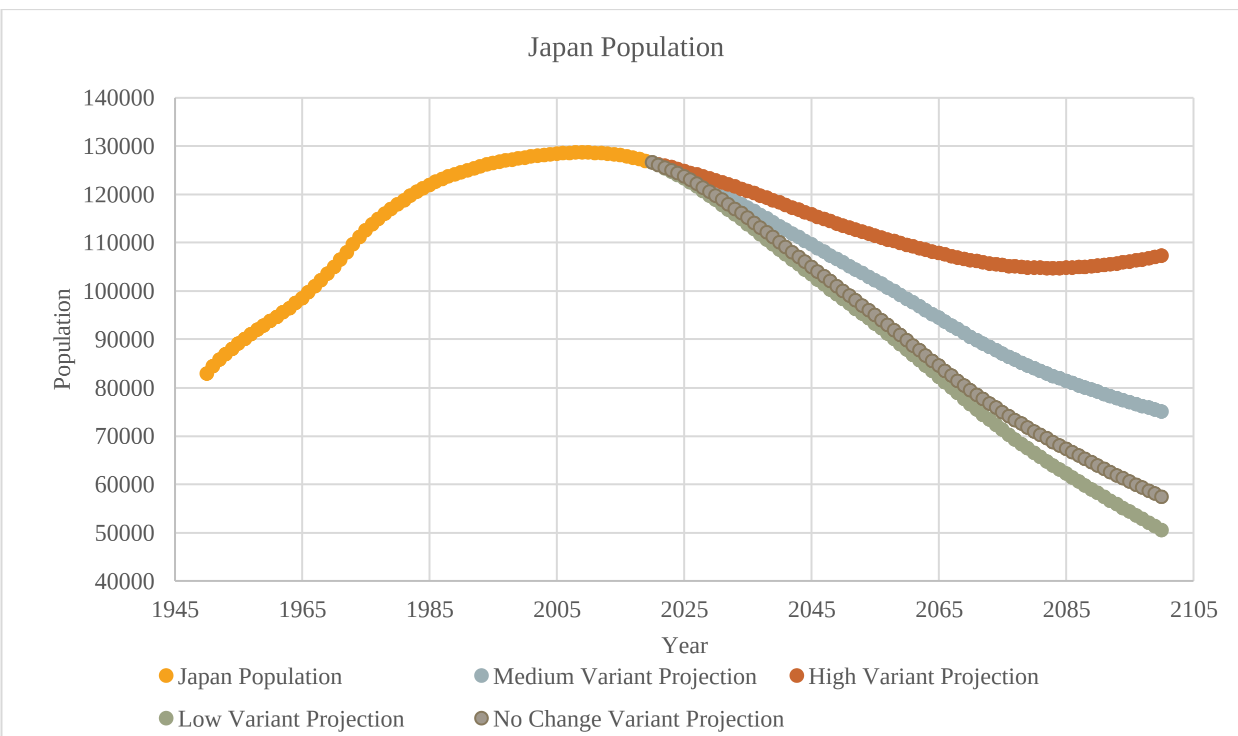

Figure 17. Population of Japan with UNPD population projection variants (UNPD 2019).

To understand the amount of plastic in Japan, the previously identified amount of plastic per person in the UBE (Section 4.1.2) was multiplied by the population of Japan. However, the question is the plastic in the UBE of the coastal zone. To quantify this, the data was multiplied by the coastal population (Fig. 18). This determines the flow of the exposed assets into the coastal UBE of Japan from 1950 to 2015. To determine the risk in 30, 50, or 100 years, the value of the exposed assets is equal to the sum of the plastic from 1985 to 2015. This assumes that the amount per person does not increase, which is not likely, but the estimation will remain conservative with this assumption. The value of exposed assets in the UBE resulted in the sum of the 30 years to be equal to 40.5 million tons of plastic. It is important to note that the waste stream is not clearly identified but is estimated by not including more than 30 years of accumulation in the stock. It is assumed that some use times are longer and that some material is left within the system after the use time has ended. This allows for the 30-year accumulation estimate.

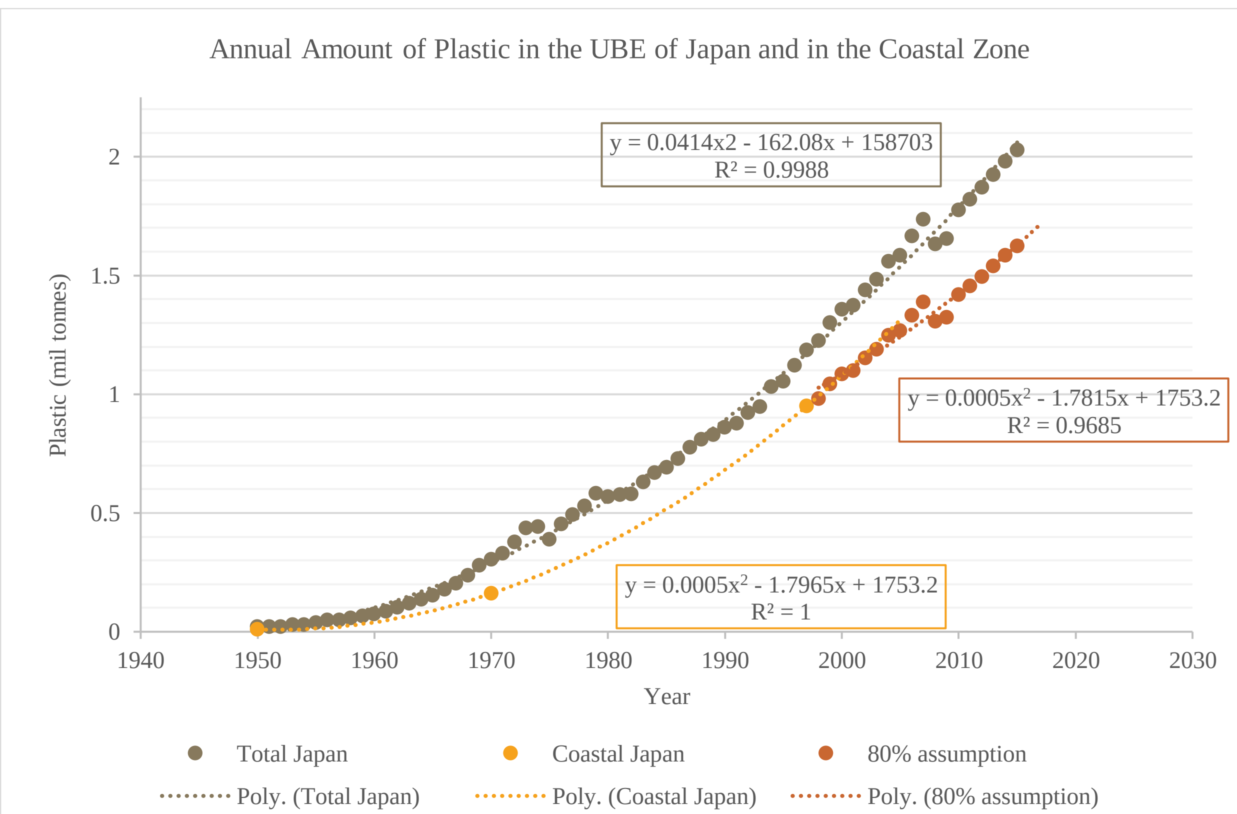

Figure 18. The annual amount of plastic in whole of Japan UBE compared to the coastal UBE.

4.2.4 RISK OF PLASTIC MARINE DEBRIS FROM THE JAPAN URBAN BUILT ENVIRONMENT

The variables of the Risk Eq. (1) have been outlined in detail, establishing the relevant hazards, the fragilities of the UBE in the coastal zone, and estimating the amount of plastic exposure in the UBE to those hazards. The current and future PDF of tsunamis in Japan is not expected to change in the near future. The risk associated with the coastal UBE to the marine biosphere in terms of PMD is outlined in the fragility scenarios. There are three scenarios outlining how much damage, in relation to the Tohoku tsunami, is created from smaller wave heights.

- Scenario A: The tsunami $WH_{(A)}$ creates 80% of the damage of the tsunami $WH_{(B)}$
- Scenario B: The tsunami $WH_{(A)}$ creates 60% of the damage of the tsunami $WH_{(B)}$
- Scenario C: The tsunami $WH_{(A)}$ creates 40% of the damage of the tsunami $WH_{(B)}$

The risk assessment (Fig. 19) required the understanding of three variables. First, understanding the PDF of tsunami waves with different WHs. Second, given that 5% of the coastal UBE of Japan created PMD by the 30+ m WH of the Tohoku tsunami, fragility scenarios were created to understand the relationship between wave height and PMD. Third, the value of the exposure of the coastal zone in terms of plastic with the assumption that the portion of the population living in the coastal UBE remained at 80% of the total. It is clear that the risk of the largest tsunami wave height category (30+ m) occurring damage scenario, $WH_{(A)}$ of 1-1.9 m would result in 20,000 tons of PMD by 2050 would result in approximately 730,000 tons of PMD. Given the 40% 2100.

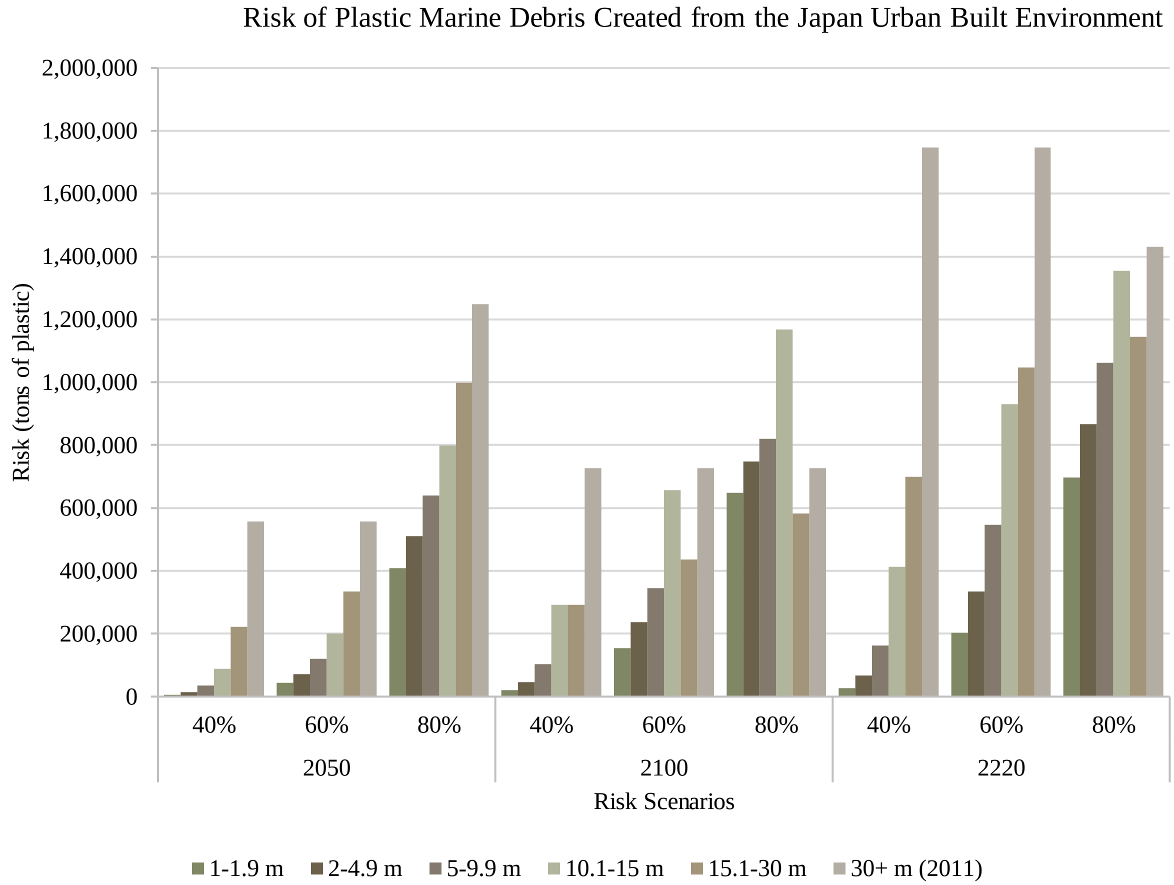

Figure 19. Risk Scenario. Risk of 1 or more tsunami events, specified by wave height, in Japan in 30, 80 or 200 years where $WH_{(A)}$ creates 40%, 60% and 80% of the damages as $WH_{(B)}$.

4.3 CASE STUDY: THE COMMONWEALTH OF THE BAHAMAS

4.3.1 THE HAZARD PROBABILITY DENSITY FUNCTION

Cyclones are an atmospheric and hydrological hazard that are formed in warm ocean waters creating low pressure zones (NHC 2021b). The tropical waters near the equator have allowed for cyclonic formation throughout history, resulting in many landfalls on the Bahamas. To determine the PDF current probability of this landfall happening on the Bahamas, cyclone data was collected from NOAA Historical Hurricane Tracks (NOAA 2021c). The search parameters were as follows: Location: The Bahamas; Radius: 0 km; Categories: HC5, HC4, HC3, HC2, HC1, TS; Months:

ALL; Years: ALL [1830-2021]; ENSO: ALL; Minimum Pressure (mb) below: 1151; Include Unknown Pressure Rating: TRUE.

The output was the total list of cyclones that passed by the island nation, including the surrounding coastal waters. Each cyclone was assessed to determine if there was landfall and the maximum strength of each cyclone at landfall. Landfall is identified as the storm path passing within 5 mi of a Bahamas Island. The storm strengths include Tropical Storm (TS), Hurricane Category 1 (HC1), Hurricane Category 2 (HC2), Hurricane Category 3 (HC3), Hurricane Category 4 (HC4), Hurricane Category 5 (HC5). The recurrence time for each category cyclone was identified and used to find μ as seen in Table 5. The Poisson Eq. (2) determined the probability for each storm strength was determined for 30 years (2050), 80 years (2100), and 200 years (2220) as seen in Table 5.

Climate change is greatly impacting the atmosphere-ocean systems, including cyclones. Cyclones are predicted to increase in intensity (Marsooli *et al.* 2019). While the change in frequency is still being determined, the increase in intensity allows for small cyclones to become larger hurricane categories. The warming ocean waters also allow for changes in the potential latitudes that cyclones can form. The change in intensity of cyclones was applied to the current PDF to understand the potential future PDF of cyclones making landfall in the Bahamas Islands. To do this, the recurrence times for the storms were moved down 1 strength. For example, the recurrence time of HC1 in the future uses the recurrence time of historic TS. The new recurrence times were used to find new μ variables for each category storm for each time in question. The Poisson Equation is utilized to find the potential future PDF of cyclones making landfall in the Bahamas Islands in 2050, 2100, and 2220, as seen in Table 6.

Table 5. Poisson Probability of no events, 1 event, and 1 or more cyclone events occurring in 30, 80, and 200 years by cyclone storm strength base on past cyclone data.

Poisson Probability for Cyclones in the Bahamas with Past Recurrence Times						
Category	R	t	μ	no events in t years	1 event in t years	1 or more events in t years
TS	1.9425	2050	15.44	1.96E-07	3.03E-06	1.00E+00
		2100	41.18	1.30E-18	5.36E-17	1.00E+00
		2220	102.96	1.93E-45	1.99E-43	1.00E+00
H1	5.3793	2050	5.58	3.78E-03	2.11E-02	9.96E-01
		2100	14.87	3.48E-07	5.17E-06	1.00E+00
		2220	37.18	7.13E-17	2.65E-15	1.00E+00
H2	9.9375	2050	3.02	4.89E-02	1.47E-01	9.51E-01
		2100	8.05	3.19E-04	2.57E-03	1.00E+00
		2220	20.13	1.82E-09	3.66E-08	1.00E+00
H3	7.1364	2050	4.20	1.49E-02	6.28E-02	9.85E-01
		2100	11.21	1.35E-05	1.52E-04	1.00E+00
		2220	28.03	6.74E-13	1.89E-11	1.00E+00
H4	11.6154	2050	2.58	7.56E-02	1.95E-01	9.24E-01
		2100	6.89	1.02E-03	7.03E-03	9.99E-01
		2220	17.22	3.33E-08	5.73E-07	1.00E+00
H5	22.0000	2050	1.36	2.56E-01	3.49E-01	7.44E-01
		2100	3.64	2.63E-02	9.58E-02	9.74E-01
		2220	9.09	1.13E-04	1.02E-03	1.00E+00

Comparing the PDF of cyclones from historic data to the potential PDF of the future allows for the changing hazard spectrum to be identified. It is clear that the probability of another HC5 storm making landfall in the Bahamas by 2050 changes from 74% probability to 92%. This change in the hazard spectrum has a potentially large impact on the future of PMD. However, the future PDFs are not considered in the risk equation because the estimations are to remain conservative.

Table 6. Poisson Probability of no events, 1 event, and 1 or more cyclone events occurring in 30, 80, and 200 years by cyclone storm strength with recurrence times of the future, where the future storm strength have the recurrence times of the storm strength weaker in the past. For example, future HC5 has recurrence times of past HC4, future HC4 has those of past HC3, and so on, while future TS has the recurrence time that is half the recurrence time of past TS.

Poisson Probability for Cyclones in the Bahamas with Future Recurrence Times						
Category	R	t	μ	no events in t years	1 event in t years	1 or more events in t years
TS	1.9425	2050	30.89	3.85E-14	1.19E-12	1.00E+00
		2100	82.37	1.69E-36	1.39E-34	1.00E+00
		2220	205.92	3.73E-90	7.67E-88	1.00E+00
H1	5.3793	2050	15.44	1.96E-07	3.03E-06	1.00E+00
		2100	41.18	1.30E-18	5.36E-17	1.00E+00
		2220	102.96	1.93E-45	1.99E-43	1.00E+00
H2	9.9375	2050	5.58	3.78E-03	2.11E-02	9.96E-01
		2100	14.87	3.48E-07	5.17E-06	1.00E+00
		2220	37.18	7.13E-17	2.65E-15	1.00E+00
H3	7.1364	2050	3.02	4.89E-02	1.47E-01	9.51E-01
		2100	8.05	3.19E-04	2.57E-03	1.00E+00
		2220	20.13	1.82E-09	3.66E-08	1.00E+00
H4	11.6154	2050	4.20	1.49E-02	6.28E-02	9.85E-01
		2100	11.21	1.35E-05	1.52E-04	1.00E+00
		2220	28.03	6.74E-13	1.89E-11	1.00E+00
H5	22.0000	2050	2.58	7.56E-02	1.95E-01	9.24E-01
		2100	6.89	1.02E-03	7.03E-03	9.99E-01
		2220	17.22	3.33E-08	5.73E-07	1.00E+00

4.3.2 THE BAHAMAS ISLANDS FRAGILITIES ASSESSMENT, 2019

The Commonwealth of The Bahamas is an island chain located southeast of Florida, US and northeast of Cuba. The country consists of 700 islands and 2,400 cays totaling an area of 13877 square km, but only 30 islands are inhabited and only 19 of those are the principal islands (Government of the Bahamas 2011). The population in 2019 was 389,486 people (UNPD 2019).

HURRICANE DORIAN, 2019

Hurricane Dorian was the most devastating hurricane to hit the north-western Bahamas in modern records (Avila *et al.* 2020). The NHC is a part of the US NOAA and National Weather Service (NWS) which is responsible for tracking, recording, and predicting weather systems (NHC 2021d). The NHC tracks and predicting TSs and hurricanes from beginning to end. The storms are then recorded, including the full track, the changing in winds speeds and pressure changes, and including the resulting damage (Avila *et al.* 2020). Hurricane Dorian began August 24th, 2019 and terminated September 7th, 2019. The following description of the cyclone hazard was summarized from the NHC tropical cyclone report (Avila *et al.* 2020).

Hurricane Dorian began as a large tropical wave off the west coast of Africa on August 19th, 2019. Moving westward, the storm continued to develop and showed cyclonic circulation and was categorized as a tropical depression on August 24th, 2019. Cloud pattern organization increased, and an 'eye-like feature' allowed the storm to be categorized as TS Dorian at 1800 Coordinated Universal Time (UTC) the same day. TS Dorian made landfall over Barbados 0130 UTC August 27th with maximum winds of 45 kt. Dorian continued to strengthen moving westward, creating an eye, and northwestward through a very warm ocean. The favoring conditions allowed Dorian to strengthen to a HC3 by 1800 UTC August 30th. By 0000 UTC on August 31st, Hurricane Dorian had estimated surface wind speeds of 115 kt and was continuing to intensify to a HC5 with an eye diameter of 12 n mi. At 1640 UTC September 1st Hurricane Dorian made landfall over Elbow Cay, Great Abaco in the northwest Bahamas Islands. The HC5 was slowed by high pressure in the north and stayed over Great Abaco several hours. The Hurricane's force declined but still remained at least tropical storm force winds to remain pounding Great Abaco. Dorian moved off and began towards Grand Bahama Island making landfall again at 0215 UTC September 2nd with 155 kt winds, decreasing to 140 kt winds 6 hours later by the time it moved off the coast.

Hurricane Dorian turned north-northwest up towards the eastern coast of Florida, weakening, and restrengthening to make another landfall over Cape Hatteras with HC2 winds at 1230 UTC on September 6th. Dorian re-entered the Atlantic weakened and continued up the east coast to Nova Scotia, Canada. Dorian then became extratropical on the morning of September 8th moving off the east coast of Canada and was absorbed by a larger extratropical low 24 hours later far over the Atlantic Ocean (Avila *et al.* 2020).

THE RESULTING DISASTER

Hurricane Dorian remained over the Bahama Islands, specifically Great Abaco Island and Grand Bahamas Island, for many days, pounding the area with rain and winds and, when finally, it moved on, large storm surges inundated the islands. The disaster resulting from this great storm was catastrophic. The NHC estimated the number of deaths, number of people missing, and the general impact of Dorian in the Bahamas (Table 7). The Bahamas census of 2000 stated that the total population was 298,045 with 90% living on the following islands. New Providence with 69.9%, Grand Bahama and Great Abaco islands with 15.5% (Government of the Bahamas 2011). Assuming these percentages remained the same, in 2019 Grand Bahama and Great Abaco islands would have had a total population of 60,370 people.

Table 7. This table shows the casualties and damage from Hurricane Dorian in the Bahama Islands. [1] is from the Health Minister in the Bahamas, [2] is from the Bahamas Weather Service. Information from table source: Avila *et al.* (2020).

Hurricane Dorian Disaster Table	
Deaths [1]	200+ people
Deaths [2]	74 people
Missing at the time of the Report [2]	245 people
Homeless and/or jobless	29,500 people
Total Damage	$ 3.4 Billion USD

After Dorian, the Inter-American Development Bank (IDB) and the UN Economic Commission for Latin America and the Caribbean (ECLAC) were also tasked with assessing the resulting damage in a detailed summary of the effects of Hurricane Dorian on the Bahamas. It includes the social, infrastructure, production, and environmental costs created by direct physical damage, revenue, and other income losses, and additional costs such as debris removal (IDB 2019). Recognizing that there are many influences in destruction, understanding the strength and intensity of a hazard and the resulting damage, the fragilities become clear.

THE FRAGILITIES OF THE URBANCOAST

The fragilities of the Bahamas UBE can be determined by using the amount of damage compared to the areas that were not damaged. First, it is understood that Hurricane Dorian caused 70% of the UBE on Abaco Island to be destroyed, 15% on Grand Bahama Island, and 9% on the other islands in the Bahamas (IDB 2019). Then, the portion of the total UBE must be understood. This was done by finding the ratio of those two islands and those marked as 'others' to the total land area from (Government of the Bahamas 2012). The ratio of the population in these groups was also identified (Government of the Bahamas 2012). Combining these ratios gives a percent impact of Hurricane Dorian to the entire country. Table 8 shows this math, which resulted in 18.22% of the Bahamas to be destroyed by Hurricane Dorian.

Table 8. Portion of the Bahamas Islands impacted by Hurricane Dorian (IDB 2019).

Summary Effects of Hurricane Dorian			
Great Abaco Island	70%	14.63%	10.24%
Grand Bahamas Islands	15%	4.99%	0.75%
All other Inhabitated Islands	9%	80.39%	7.23%
Total Impact of Hurricane Dorian			18.22%

From here, scenarios are created to estimate the fragilities of the UBE in the Bahamas. It is unclear and undocumented how much of the destroyed UBE was washed into the ocean, so scenarios were created to describe this (Table 9) to be used in potential risk for a Hurricane Dorian size storm. To understand the fragilities with respect to cyclones of various storm strength, scenarios are necessary. Storm categories and the resulting damage have no known correlation other than that a 'weaker' strength storm creates less damage. However, the ratio of this relationship is unknown. Scenarios are created estimating the amount of damage resulting from the storm. This was done by assuming that HC_a creates (x) amount of damage as HC_{a+1}, where (x) is 80%, 60%, or 40%. For example, HC5 represents the damage that took place during Hurricane Dorian. The scenarios are based on the proportion of the UBE destroyed during Hurricane Dorian. HC4 could result in 80% of the damage that HC5 created. A HC3 storm under this scenario would result in 80% of the damage of HC4. This applies to all cyclone categories The scenarios are *x* is equal to 80%, 60%, or 40% of the damage created by Hurricane Dorian. The scenarios estimating the damage are shown in Table 9.

Table 9. The fragility scenarios for the Bahamas Islands.

Storm Category	Damage Scenario	Material Damaged in the Bahamas (%)	40% enters the ocean	20% enters the ocean	10% enters the ocean
Tropical Storm	80%	5.97%	2.39%	1.19%	0.60%
HC1		7.46%	2.99%	1.49%	0.75%
HC2		9.33%	3.73%	1.87%	0.93%
HC3		11.66%	4.66%	2.33%	1.17%
HC4		14.58%	5.83%	2.92%	1.46%
HC5 (Dorian)		18.22%	7.29%	3.64%	1.82%
Tropical Storm	60%	1.42%	0.57%	0.35%	0.14%
HC1		2.36%	0.94%	0.59%	0.24%
HC2		3.94%	1.57%	0.98%	0.39%
HC3		6.56%	2.62%	1.64%	0.66%
HC4		10.93%	4.37%	2.73%	1.09%
HC5 (Dorian)		18.22%	7.29%	4.56%	1.82%
Tropical Storm	40%	0.19%	0.07%	0.05%	0.02%
HC1		0.47%	0.19%	0.12%	0.05%
HC2		1.17%	0.47%	0.29%	0.12%
HC3		2.92%	1.17%	0.73%	0.29%
HC4		7.29%	2.92%	1.82%	0.73%
HC5 (Dorian)		18.22%	7.29%	4.56%	1.82%

In each scenario, a HC5 creates 18.2% of the material in the Bahamas UBE to be destroyed. If 40% of this enters the ocean, 7.29% of the UBE will become PMD. Creating this spectrum of fragilities allows for the full understanding of potential risk of the Bahamas UBE.

4.3.3 THE VALUE OF THE EXPOSED ASSETS

The Commonwealth of the Bahamas is an island nation whose coastal population is defined as the total population, rather than a portion of the population. The nation's population from 1950 to 2019 (UNPD 2019) is utilized in the Model Eq. (5). The population in 1950 was 79,090 and in

2015 was 374,200. Fig. 20 shows the population from 1950 to 2019 and UNPD projected population variants from 2020 to 2100.

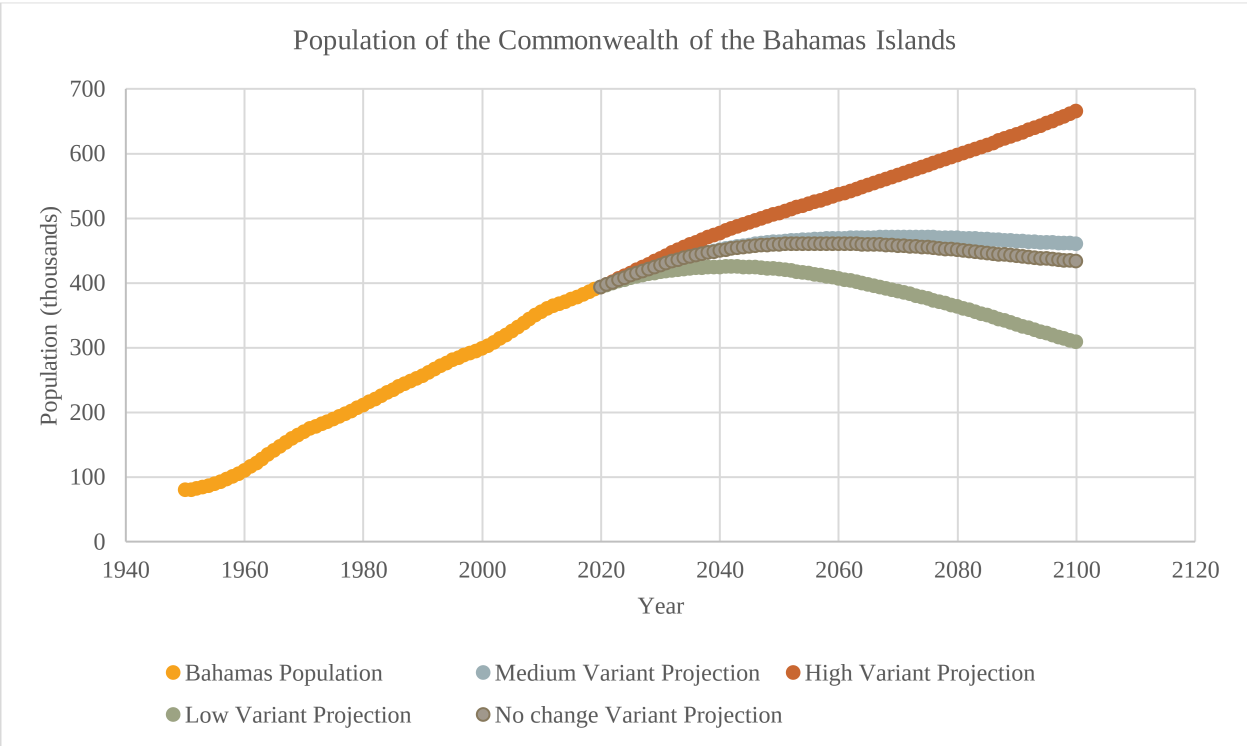

Figure 20. Population of the Commonwealth of the Bahamas (UNPD 2019).

The population has been increasing nearly linearly since 1950. The expectation is for the projected population to level off and begin declining in the future, except for the high variant which continues to increase. The GAAPP and the annual population is used to estimate the value of the exposed assets in the amount of plastic material in the Commonwealth of the Bahamas, as seen in Fig. 21.

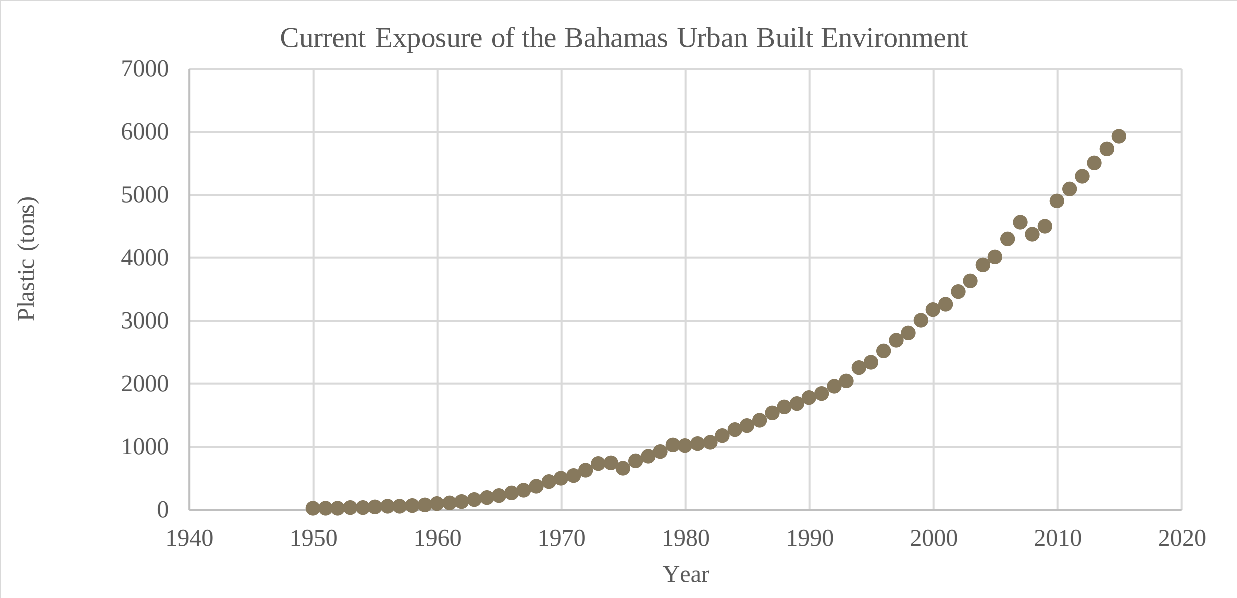

Figure 21. The current amount of exposure in the Bahamas Islands in terms of PMD. The total plastic and UBE plastic in the Bahamas are the same because the islands are relatively flat and therefore all plastic could be open for transport, rather than that just in the UBE as construction and consumer uses.

In 2000, the amount of plastic produced was 3.2 thousand tons and, in 2015, 5.9 thousand tons of plastic is estimated to be introduced into the coastal zone. The value of the exposed assets, in terms of plastic tons, is projected to continue increasing. The future value of exposed assets is estimated through population scenarios and the GAAPP from 2015. This would result in low-end estimations of the plastic material.

4.3.4 RISK OF PLASTIC MARINE DEBRIS FROM THE BAHAMAS URBAN BUILT ENVIRONMENT

The variables of the risk assessment associated with the case study of the Bahamas have been discussed. To estimate the risk for the Bahamas, a few scenarios have been created. The scenarios include the probability of 1 or more cyclones occurring (Table 5), the strength of storms related to Hurricane Dorian (Table 9), and the amount of debris that enters the ocean (Fig. 21). The storm strength scenarios were created because there was a lack of information that related hurricane storm strength to amount of damage in the Bahamas. The hurricane categories are related to maximum sustained wind speeds (NHC 2021c). The resulting damage does not have a known scale and is different for every storm depending on winds speed, momentum across an area, and storm surge. The scenarios are created to understand the risk of cyclonic damage related to a hurricane category rather than the cyclone sustained wind speeds. All scenarios assess the risk associated with 1 or more cyclones storms occurring in 30 years (2050), and 80 years (2100), and 200 years (2220) as seen in Fig. 22.

4.4 CASE STUDY: JAKARTA, INDONESIA

Jakarta, Indonesia is located in a tectonically active area. However, the hazard that threatens this coast is that of SLR, due mainly to land subsidence. The case study of Jakarta is different from the other two because the hazard is continuous, compared to the discrete events, and the fragilities are based on the retreat plan, rather than from an event. Jakarta is the first city to plan a retreat and this risk assessment identifies the risk of this retreatment in Jakarta.

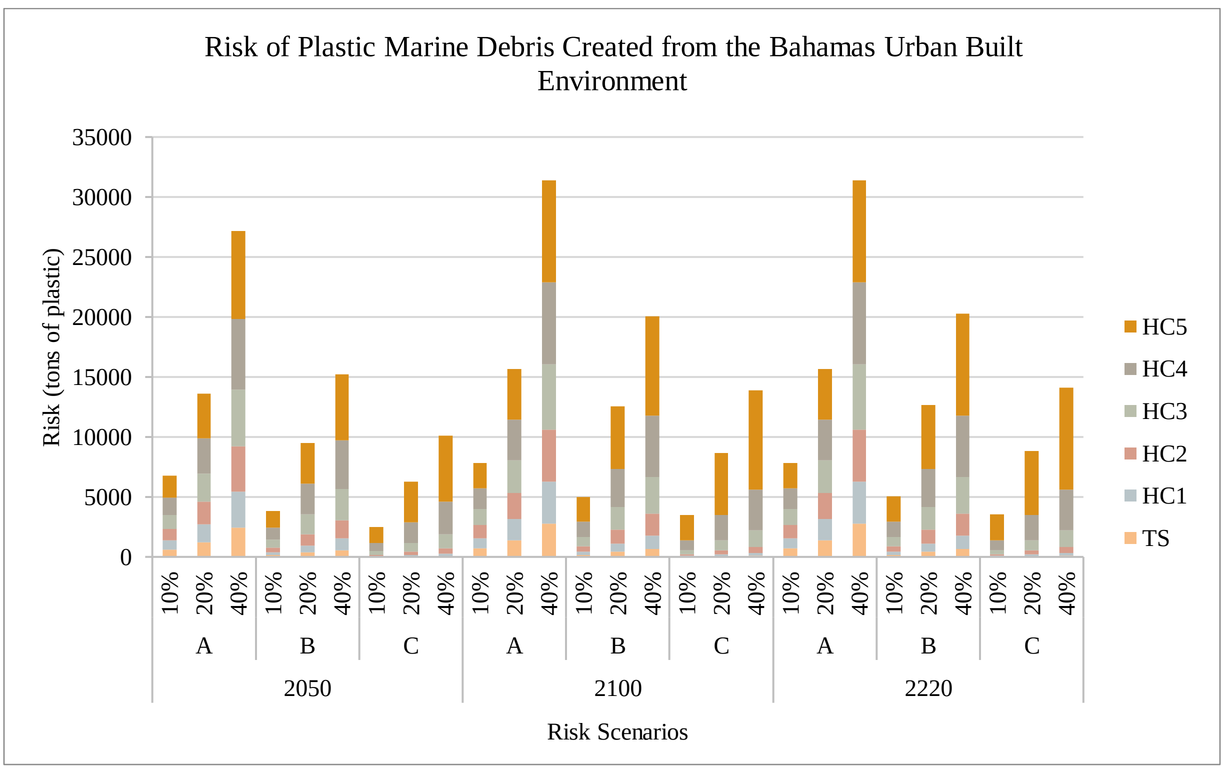

Figure 22. Risk Scenarios. Risk of 1 or more cyclone events making landfall in the Bahamas Islands in 30, 80, and 100 years where HCa creates A (40%), B(60%), or C(80%) of the damages as $HC_{(a+1)}$ and the fragilities are 10%, 20%, and 40% of the damaged material enters the ocean.

4.4.1 HAZARD PROBABILITY DENSITY FUNCTION

Flooding is a major hazard in Jakarta, Indonesia that will continue to increase as land subsidence continues. In this case, it is important to understand that the river flood events are not insignificant, but the impact of land subsidence is greater. To understand the probability of flooding specifically, the PDF of flood events is established using the discrete event method, the Poisson Distribution Equation. Data regarding the flood events is taken from EM-DAT, the International Disaster Database hosted by Centre for Research on the Epidemiology of Disasters (CRED) (CRED 2021). First, the PDF of flood events from EM-DAT identifies the flooding in all of Indonesia, by area. The database also lists the number of people affected for nearly all the events and for some events, the amount of area the flood covers (km^2) is listed (CRED 2021). The PDF by size of flood event cannot yet be distinguished. An assumption can be made that flood events are greater than 0.5 m because less than this is not notable. The Poisson Eq. (2) of these events is outlined in Table 10.

Table 10. Poisson Probability of no events, 1 event, and 1 or more events occurring in 10, 30, 80, and 200 years.

Poisson Probability							
k = x	t	year	R	μ	no events in t years	1 event in t years	1 or more events in t years
0	30	2050	0.289	104	7.68E-46	7.98E-44	1.00E+00
1	80	2100		277	4.94E-121	1.37E-118	1.00E+00
	200	2220		693	1.72E-301	1.19E-298	1.00E+00

Land subsidence in Jakarta is occurring rapidly but not regularly over the city (Abidin *et al.* 2015). There is a range of subsidence rates over the city area ranges from 1-10 cm/yr (Abidin *et al.* 2015). The average change is 2.5cm/yr (Budiyono *et al.* 2016). The hazard scenarios (Fig. 23) are 2.5 cm/yr, 3 cm/yr, 5 cm/yr, 7 cm/yr, 10 cm/yr to reach the range of land subsidence rates.

The hazard of flooding is changing presently and in the future due to land. There is not a single database for land subsidence in Indonesia for years 1950-2020, but Abidin *et al.* (2001)

gives data for 1982, 1991, and 1997 and Abidin *et al.* (2015) provides more recent estimations. Budiyono *et al.* (2016) also discusses the risk of flooding in Jakarta, including land subsidence, precipitation, sea level, and land usage. Rainfall and precipitation are expected to change in the future as well. Budiyono *et al.* (2016) provides analysis and data for precipitation PDF. Land subsidence is a continuous variable; therefore, the probability is 1 because the subsidence will continue. Scenarios of land subsidence rates have been created in Fig. 23.

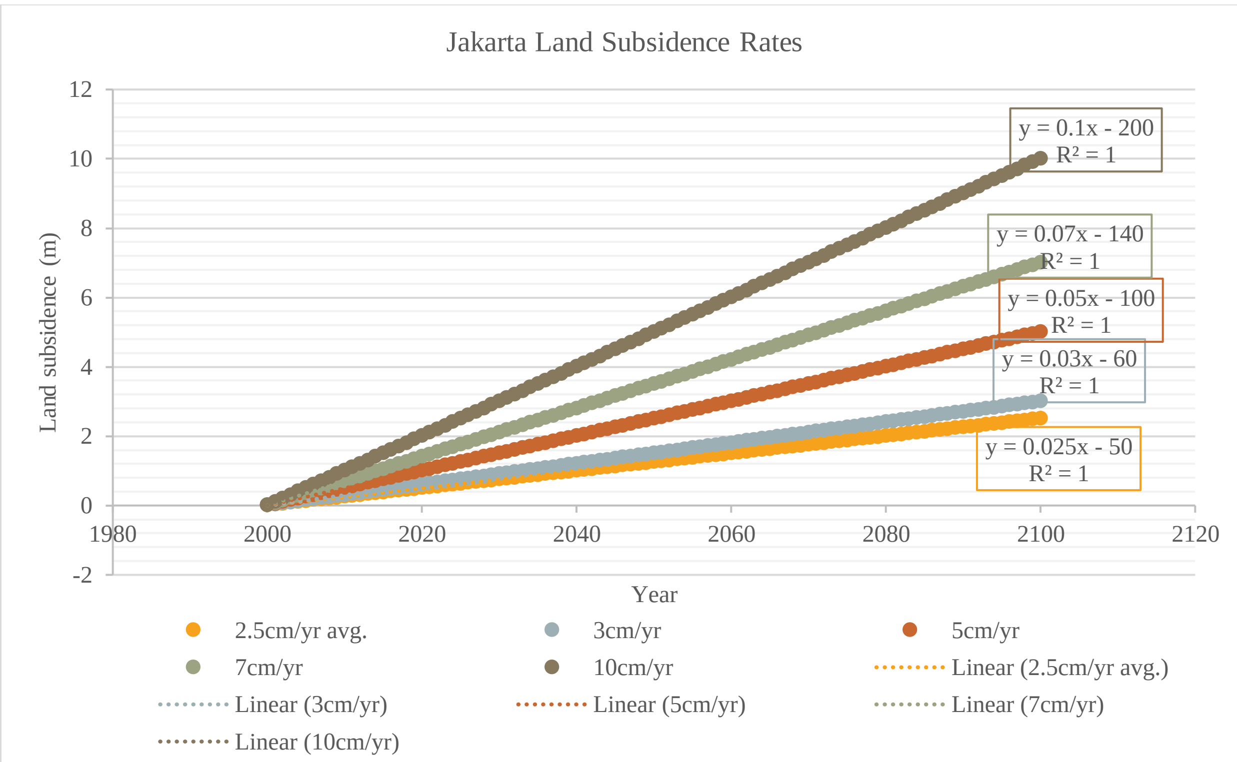

Figure 23. Land subsidence data for 2.5cm/yr (Budiyono *et al.* 2016), 3 cm/yr, 5 cm/yr, 7 cm/yr, 10 cm/yr (Abidin *et al.* 2015).

The probability of land subsidence is 1. However, the rate of subsidence is varied in different parts of the city. The risk assessment using the fragilities to understand this variation in terms of risk of PMD.

4.4.2 LAND SUBSIDENCE, PRESENT DAY

THE HAZARDOUS EVENT

While Indonesia is located in a very tectonically active area which includes many potential hazards such as earthquakes, tsunamis, and volcanoes, the hazard this study focuses on is flooding. Flooding in this case study is caused mainly by land subsidence and, to a small degree, precipitation resulting in river floods (Budiyono *et al.* 2016). The first two case studies represent short-term single events that have resulted in a disaster. For this case, the hazard is ongoing and therefore the disaster is ongoing. Historically, Jakarta has had reports of flooding as early as 1621 (BBWS,2014). In the 1800s a few large flood events occurred which resulted in the Dutch government creating dams and flood canals (Asdak *et al.* 2018). The monsoon rains have been a cause of this flooding; however, the monsoon rains are growing heavier which has already resulted in severe river flooding in 1996, 2002, 2007, 2013, and 2014 (Asdak *et al.* 2018) due to the rivers at full capacity. The hazardous event that determines fragilities is the land subsidence that inundates the city. The fragilities are identified through scenarios of retreat. These scenarios ask the question: How much material is left behind after the retreatment begins?

THE RESULTING DISASTER

The fragilities from land subsidence are determined through scenarios of material loss. However, the river flood events in January 2013 resulted in 40 deaths and 45,000 refugees, and substantial economic damage (Kure *et al.* 2014), caused a loss of 15 billion IDR (Oppusunggu & Tantular 2015). In February 2007, extensive economic loss between 4.1 and 7.3 billion IDR (Sagala *et al.* 2013) and a calamity loss reached 100 mill IDR per day (Oppusunggu & Tantular 2015). The disasters described here show a small amount of the damage of the UBE created by flooding.

FRAGILITIES OF THE URBAN COAST

Land subsidence is, and will continue, to cause the largest disaster. However, this is dependent on the amount of material left behind. The fragilities (Table 11) of the coastal UBE in Jakarta, Indonesia are identified from scenarios based on the percent material left behind. All of the material left behind during a retreat will enter the ocean, so this is the fragility itself.

Table 11. The fragility scenarios of the UBE of Jakarta where different portions of material are left behind.

Retreat Scenarios	***Material Left Behind***
A	*20%*
B	*30%*
C	*40%*
D	*50%*
E	*60%*
F	*70%*
G	*80%*
H	*90%*

With a faster subsidence rate, it can be assumed that the amount of material left behind is greater. There is less time to deconstruct the buildings and remove the plastic material from the coastal zone. The high-end scenarios represent the largest amount of material left behind with the varying subsidence rate. The medium scenario represents the amount of material left behind if guidance and some care was put into the removal of the city's material. The low-end scenario represents the amount where a lot of precautions are taken to remove the plastic from the coastal zone. These scenarios have no evidential basis, as retreatment of this size has not been executed before. The percentages provide for an estimation of the fragilities of the UBE.

4.4.3 VALUE OF THE EXPOSED ASSETS

This case study focuses specifically in Jakarta, Indonesia, a city with a maximum elevation of 60 m (Yamazaki *et al.* 2021). The coastal zone is defined as the entire city. To estimate the value of exposed assets in terms of amount of plastic in the city, the population has to be extracted for the city, specifically. The UNPD (2019) specifies population by country, not by city. However, it is still used to understand the portion of the population living in Jakarta compared to the country as a whole. The population of Jakarta was used from World Population Review (WPR 2021).

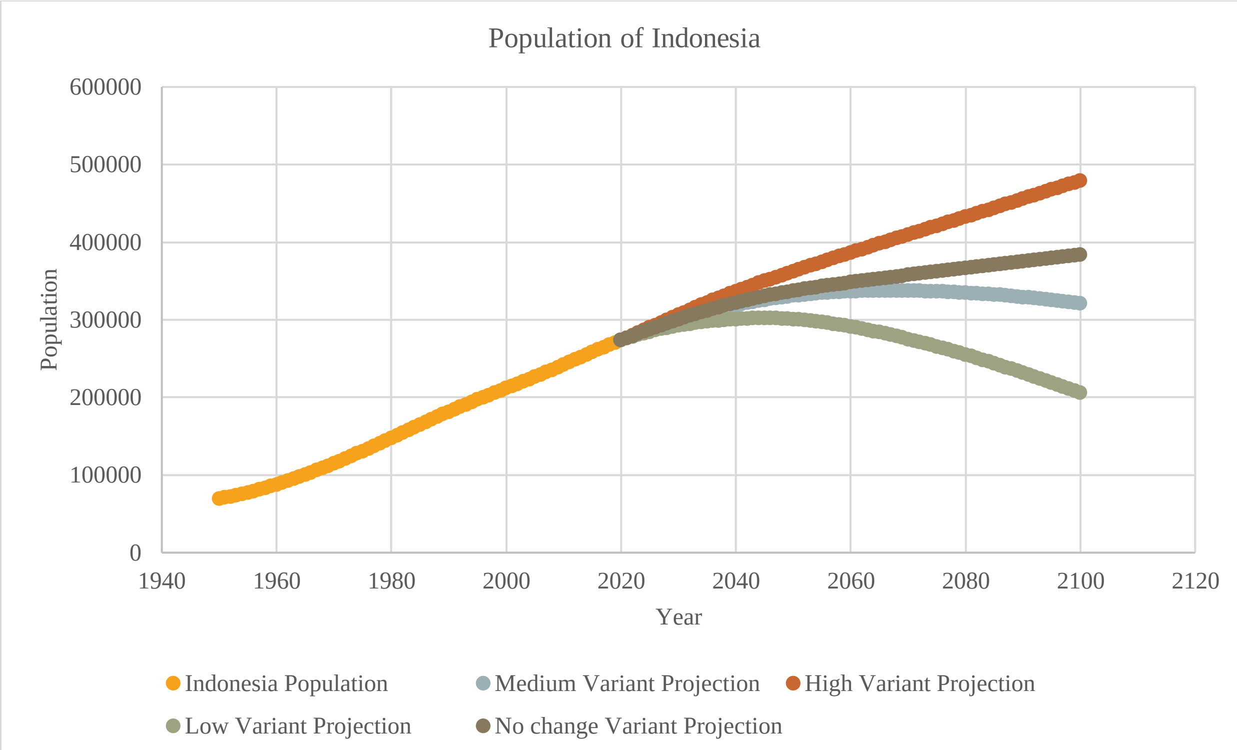

Figure 24. Population of Indonesia (UNPD 2019).

The population in Indonesia in 1950 was 69,543,321 and in 2015 the population was 258,383,257 people, while the population in the city ofJakarta in 1950 was 1,452,000 and in 2015 it was 10,173,388 people. Fig. 24 shows the population in Indonesia from 1950 to 2015 and Fig. 25 is the population in Jakarta for the same time span. Understanding that the portion of the population living in Jakarta ranges is approximate 3.9% in 2010, this proportion is applied to the UNPD (2019) projections from 2016 to 2100 in order to determine the possible population in Jakarta. Again, this assumption says the ratio between total population and the population in Jakarta remains the same, however, the retreat plans have not been identified and therefore the population projections are unknown. The most influential variable here is fragilities determining the amount of material left behind.

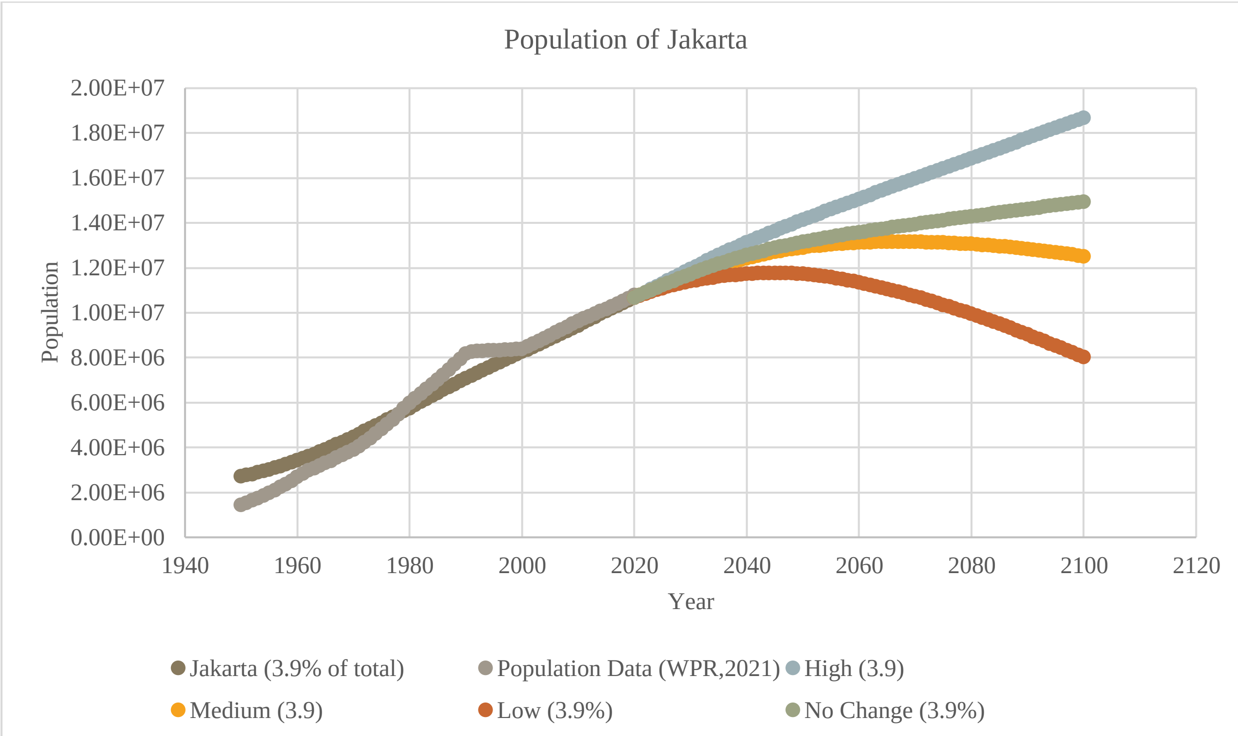

Figure 25. Population of Jakarta, Indonesia (WPR 2021).

The population of Jakarta is multiplied by the estimated amount of plastic per person in the UBE. Fig. 26 shows the results. The value of the exposed assets in 2000 is 89.3 thousand tons of plastic while the amount of plastic in 2015 is 161.2 thousand tons.

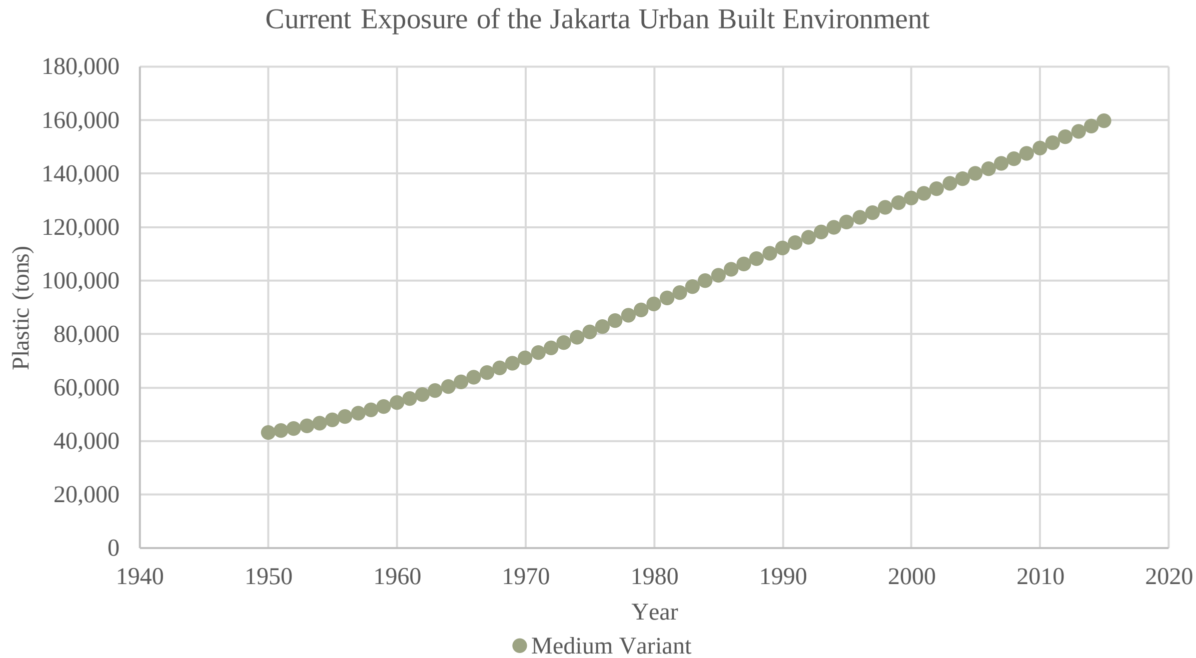

Figure 26. The amount of exposed assets annually in the Jakarta, Indonesia (the UBE) in terms of tons of plastic.

4.4.4. RISK OF PLASTIC MARINE DEBRIS FROM THE JAKARTA, INDONESIA URBAN BUILT ENVIRONMENT

The risk in Jakarta, Indonesia is not determined the same way as Japan or the Bahamas because the probability of hazards is not the same. Jakarta's current and future hazard is land subsidence. This is an ongoing observation of the land that is causing extreme local sea level rise that will continue to rise at a steady pace. While different parts of the city are sinking at varying rates, the probability of occurrence is 1. The assumptions made to estimate this risk include that the land will continue subsiding, and that the value of the exposed assets is the sum of the annual plastic production between 2005 and 2015. While there is a waste variant not included, there is plastic older than that introduced in 2005 in the system and there is new plastic continuing to be introduced. The assumption that the total plastic for this timespan is reasonable, and likely a conservative estimate of the value of exposed assets. The scenarios in this case are based on the fragilities. Jakarta is retreating due to the rapidly rising sea level, the portion of material that is left behind during this retreatment is unknown and therefore a scenario approach is used (Fig. 27). The fragilities range from 20% to 90%. With a rapid land subsidence, it is likely that much of the material will remain, however, it can be assumed that at least 10% of the plastic will retreat with the people. With a slower subsidence rate, there is time to deconstruct the UBE and remove the harmful materials of the coast, potentially leave only 20% of the plastics. There is not a component that further estimates how much of this material enters the ocean because if it is left behind, it will be inundated and in the ocean system.

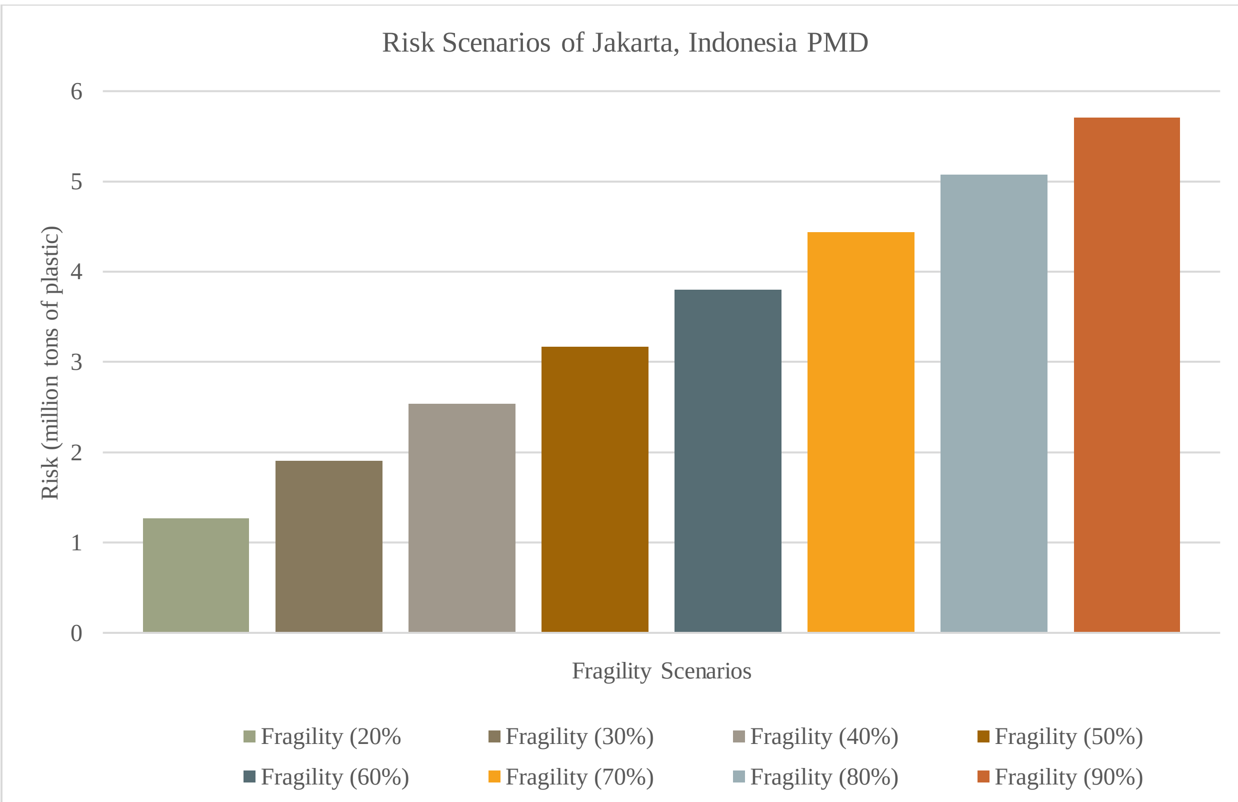

Figure 27. Risk graph showing scenarios of fragilities. The fragilities are based on how much material is left behind during retreatment (20% to 90%).

CHAPTER 5

DISCUSSION

The risk of PMD originating in the urban coast is increasing. The urban coastal zone is growing. Population is increasing and therefore the materials that potentially could result in PMD in the coastal in the coastal zone are growing. The use of plastic in the built environment and in consumer goods has resulted in the increase of plastic production per person, globally. When considering the coastal UBE, this increase of plastic poses a great risk to the marine biosphere.

To estimate this risk quantitatively in terms of the amount of PMD that might enter the ocean and impact the marine biosphere from the urban environments a risk equation with three distinct factors was utilized: PDFs of a hazard to the UBE, the fragilities of the UBE to the relevant hazards, and the value of the exposed assets expressed in the amount of plastic stored in these assets. Typically, the fragilities and the value of exposed assets are discussed and determined in terms of cost, whereas this study determines value in terms of amount of plastic.

Historically, on human timescales, the coastal zone has experienced hazards such as cyclones, river flooding, and storm surges. However, thechanging climate has allowed for a changing hazard spectrum. Cyclones are increasing in intensity and therefore, are allowing for more tropical storms to become stronger category hurricanes. While some hazards are not expected to have major changes in occurrence, such as earthquakes and tsunamis, growing coastal UBEs and the fragilities within them still allow for changing risks.

The fragilities have been established through understanding the impact of hazardous events on a system and creating scenarios to estimate potential fragilities that allow for PMD to enter the ocean. The Tohoku tsunami in 2011 that impacted the Japanese coast allowed for an understanding of varying wave height impact on the UBE. Hurricane Dorian, the largestknown hurricane, detailed the impact of a HC5 on the Bahamas Islands. While these were event based, understanding the fragilities of a case study with an ongoing hazard is dependent on scenarios regarding the amount of material left behind during retreatment.

The research conducted here attempted to estimate the amount of plastic in the urban coast through a detailed model of the UBE. However, the lack of data regarding the use of plastics did not allow for a full SFM to be calibrated and validated. Instead, a generalized estimate for the amount of plastic in the coastal UBE was created in three case study locations using population and plastic amounts per person. The plastic amount per person was estimated based on the available data on production over time. There was not data available for understanding plastic production and usage independent of PlasticsEurope, the organization of the plastic producing companies that account for nearly 90% of the plastic producers. Instead, the estimation of the exposed assets relies on general, global annual average amount of plastic produced per person. This was then applied to the case study locations with coastal population estimates.

The risk assessment established an understanding of how much plastic is potentially in the coastal zone. In Japan, with 1 or more tsunami waves of 1 m - 2m, the conservative risk scenario of a wave height creating 1% of the damage that the Tohoku tsunami created and only 10% of that entering the ocean is 369 tons of plastic moving from the UBE to the ocean in 10 years. When looking at the conservative risk scenario in the Bahamas Islands, 1 or more tropical storms creating 40% of the damage that Hurricane Dorian did in the next 10 years results in 9 to 37 tons of plastic (10% - 40% of damaged material) entering the ocean. Understanding the risk in Jakarta is not by time, but by retreatment type. Conservatively, if 20% of the UBE is left behind 272,844 tons of PMD is created. If only a quarter of Jakarta retreats and leave 20% of the UBE behind and 1 or more tsunamis with a wave height less than 2 meters occurs in Japan and 1 or more tropical storm occurs in the Bahamas and creates 1% of the damage of Dorian, approximately 69,000 tons of plastic are at risk of becoming PMD. This poses a significant hazard to the ocean and the marine biosphere.

When considering the risk globally, this risk of plastic originating in the coastal zone poses a major hazard to the ocean, which adds to the other anthropogenic hazards such as acidification, heating, and nutrient overload. By 2100, it is projected that eight of the 10 largest cities are in the coastal zones. Even without the hazards of cyclones or regular tsunamis, the growing exposure creates a GCR of plastic entering the marine biosphere from the UBE. The risk assessment has made clear that 1. plastic production and usage is not being monitored; 2. climate change poses a change spectrum of hazards to the coastal zones; 3. the risk associated with plastic accumulating in the coastal zone poses a severe hazard to the ocean and future generations.

REFERENCES

Abidin, H. Z., Djaa, R., Darmawan, D., Hadi, S., Akbar, A., Rajiyowiryono, H., Sudibyo, Y., Meilano, I., Kasuma, M. A., Kahar, J., & Subarya, C. (2001) Land subsidence of jakarta (indonesia) and its geodetic monitoring system, *Nat.Haz.*, **23**, 265–387.

Abidin, H. Z., Andreas, H., Gumilar, I., & Brinkman, J. J. (2015) Study on the risk and impacts of land subsidence in jakarta, *Proc. IAHS*, **372**, 115–120.

Asdak, C., Supian, S., & Subiyanto, (2018) Watershed management strategies for flood mitigation: a case study of jakarta's flooding, *Weather Clim. Extremes*, **21**, 117–122.

Avila, L. A., Stewart, S. R., Berg, R., & Hagen, A. B. (2020) National hurricane center tropical cyclone report tropical storm dorian (AL042013), Tech. rep., *National Hurricane Center*, Available at https://www.nhc.noaa.gov/data /tcr/AL052019Dorian.pdf.

Avin, B., Wintle, B. C., Weitzdorfer, J., Heigeartaigh, S.O., Sutherland, W. J., & Rees, M. J. (2018) Classifying global catastrophic risks, *Futures*, DOI: 10.1016/j.futures.2018.02.001.

Baart, F., Bakker, M. A. J., van Dongeren, A., den Heijer, C., van Heteren, S., Smit, M. W. J., van Koningsveld, M., & Pool, A. (2011) Using 18th century storm-surge data from the dutch coast to improve the confidence in flood-risk estimates, *Nat. Hazards Earth Syst. Sci.*, **11**(10), 2791–2801.

Baztan, J., Chouinard, O., Jorgensen, B., Tett, P., Vanderlinden, J., & Vasseur, L. (2015) Introduction, in *Coastal Zones*, ed. J Baztan, J., Chouinard, O., Jorgensen, B., Tett, P., Vanderlinden, J., & Vasseur, L., pp. xxi- xxiii, Elsevier. DOI: 10.1016/B978-0-12-802748-6.02001-5.

Bevacqua, E., Maraun, D., Vousdoukas, M. I., Voukouvalas, E., Vrac, M., Mentaschi, L., & Widmann, M. (2019) Higher probability of compound flooding from precipitation and storm surge in europe under anthropogenic climate change, *Sci. Adv.*, **5**(9), 1-7.

British Geological Survey (2021) What causes earthquakes? discovering geology - earthquakes, *United Kingdom Research and Innovation (UKRI)*. Available at: https://www.bgs.ac.uk/discovering-geology/earth-hazards/earthquakes/what-causes-earthquakes.

Bostrom, N. & Cirkovic, M. (2008) Introduction, in *Global Catastrophic Risks* ed. Bostrom, N. & Cirkovic, M., pp. 1-30, Oxford University Press. Available at: http://global-catastrophic-risks.com/docs/Chap01.pdf.

Britannica (2021) Indonesia, *Encyclopedia Britannica*. Available at: https://www.britannica.com /place/Indonesia.

Brown, V., Harris, J., & Russell, J. (2010) *Tackling Wicked Problems: Through the Transdisciplinary Imagination*, London, UK: Taylor & Francis.

Budiyono, Y., Aerts, J. C. J. H., Tollenaar, D., & Ward, P. J. (20160 River flood risk in jakarta under scenarios of future change, *Nat. Hazards Earth Syst. Sci.*, **16**(3), 757–774.

CRED (2021) Flood events in indonesia, *EM-DAT: Centre for Research on the Epidemiology of Disasters (CRED).* Available at: https://www.emdat.be. Accessed 08.2021.

DHHS (2004) Obesity and the built environment, *Department of Health and Human Services.* Available at http://grants.nih.gov/grants/guide/rfa-files/RFA-ES-04-003.html, RFA-ES-04-003.

Emanuel, K. (2003) Tropical cyclones, *Annu. Rev. Earth Planet Sci.*, **31**(1), 75–104.

Engler, R. E. (2012) The complex interaction between marine debris and toxic chemicals in the ocean, *Environ. Sci. Technol.*, **46**(22), 12302 12315, PMID: 23088563.

Foulger, G. R., Wilson, M. P., Gluyas, J. G., Julian, B. R., & Davies, R. J. (2018) Global review of human-induced earthquakes, *Earth Sci. Rev.*, **178**, 438 – 514.

Frame, D., Rosier, S., Noy, I., Harrington, L., Carey-Smith, t., Sparrow, S., Stone, D., & Dean, S. M. (2020) Climate change attribution and the economic costs of extreme weather events: a study on damages from extreme rainfall and drought, *Clim. Chang.*, **162**, 781–797.

Frihy, O. & El-Sayed, M. (2013) Vulnerability risk assessment and adaptation to climate change induced sea level rise along the mediterranean coast of egypt, *Mitigation Adapt. Strategies Global Change*, **18**, 1215 - 1237.

Geyer, R., Jambeck, J., & Law, K. (2017) Production, use, and fate of all plastics ever made, *Sci. Adv.*, **3**(7), 1-5. DOI: 10.1126/sciadv.1700782.

Geyer, R., Jambeck, J., & Law, K. (2017) Supplemental materials for: Production, use, and fate of all plastics ever made, *Sci. Adv.*, **3**(7), 1-5. DOI: 10.1126/sciadv.1700782.

Goldewijk, K. K., Beusen, A., Doelman, J., & Stehfest, E. (2017) Anthropogenic land use estimates for the holocene; hyde 3.2, *Earth Syst. Sci. Data*. **9**(2). 927-953.

Government of the Bahamas, (2011) Overview of the bahamas, *Government of The Bahamas (GOB)*, Available at: Overview of The Bahamas.

Government of the Bahamas (2012) 2010 census of population and housing, (No. 1), The Commonwealth of the Bahamas: Department of Statistics.

Grinsted, A., Moore, J. C., & Jevrejeva, S. (2013) Projected atlantic hurricane surge threat from rising temperatures, *PNAS*, **110**(14), 5369–5373.

Haasnoot, M., Brown, S., Scussolini, P., Jimenez, J. A., Vafeidis, A. T., & Nicholls, R. J. (2019) Generic adaptation pathways for coastal archetypes under uncertain sea-level rise, *Environ. Res. Commun.*, **1**(7), 071006.

Hall (2014) Indonesia tectonics: subduction, extension, provenance and more, ed. Southeast Asia Research Group. Proceedings of the *Indonesian Petroleum Association 38th Annual Convention and Exhibition*, Available at http://searg.rhul.ac.uk/pubs/hall 2014

Hallegatte, S., Ranger, N., Mestre, O., Dumas, P., Corfee-Morlot, J., Herweijer, C., & Muir Wood, R. (2011) Assessing climate change impacts, sea level rise and storm surge risk in port cities: a case study on copenhagen., *Clim. Chang.*, **104**, 113-137.

Hampel, A., Hetzel, R., & Maniatis, G. (2010) Response of faults to climate- driven changes in ice and water volumes on earth's surface, *Philos. Trans. R. Soc. London, Ser. A*, **368**, 2501–2517.

Hinrichsen, D. (1999) The coastal population explosion, in Trends and Future Challenges for U.S. National Ocean and Coastal Policy, *The Next 25 Years: Global Issues*.

Holland, G. & Bruyére, C. L. (2014) Recent intense hurricane response to global climate change, *Clim. Dyn.*, **42**, 617-627.

Hsu, T.-W., Shih, D.-S., Li, C.-Y., Lan, Y.-J., & Lin, Y.-C. (2017) A study on coastal flooding and risk assessment under climate change in the mid- western coast of taiwan, *Water*, **9**(390). 1-13.

Hunt, A. & Watkiss, P. (2011) Climate change impacts and adaptation in cities: a review of the literature, *Clim. Chang.*, **104**, 13-49.

IDB (2019) Assessment of the effects and impacts of hurricane dorian in the bahamas: executive summary, *Inter-American Development Bank.* Available at http://idbdocs.iadb.org/wsdocs /getdocument.aspx?docnum=EZSHARE-1256154360-486.

IPCC (2007) *Climate Change 2007: Synthesis Report. Contribution of Working Groups I, II and III to the Fourth Assessment Report of the Intergovernmental Panel on Climate Change*. [Core Writing Team, Pachauri, R.K and Reisinger, A. (eds.)]. IPCC, Geneva, Switzerland.

Jensen, J. & Muller-Navarra, J. (2008) Storm surges on the german coast, *Die Kuste*, **74**, 92 – 124.

Kishtawal, C. M., Jaiswal, N., Singh, R., & Niyogi, D. (2012) Tropical cyclone intensification trends during satellite era (1986–2010), *Geophys. Res. Lett.*, **39**(10).

Koshimura, S., Hayashi, S., & Gokon, H. (2014) The impact of the 2011 tohoku earthquake tsunami disaster and implications to the reconstruction, *Soils Found.*, **54**(4), 560–572.

Kundu, B., Vissa, N. K., & Gahalaut, V. K. (2015) Influence of anthropogenic groundwater unloading in indo-gangetic plains on the 25 april 2015 mw 7.8 gorkha, nepal earthquake, *Geophys. Res. Lett.*, **42**(24), 10,607– 10,613.

Kure, S., Farid, M., Fukutani, Y., Muhari, A., Bricker, J., & Udo, K. (2014) Several social factors contributing to floods and characteristics of the january 2013 flood in jakarta, indonesia, *Japan Soc. Civil Engin. P. Global Environ.*, **70**, 211–217.

Leopold, L. B.(1994) Flood hydrology and the floodplain, *J. Contemp. Water Res. Ed.* University *of California*, **95**(1), 11-14.

Liu, C., Linde, A. T., & Sacks, I. S. (2009) Slow earthquakes triggered by typhoons, *Nature*, **459,** 833–836.

Lujala, P., Lein, H., & Rød, J. K. (2015) Climate change, natural hazards, and risk perception: the role of proximity and personal experience, *Local Environ.*, **20**(4), 489–509.

Marsooli, R., Lin, N., Emanuel, K., & Feng, K. (2019) Climate change exacerbates hurricane flood hazards along us atlantic and gulf coasts in spatially varying patterns, *Nat. Comm.*, **10**(3785).

Martin, D. (2021) Plasticseurope, Personal Communication.

McGranahan, G., Balk, D., & Anderson, B. (2007) The rising tide: assessing the risks of climate change and human settlements in low elevation coastal zones, *Environ. Urban.*, **19**(1), 17–37.

Merriam-Webster (2020) Fragile, *Merriam-Webster*, available at: www.merriam-webster.com /dictionary/fragile.

Merriam-Webster (2020) Hazard, *Merriam-Webster*, available at: www.merriam-webster.com /dictionary/hazard.

MIAC (2020) *Statistical Handbook of Japan*, Statistics Bureau, Ministry of Internal Affairs and Communications (MAIC).

Mimura, N., Yasuhara, K., Kawagoe, S., Yokoki, H., & Kazama, S. (2011) Damage from the great east japan earthquake and tsunami - a quick report, *Mitigation Adapt. Strategies Global Change*, **16**, 803-818.

NCEI (2021) National geophysical database center: Global historical tsunami database, *National Oceanic and Atmospheric Administration: National Centers for Environmental Information.* doi:10.7289/V5PN93H7.

Neely, W. & Read, B. (2019) *The Greatest and Deadliest Hurricanes to Impact the Bahamas: The Stories Behind the Great Storms*, ebook: iUniverse.

Neumann, B., Vafeidis, A., Zimmermann, J., & Nicholls, R. (2015) Future coastal population growth and exposure to sea-level rise and coastal flooding - a global assessment, *PLoS ONE*, **10**(3).

NHC (2021) Storm surge overview. *National Oceanic and Atmospheric Administration National Hurricane Center (NHC).* Retrieved June, 2021, from https://www.nhc.noaa.gov/surge/.

NHC (2021) Saffir-simpson hurricane wind scale. *National Oceanic and Atmospheric Administration National Hurricane Center (NHC).* Retrieved June, 2021, from https://www.nhc.noaa.gov/aboutsshws.php.

NHC (2021) Tropical cyclone climatology. *National Oceanic and Atmospheric Administration National Hurricane Center (NHC).* Retrieved July, 2021, from https://www.nhc.noaa.gov/climo/.

NHC (2021) About the national hurricane center. *National Oceanic and Atmospheric Administration National Hurricane Center (NHC).* Retrieved June, 2021, from https://www.nhc.noaa.gov /aboutintro.shtml.

Nilsson, C. & Grelsson, G. (1995) The fragility of ecosystems: A review, *J. Appl. Ecol.*, **32**(4), 677-692.

NOAA (2014) Marine debris program: Modeling the movement of tsunami debris. *National Oceanic and Atmospheric Administration (NOAA) Office of Response and Restoration.* Retrieved August, 2021, from https://marinedebris.noaa.gov/japan-tsunami-marine-debris/modeling-movement-tsunami-debris.

NOAA (2021) Tsunamis. *National Oceanic and Atmospheric Administration (NOAA)*. Retrieved August, 2021, from https://www.noaa.gov/education/resource-collections/ocean-coasts/tsunamis.

NOAA (2021) Historical hurricane tracks. *National Oceanic and Atmospheric Administration*

(NOAA) Office of Coastal Management DigitalCoast. Retrieved August, 2021, from https://coast.noaa.gov/digitalcoast/tools/hurricanes.html.

Norio, O., Ye, T., Kajitani, Y., Shi, P., & Tatano, H. (2011) The 2011 eastern japan great earthquake disaster: Overview and comments, *International Journal of Disaster Risk Science*, **2**(1), 34-42.

National Police Agency (2011) Police countermeasures and damage situation associated with 2011 tohoku district - off the pacific ocean earthquake march 10, 2021, National Police Agency of Japan Emergency Disaster Countermeasures Headquarters

NSIDC (2021) Cryosphere glossary: isostatic rebound, *National Snow & Ice Data Center*. Retrieved March, 2021, from https://nsidc.org/cryosphere/glossary/term/isostatic-rebound

Oppusunggu, R. & Tantular, R. (2015) Creating people's awareness and pushing active contribution. case: Wider public engagement on flood and land use problems in jakarta and surroundings, *Proc. Social Behav. Sci.*, **184**, 240-244.

Paping, R. (2014) cities and countryside, in *General Dutch Population development 1400-1850, 1st ESHD conference*. Conference date: 15-09-2014 Through 17-09-2014.

Pfahl, S., O'Gorman, P., & Fischer, E. (2017) Understanding the regional pattern of projected future changes in extreme precipitation, *Nat. Climate Chang.*, **7**, 423–427.

Pinto, C. A. & Garvey, P. R. (2012) *Advanced Risk Analysis in Engineering Enterprise Systems*, CRC Press: Kindle Edition.

Plag, H.-P. & Jules-Plag, S. (2013) Sea-level rise and coastal ecosystems, in *Climate Vulnerability: Understanding and Addressing Threats to Essential Resources*, ed. R. A. Pielke Sr., T. Seastedt, & K. Suding, **4**, 163-184, Elsevier.

PlasticsEurope (2021) About us: Who we are, *PlasticsEurope.* Retrieved September, 2021, from https://www.plasticseurope.org/en/about-us/who-we-are.

Rekacewicz, P. (2002) Human actions leading to coastal degradation, *GRID-Arendal*. Retrieved November, 2019, from https://www.grida.no/resources/5631.

Ritchie, H. & Roser, M. (2018) Urbanization, *Our World in Data*. Retrieved December, 2020, from https://ourworldindata.org/urbanization.

Rittel, H. & Webber, M.(1972) Dilemmas in a general theory of planning, *Policy Sci.*, **4**(2), 155-169.

Rockstrom, J., Steffen, W., Noone, K., Persson, A., Chapin, F. S., Lambin, E. F., Lenton, T. M., Scheffer, M., Folke, C., Schellnhuber, H. J., Nykvist, B., de Wit, C. A., Hughes, T., van der Leeuw, S., Rodhe, H., Sorlin, S., Snyder, P. K., Costanza, R., Svedin, U., Falkenmark, M., Karlberg, L., Corell, R. W., Fabry, V. J., Hansen, J., Walker, B., Liverman, D., Richardson, K., Crutzen, P., & Foley, J. A. (2009) A safe operating space for humanity, *Nature*. **461**, 472–475.

Roser, M., Ritchie, H., & Ortiz-Ospina, E. (2013) World population growth, *Our World in Data*. Retrieved December, 2019, from https://ourworldindata.org/world-population-growth.

Robke, B. & Vott, A. (2017) The tsunami phenomenon, *Prog. Oceanogr.*, **159**, 296 – 322.

Sagala, S., Lassa, J., Yasaditama, H., & Hudalah, D. (2013) The evolution of risk and vulnerability in greater jakarta: Contesting government policy in dealing with a megacity's exposure to flooding, *IRGSC Working Paper*. **2**,18.

Sale, P. F., Agardy, T., Ainsworth, C. H., Feist, B. E., Bell, J. D., Christie, P., Hoegh-Guldberg, O., Mumby, P. J., Feary, D. A., Saunders, M. I., Daw, T. M., Foale, S. J., Levin, P. S., Lindeman, K. C., Lorenzen, K., Pomeroy, R. S., Allison, E. H., Bradbury, R., Corrin, J., Edwards, A. J., Obura, D. O., Sadovy de Mitcheson, Y. J., Samoilys, M. A., & Sheppard, C. R. (2014) Transforming management of tropical coastal seas to cope with challenges of the 21st century, *Mar. Pollut. Bull.*, **85**(1), 8–23.

Sheavly, S. B. & Register, K. (2007) Marine debris and plastics: Environmental concerns, sources, impacts and solutions, *J. Polymers Environ.*, 15, 301–305.

Sigmundsson, F., Pinel, V., Lund, B., Albino, F., Pagli, C., Geirsson, H., & Sturkell, E. (2010) Climate effects on volcanism: influence on magmatic systems of loading and unloading from ice mass variations, with examples from iceland, *Philos. Trans. R. Soc. London, Ser. A*, **368**(1919), 2519 - 2534.

Skliris, N., Zika, J. D., Nurser, G., Josey, S. A., & Marsh, R. (2016) Global water cycle amplifying at less than the clausius-clapeyron rate, *Sci. Rep.*, **6**(38752).

Slovic, P.(1987) Perception of risk, *Science*, **236**(4799), 280 - 285.

Sterzel, T., Ludeke, M. K. B., Walther, C., Kok, M. T., Sietz, D., & Lucas, P. L. (2020) Typology of coastal urban vulnerability under rapid urbanization, *PLoS ONE*, **15**(1), 1-24.

Sun, X., Li, R., Shan, X., Xu, H., & Wang, J. (2021) Assessment of climate change impacts and urban flood management schemes in central shanghai, *Int. J. Disaster Risk Reduct.*, **65**(102563).

Tabari, H. (2020) Climate change impact on flood and extreme precipitation increases with water availability, *Sci. Rep.*, **10**(13768).

Taubenbock, H., Debray, H., Qiu, C., Schmitt, M., Wang, Y., & Zhu, X. (2020) Seven city types representing morphologic configurations of cities across the globe, *Cities*, **105**(102814).

UN (2019). World population prospects 2019: highlights (ST/ESA/SER.A/423). United Nations, Department of Economic and Social Affairs, Population Division

UN (2019) World population prospects, germany. *Population Division World Population Prospects 2019*. Retrieved September, 2020, from https://population.un.org/wpp/Graphs/Probabilistic/POP/TOT/276.

UN (2019) World population prospects, netherlands. *Population Division World Population Prospects 2019*. Retrieved September, 2020, from https://population.un.org/wpp/Graphs/Probabilistic/POP/TOT/528.

UNEP (2009) *Marine Litter: A Global Challenge*, Nairobi: United Nations Environmental Programme (UNEP).

UNPD (2019) World population prospects 2019, total population - both sexes.csv. *Population Division World Population Prospects 2019*. Retrieved January, 2020, from https://population.un.org/wpp/Download/Standard/Population/.

USGS (2021) Introduction to subduction zones: Amazing events in subduction zones. *United State Geologic Survey*. Retrieved September, 2021, from https://www.usgs.gov/special-topic/subduction-zone/science.

Vousdoukas, M., Voukouvalas, E., Annunziato, A., Giardino, A., & Feyen, L. (2016) Projections of extreme storm surge levels along europe, *Clim. Dyn.*, **47**, 3171-3190.

Wijayanti, P., Zhu, X., Hellegers, P., Budiyono, Y., & van Ierland, E. C. (2017) Estimation of river flood damages in jakarta, indonesia, *Nat. Haz.*, **86**, 1059-1079.

Wikipedia (2020) List of deadliest floods. *Wikipedia, the free encyclopedia*. Retrieved August, 2020, from https://en.wikipedia.org/wiki/List_of_deadliest_floods.

Wikipedia (2020) List of floods in the Netherlands. *Wikipedia, the free encyclopedia*. Retrieved August, 2020, from https://en.wikipedia.org/wiki/List_of_floods_in_the_Netherlands.

Wikipedia (2020) List of floods in Europe. *Wikipedia, the free encyclopedia*. Retrieved August, 2020, from https://en.wikipedia.org/wiki/List_of_floods_in_Europe.

WMO (2011) Guide to storm surge forecasting (WMO-No 1076). World Meteorological

Organization.

WPR (2021) Jakarta population data (urban area). *World Population* Review. Retrieved July, 2021, from https://worldpopulationreview.com/world-cities/jakarta-population.

Wuebbles, D.J., D.R. Easterling, K. Hayhoe, T. Knutson, R.E. Kopp, J.P. Kossin, K.E. Kunkel, A.N. LeGrande, C. Mears, W.V. Sweet, P.C. Taylor, R.S. Vose, & M.F. Wehner (2017) Our globally changing climate. *in Climate Science Special Report: Fourth National Climate Assessment*, **1** [Wuebbles, D.J., D.W. Fahey, K.A. Hibbard, D.J. Dokken, B.C. Stewart, and T.K. Maycock (eds.)]. U.S. Global Change Research Program, Washington, DC, USA, pp. 35-72, doi: 10.7930/J08S4N35.

Yamazaki, D., Ikeshima, D., Tawatari, R., Yamaguchi, T., O'Loughlin, F., Neal, J. C., Sampson, C. C., Kanae, S., & Bates, P. D. (2021) A high-accuracy map of global terrain elevations: Jakarta special capital region topographic map, elevation, relief. *Topographic Maps*. Retrieved September,2021, from https://en-gb.topographic-map.com/maps/s7ak/Jakarta-Special-Capital-Region/.

VITA

Kelly C. Jones
Old Dominion University
Department of Ocean and Earth Sciences
4600 Elkhorn Ave
Norfolk VA 23529

EDUCATION

2019 – 2021	**Master of Science in Ocean & Earth Science** *Old Dominion University*
2014 - 2018	**Bachelor of Arts in Geology** *Hartwick College*, Oneonta, NY

PRESENTATIONS & CONFERENCE PROCEEDINGS

Jones,K. and Plag, H.P. 2021. The Risk of Current and Future Plastic Marine Debris Originating in the Coastal Urban Built Environment. *American GeoPhysical Union Fall Meeting* eLigtening Session, Dec. 2021.

Jones, K., Plag, H.P., and Martin, D. 2021. Estimating the Risk of Future Marine Debris Resulting from the Coastal Built Environment.*Integrated Marine Debris Observing System (IMOS) Event to the UN Decade Lab for a Clean Ocean hybird event.* Poster Hall Nov. 10-30 2021.

Plag, H.P., Jones, K., Kimberly, A., and Martin, D., R. 2021. A Virtual Center for the Community Addressing the Challenge of Marine Debris. Oceans 2021, Sept. 20-23, 2021, San Diego, USA. Available at: https://proceedings.oceans2021.org/viewpaper.cfm?ID=1040&pc=59123 057.

Plag, H.P., Jones, K., Kimberly, A., and Martin, D., R. 2021b. A Virtual Center for the Community Addressing the Challenge of Marine Debris. Integrated Marine Debris Observing System Event to the UN Decade Lab for a Clean Ocean hybird event. Poster Hall Nov. 10-30, 2021.

Jones, K. 2021. Plastics in the Urban Coast Prestation. Track on Marine Debris for the Evolving and Sustaining OBPS Workshop IV.

Jones, K., Martin, D., Plag, H.-P., 2019. The Coastal Built Environment: A Source of Current and Future Marine Debris? Poster at the workshop on Marine Debris Indicators: What's Next? Brest, France, December 16-18, 2019.

Martin, D., Jones, K., Plag, H.-P., 2019. Modeling the Life Cycle of Plastic: From Marine Debris to the Source. Poster at the workshop on Marine Debris Indicators: What's Next? Brest, France, December 16-18, 2019.

AWARDS AND CERTIFICATES

Summer 2021	Old Dominion University Graduate School Summer Award
Fall 2021	Impact Learning Community Peer Mentor
Summer 20201	Graduate Certificate in Conservation Leadership

LEADERSHIP

July 2020 – June 2021	Ocean and Earth Science Graduate Student Organization President